

---


Electronic Theses and Dissertations, 2004-2019

---

2007

## Advances In Fire Debris Analysis

Mary Williams  
*University of Central Florida*

 Part of the [Chemistry Commons](#), and the [Forensic Science and Technology Commons](#)  
Find similar works at: <https://stars.library.ucf.edu/etd>  
University of Central Florida Libraries <http://library.ucf.edu>

This Masters Thesis (Open Access) is brought to you for free and open access by STARS. It has been accepted for inclusion in Electronic Theses and Dissertations, 2004-2019 by an authorized administrator of STARS. For more information, please contact [STARS@ucf.edu](mailto:STARS@ucf.edu).

---

### STARS Citation

Williams, Mary, "Advances In Fire Debris Analysis" (2007). *Electronic Theses and Dissertations, 2004-2019*. 3412.  
<https://stars.library.ucf.edu/etd/3412>

ADVANCES IN FIRE DEBRIS ANALYSIS

by

MARY R. WILLIAMS  
B.S. University of Central Florida, 1999

A thesis submitted in partial fulfillment of the requirements  
for the degree of Master of Science  
in the Department of Chemistry  
in the College of Sciences  
at the University of Central Florida  
Orlando, Florida

Spring Term  
2007

© 2007 Mary R. Williams

## **ABSTRACT**

Fire incidents are a major contributor to the number of deaths and property losses within the United States each year. Fire investigations determine the cause of the fire resulting in an assignment of responsibility. Current methods of fire debris analysis are reviewed including the preservation, extraction, detection and characterization of ignitable liquids from fire debris. Leak rates were calculated for the three most common types of fire debris evidence containers. The consequences of leaking containers on the recovery and characterization of ignitable liquids were demonstrated. The interactions of hydrocarbons with activated carbon during the extraction of ignitable liquids from the fire debris were studied. An estimation of available adsorption sites on the activated carbon surface area was calculated based on the number of moles of each hydrocarbon onto the activated carbon. Upon saturation of the surface area, hydrocarbons with weaker interactions with the activated carbon were displaced by more strongly interacting hydrocarbons thus resulting in distortion of the chromatographic profiles used in the interpretation of the GC/MS data. The incorporation of an additional sub-sampling step in the separation of ignitable liquids by passive headspace sampling reduces the concentration of ignitable liquid accessible for adsorption on the activated carbon thus avoiding saturation of the activated carbon. A statistical method of covariance mapping with a coincident measurement to compare GC/MS data sets of two ignitable liquids was able to distinguish ignitable liquids of different classes, sub-classes and states of evaporation. In addition, the method was able to distinguish 10 gasoline samples as having originated from different sources with a known statistical certainty. In a blind test, an unknown gasoline sample was correctly identified from the set of 10 gasoline samples without making a Type II error.

*To My Husband Darrin*

## **ACKNOWLEDGMENTS**

This work was supported under State of Florida Type II Center funding to the University of Central Florida and National Center for Forensic Science. The work was done at the National Center for Forensic Science, a National Institute of Justice program hosted by the University of Central Florida, and a member of the Forensic Science Resource Network.

## TABLE OF CONTENTS

LIST OF FIGURES .....	viii
LIST OF TABLES .....	x
CHAPTER ONE: INTRODUCTION.....	1
CHAPTER TWO: FIRE DEBRIS EVIDENCE .....	4
Collection of Fire Debris Evidence.....	4
Point of origin.....	5
Cause.....	5
Collection.....	6
Extraction of Ignitable Liquid from Fire Debris.....	6
Steam Distillation .....	7
Solvent Extraction .....	7
Headspace Vapor Sampling.....	8
Dynamic Headspace Concentration.....	8
Passive Headspace Concentration with Activated Carbon.....	9
Headspace Concentration with Solid Phase Microextraction.....	10
Detection of Ignitable Liquids .....	11
Gas Chromatography .....	11
Gas Chromatography – Mass Spectrometry .....	13
Two Dimensional Gas Chromatography with Mass Spectrometry .....	14
Gas Chromatography – Mass Spectrometry – Mass Spectrometry .....	16
Analysis of Ignitable Liquids.....	17
Pattern Recognition .....	17
Extracted Ion Profiling .....	18
Target Ion Analysis.....	20
Classification .....	21
CHAPTER THREE: EXTRACTION OF IGNITABLE LIQUIDS FROM FIRE DEBRIS BY PASSIVE HEADSPACE SAMPLING WITH ACTIVATED CARBON .....	30
Introduction.....	30
Methods and Materials.....	31
Results.....	33
Hydrocarbon Molecule Interactions with Activated Carbon.....	33
Effects of Adsorbent Size and Liquid Volume on Hydrocarbon Recovery .....	40
Discussion.....	49
CHAPTER FOUR: COLLECTION AND STORAGE OF FIRE DEBRIS EVIDENCE .....	56
Introduction.....	56
Methods and Materials.....	57
Results.....	61
Commercial Container Leak Rates.....	61
Effects of Container Leaks .....	66
Discussion.....	71
CHAPTER FIVE: ANALYSIS OF FIRE DEBRIS EVIDENCE BY COVARIANCE MAPPING .....	74
Introduction.....	74

Methods and Materials.....	75
Results.....	78
Covariance Mapping.....	78
Characterization of Ignitable Liquids.....	81
Comparison of Gasoline Samples by Covariance Mapping.....	85
Discussion.....	93
CHAPTER SIX: DISCUSSION.....	95
APPENDIX: PERMISSION LETTER.....	100
REFERENCES.....	102



## LIST OF FIGURES

Figure 1: Schematic of Gas Chromatograph.....	12
Figure 2: Schematic of a Quadrupole Mass Spectrometer.....	14
Figure 3: Schematic of a Two Dimensional Gas Chromatograph.....	15
Figure 4: Total Ion Chromatogram on n-Alkanes from n-Hexane to n-Eicosane .....	22
Figure 5: Total Ion Chromatogram of Gasoline .....	24
Figure 6: Total Ion Chromatogram of a Heavy Petroleum Distillate .....	24
Figure 7: Total Ion Chromatogram of an Isoparaffinic Product.....	26
Figure 8: Total Ion Chromatogram of an Aromatic Product .....	26
Figure 9: Total Ion Chromatogram of a Naphthenic Paraffinic Product .....	27
Figure 10: Total Ion Chromatogram of a Normal Alkane Product.....	27
Figure 11: Total Ion Chromatogram of a De-aromatized Product.....	28
Figure 12: Total Ion Chromatogram of an Oxygenated Product.....	28
Figure 13: Experimental Setup .....	32
Figure 14: Activated Carbon Surface Area Covered by Adsorbed Hydrocarbons as Calculated from the van der Waals Area of Each Hydrocarbon.....	34
Figure 15: Additional Adsorption of Hydrocarbon Molecules onto Activated Carbon .....	36
Figure 16: Displacement and Loss of Hydrocarbon Molecules Previously Adsorbed onto Activated Carbon .....	37
Figure 17: Adsorbed Hydrocarbon Molecules Remaining on Activated Carbon after a Second Heating Period .....	39
Figure 18: Hydrocarbon Molecule Loss from Activated Carbon after a Second Heating Period	40
Figure 19: Distribution of Mole Fractions of Hydrocarbons Adsorbed on Various Sizes of Activated Carbon .....	42
Figure 20: Mole Fraction Distribution of Hydrocarbons Recovered from Activated Carbon.....	45
Figure 21: Chromatogram of 12 $\mu$ l of Gasoline after Extraction from Activated Carbon .....	46
Figure 22: Chromatogram of 0% Weathered Gasoline.....	46
Figure 23: Chromatogram of 96 $\mu$ l of Gasoline after Extraction from Activated Carbon .....	47
Figure 24: Chromatogram of 75% Weathered Gasoline.....	47
Figure 25: Chromatogram of Hydrocarbons Recovered from 96 $\mu$ l of 0% Weathered Gasoline Deposited onto Carpet.....	48
Figure 26: Chromatogram of Hydrocarbons Recovered from a Sub-sample of Carpet Spiked with 96 $\mu$ l of 0% Weathered Gasoline.....	49
Figure 27: Mole Fractions of Adsorbed Hydrocarbons on Activated Carbon Plotted as a Function of the Square of the Molecular Polarizability ( $\alpha^2$ ).....	54
Figure 28: Experiment Setup .....	59
Figure 29: Mole Fractions of Recovered Hydrocarbons from Activated Carbon Disks at Various Depths within the Container with a Volume 12 $\mu$ l Hydrocarbon Solution .....	62
Figure 30: Mole Fractions of Recovered Hydrocarbons from Activated Carbon Disks at Various Depths within the Container with a Volume 96 $\mu$ l Hydrocarbon Solution .....	63
Figure 31: Ratio of Hydrocarbons in the Vapor Phase to Hydrocarbons Adsorbed.....	65
Figure 32: Container Leak Rates .....	66

Figure 33: Hydrocarbon Mole Fractions from the 10 $\mu$ l Volume Deposited into Each Container Type of Hydrocarbons that Leaked from the Container and Hydrocarbons that Remained in the Container.....	68
Figure 34: Hydrocarbon Mole Fractions from the 18 $\mu$ l Volume Deposited into Each Container Type of Hydrocarbons that Leaked from the Container and Hydrocarbons that Remained in the Container.....	69
Figure 35: Demonstration of Hydrocarbon Transfer from Environment into Empty Jar .....	70
Figure 36: Demonstration of Cross Contamination.....	71
Figure 37: A Graphical Representation of a Covariance Matrix being generated from a GC-MS data set .....	79
Figure 38: Covariance Map of Gasoline.....	80
Figure 39: Covariance Maps of Ignitable Liquids .....	83
Figure 40: Frequency Distribution Plot of 30 same sample distances ( $D_{SS}$ ) and 405 different sample distances ( $D_{DS}$ ).....	86
Figure 41: Depiction of Two Probability Distributions.....	89
Figure 42: The Calculated Power for $n_{SS}$ and $n_{DS}$ at a significance level $\alpha$ of 0.05.....	90

## LIST OF TABLES

Table 1: Common Ions of Each Class of Compounds.....	19
Table 2: Target Compounds in Gasoline and Medium Petroleum Distillates Found in the Standard Testing Method ASTM E1618-01.....	21
Table 3: Summary of Experimental Conditions for each Container.....	35
Table 4: Hydrocarbon Mole Fractions from Recovered Liquid .....	43
Table 5: Hydrocarbon Mole Fraction of Vapor Phase.....	44
Table 6: Gasoline Sources and Octane Ratings .....	76
Table 7: Samples from Ignitable Liquid Reference Collection .....	77
Table 8: Distances between Ignitable Liquid Samples .....	84
Table 9: Average Distances between Gasoline Samples .....	91
Table 10: Unknown A Comparison to Ten Gasoline Samples .....	92
Table 11: Unknown B Comparison to Ten Gasoline Samples .....	92

## **CHAPTER ONE: INTRODUCTION**

In 2005, fire killed more Americans than all natural disasters combined. The U.S. Fire Administration reported there were 3,675 civilians and 115 firefighters killed as a result of fire. Direct property loss due to fires was estimated at \$10.7 billion. An estimated 31,500 intentionally set (arson) structure fires resulted in 315 deaths and resulted in \$664 million dollars in property damage.<sup>1</sup> Fire investigations are a challenge since the evidence is partially if not totally destroyed during the event. At the scene, fire investigators establish the point of fire origination to begin the process of determining a cause. Fire debris from the point of origin is collected as evidence then analyzed in the laboratory to detect whether an ignitable liquid residue is present. The presence of an ignitable liquid residue is a key factor in establishing the cause of a fire. The volatile nature of an ignitable liquid requires the container for collection and preservation of the physical evidence is contaminant free and air tight. At the laboratory, the ignitable liquid residue must be extracted from the fire debris before detection and analysis. Several extraction methods exist, all having advantages and disadvantages, but adsorption methods are the most popular. The hydrocarbon components of the extracted ignitable liquid residue are separated then detected by chromatographic-spectrometric combined methods. The resulting data is interpreted to classify the ignitable liquid residue into a group of ignitable liquids with similar chemical and physical characteristics.

The American Society of Testing and Materials standard practice E1412-00 recommends a procedure for extracting ignitable liquid residues from fire debris by adsorption onto activated carbon suspended in the heated headspace above the fire debris sample within the collection container. Subsequent desorption of the ignitable liquid residue from the activated carbon is

accomplished by a solvent. ASTM E1412-00 provides guidelines in the extraction process to reduce the possibility of preferential adsorption of the ignitable liquid components. Limitations of extraction by passive headspace sampling have been addressed concerning the effects of adsorption time, temperature, activated carbon size, and sample concentration. The study demonstrates the effects of chromatographic profile distortion when certain parameters in the extraction process are not controlled. If a representative sample of the ignitable liquid is not obtained, analysis of the results is compromised. The study presented here encompassed a more extensive investigation into the adsorption process. Hydrocarbon molecule interactions with the activated carbon are investigated, including a determination of the activated carbon surface area. Activated carbon size and ignitable liquid volume were demonstrated to affect the chromatographic profiles due to saturation of the activated carbon. A modification to the extraction process incorporating a sub-sampling technique reduced the effects of saturation of the activated carbon.

The collection and preservation of fire debris evidence is crucial in retaining ignitable liquid residues for analysis. An effective fire debris evidence container must be vapor-tight and contaminant free. The possibility of cross-contamination is a common concern in choosing a suitable container for fire debris evidence. Containers recommended for fire debris evidence include metal “paint” cans with compression lids, glass mason jars with standard pressure-canning flats and bands, and special co-polymer bags.<sup>3, 35, 36</sup> Metal paint cans are the most frequently used fire debris evidence container. Previous studies typically determine the suitability of a container by comparing it to the preferred container or incorporating the preferred container in the experiment with the assumption it is vapor tight. Usually a reduction in ignitable liquid volume determines whether a container is not vapor tight. In the study here the leak rates

of three types of containers is determined. The consequences of using an inappropriate container for preservation of ignitable liquids are demonstrated.

Interpretation of GC-MS data by pattern recognition, extracted ion profiling and target ion profiling techniques are recommended as described within ASTM E1618-01. These techniques are utilized separately or in combination to place an ignitable liquid residue into one of nine classes. Various methods for improving detection and alternative methods for data analysis and interpretation have been studied. Methods for improving detection generally utilize an additional chromatography or spectrometry method to improve resolution of the ignitable liquid components. Statistical methods for comparing GC/MS data have been applied in the classification of ignitable liquids as well as the identification of gasoline, but still rely on pattern recognition. The study here applied covariance mapping and coincidence measurements to existing GC/MS data from the Ignitable Liquids Reference Collection and analyses of regional gasoline samples. The capability of the method to characterize ignitable liquids according to ASTM class, carbon range, and percent evaporation was determined. The application of covariance mapping with coincidence measurement and subsequent t-test was performed to ascertain if ten gasoline samples can be distinguished as having different sources of origin and can be identified with a known statistical certainty.

## **CHAPTER TWO: FIRE DEBRIS EVIDENCE**

The analysis of fire debris begins at the crime scene where most of the evidence in the form of an ignitable liquid is consumed in the fire leaving only trace amounts of its residue behind. At the fire scene, investigators determine the point of origin in order to collect any possible ignitable liquid residue. Fire debris from the point of origin is analyzed to determine if an ignitable liquid is present. The presence of an ignitable liquid is a key factor in establishing the cause of the fire. Since the ignitable liquid residue is volatile by nature, the collection of the fire debris is important in the preservation of the physical evidence. The next challenge is for the laboratory analyst to extract the ignitable liquid residue from the fire debris collected at the scene. There are several extraction methods published by the American Society for Testing and Materials each having advantages and disadvantages. Once the ignitable liquid residue is extracted, chromatographic methods of separation, usually coupled with spectrometric methods, are utilized in detecting the residue. After detection, the chromatographic and spectrometric data are interpreted to identify the ignitable liquid or classify the liquid residue into a group according to its composition.

### *Collection of Fire Debris Evidence*

Fire debris analysis begins at the fire scene where a fire investigator determines the point of origin. Fire debris is collected from the point of origin then sent to the laboratory to determine whether the fire debris contains ignitable liquid residues. Timely collection and preservation of fire debris evidence is crucial due to the volatile nature of the ignitable liquid residues. The presence of an ignitable liquid is a key factor in the determining the cause of a fire as incendiary.

### *Point of origin*

The point of origin of a fire is the location where the fire started – the place of beginning.<sup>2</sup> Determination of the point of origin involves incorporating the following information; the fire patterns left by the fire, observations reported by witnesses, analysis of the physics and chemistry in the fire initiation, and the development of the fire which would produce the conditions found at the fire scene. Examination of the fire scene usually provides the information needed for a determination of which area corresponds to the point of origin. The examination begins with a systematic procedure of identifying areas with the least amount of damage then moving toward the area of greatest damage. Once the general location of the origin is determined the specific location is identified based on the patterns produced by the movement of heat, flame, and smoke. The specific location of the origin will be where the heat ignited the first fuel.<sup>3</sup>

### *Cause*

The cause of a fire is determined by identifying the circumstances and factors which were necessary for the fire to occur. Those circumstances and factors include the device or equipment involved in the ignition, the ignition source, the material first ignited, and the circumstances or actions that brought all of these factors together allowing the fire to occur. The cause of the fire is classified as natural, accidental, undetermined, or incendiary. Classifying a fire assists in assigning responsibility and culpability. Natural fires are considered acts of God, such as lightning, earthquakes, and wind. Accidental fires are those where the proven cause doesn't involve the deliberate or intentional action of a human to ignite or spread the fire. Undetermined



fires are those where the cause can not be proven or is unknown. Incendiary fires are those fires proven to be deliberately or intentionally ignited.’

### *Collection*

If an incendiary fire is suspected, the fire investigator collects samples from potential points of origin as evidence. The evidence most frequently collected is fire debris and other materials such as flooring, carpet, baseboard, and pieces of furnishings.<sup>4</sup> These samples of fire debris are suspected of containing ignitable liquid residues. The ignitable liquid residues are what remain of an ignitable liquid which is considered a possible source of ignition. The presence or absence of an ignitable liquid provides the fire investigator with information about one of the factors evaluated in the cause of the fire. Fire debris evidence is collected into air tight containers to preserve the volatile ignitable liquid residues. The most common types of containers are metal cans, glass jars and polymer bags. There are differing opinions as to which container type is best. The presence of an ignitable liquid alone does not classify the fire as incendiary other factors and circumstances must also be identified to come to that conclusion.

### *Extraction of Ignitable Liquid from Fire Debris*

Analysts in the fire debris community have formed a committee to develop standard practices and methods in the extraction and analysis of fire debris collected from potential arson scenes. The standard practices and methods were published by the American Society for Testing and Materials (ASTM), volume 14.02. They are under the jurisdiction of ASTM Committee E30 of Forensic Science and are the responsibility of E30.01 on Criminalistics. The E30 committee reviews and updates each standard practice or method every five years to determine if it is still

relevant and to update it based upon current peer reviewed literature. Currently, there are six standard practices for the extraction of ignitable liquid residues from fire debris.

### *Steam Distillation*

The first standard extraction practice is E1385-00, Standard Practice for Separation and Concentration of Ignitable Liquid Residues from Fire Debris Samples by Steam Distillation, which is one of the oldest extraction practices. Steam distillation is a classical separation technique for extraction of hydrocarbon based liquids. The apparatus is a flask or container of appropriate size in which the fire debris can be introduced through the mouth, and a distillation trap fitted with a condensing column or a cold finger. The technique involves introducing the fire debris into a container with an appropriate amount of water and boiling. The vapors produced are condensed in the distillation apparatus. Petroleum distillate residues float on top of a column of water and are collected as visible liquids.<sup>5</sup>

### *Solvent Extraction*

The second standard extraction practice is E1386-00, Standard Practice for Separation and Concentration of Ignitable Liquid Residues from Fire Debris Samples by Solvent Extraction, a destructive technique which should only be used when a representative portion of the fire debris sample can be reserved for reanalysis. Solvent extraction is well suited for extraction of ignitable liquid residues from non porous surfaces such as glass. A representative portion of the sample is placed into a beaker with a sufficient volume organic solvent to moisten the sample. The solvent and debris are mixed to promote the extraction of the ignitable liquid residue. The solvent is decanted from the debris then passed through a filter as necessary. The organic

solvent should be evaporated with dry nitrogen, filtered air, or inert gas to concentrate the sample if necessary.<sup>6</sup>

### *Headspace Vapor Sampling*

The third standard extraction practice is E1388-00, Standard Practice for Sampling Headspace Vapors from Fire Debris Samples, which is the least sensitive of the five extraction techniques. The headspace vapor sampling technique is useful in screening fire debris samples for the presence of ignitable liquid residues. There are four apparatuses required; a heating system such as an oven, a temperature measuring device such as a thermometer, a gas-tight syringe in the range of 0.5 to 5 milliliters, and a drill or punch to puncture holes in the evidence container lid. Once the hole is punched into the container lid it must be sealed with tape across the hole or a septum inserted in the hole. The temperature measuring device is placed in the container lid of the container. The container is placed in the heating system for 20 to 60 minutes until the temperature inside the container reaches 90°C. The ignitable liquid residue is volatilized to fill the headspace of the container. Immediately after the container is removed from the oven, the syringe is inserted through the tape or septum. The syringe is flushed three times with the headspace vapor before being withdrawn with a portion of the volatilized ignitable liquid residue.<sup>7</sup>

### *Dynamic Headspace Concentration*

The fourth standard extraction practice E 1413-00, Standard Practice for Separation and Concentration of Ignitable Liquid Residues from Fire Debris Samples by Dynamic Headspace Concentration is a highly sensitive technique for obtaining low concentrations of ignitable liquid residues. The technique is potentially destructive therefore a portion of the sample should be

reserved for reanalysis. The dynamic headspace concentration technique requires a positive or negative pressure apparatus, an adsorption tube, a heating system, and a temperature measuring device. The technique involves heating the sample container to volatilize the ignitable liquid residue at the same time pushing or drawing the headspace containing the volatilized ignitable liquid through a tube containing an adsorbent material. The ignitable liquid residue is captured onto the adsorbent material which is usually activated charcoal. The adsorption tube is removed from the apparatus and cooled to room temperature before an elution solvent is passed through the tube. The elution solvent desorbs the ignitable liquids residue from the activated charcoal.<sup>8</sup>

#### *Passive Headspace Concentration with Activated Carbon*

The fifth standard extraction practice E1412-00, Standard Practice for Separation of Ignitable Liquid Residues from Fire Debris Samples by Passive Headspace Concentration with Activated Charcoal is the most common extraction technique used in the forensic laboratory for fire debris analysis today. The passive headspace concentration technique uses a heating system, a temperature measuring device, and activated charcoal to extract the residue. The technique is considered to be a non destructive technique which introduces the activated charcoal usually in the form of a rectangular strip into the headspace of the evidence container. This is accomplished by perforating the activated charcoal strip with a paperclip which is attached to a string or dental floss. The activated charcoal strip is suspended in the headspace with the end of the string hung over the lip of the container and secured with the container lid. The container is placed into a heated oven to volatilize the ignitable liquid residue into the headspace for adsorption onto the activated charcoal strip. After several hours in the oven, the container is cooled to room temperature then the activated charcoal strip is removed and placed into a sample

vial with an eluting solvent. The elution solvent, carbon disulfide or diethyl ether desorbs the ignitable liquid residue from the activated charcoal strip.<sup>9</sup>

#### *Headspace Concentration with Solid Phase Microextraction*

The sixth standard extraction practice E2154-01, Standard Practice for Separation and Concentration of Ignitable Liquid Residues from Fire Debris Samples by Passive Headspace Concentration with Solid Phase Microextraction (SPME) is the newest extraction technique. The SPME practice is best suited for the screening of fire debris samples to assess the relative concentration of the ignitable liquid or for aqueous samples. Solid phase microextraction is also considered to be a non destructive extraction technique because it recovers a small amount of the ignitable liquid residue. The required apparatus is a heating system, a temperature measuring device, a SPME fiber with holder, a punch, and septum. The SPME fiber is coated with a polymeric stationary phase which is held within a needle contained inside a holder. A SPME fiber with a 100  $\mu\text{m}$  thickness of polydimethylsiloxane (PDMS) is recommended for ignitable liquids in the  $\text{C}_{10} - \text{C}_{25}$  range and a fiber with an 85  $\mu\text{m}$  thickness of polyacrylate or a fiber with a 75  $\mu\text{m}$  thickness of Carboxen/PDMS for ignitable liquids in the  $\text{C}_1 - \text{C}_{10}$  range. After the evidence container lid is punctured a septum is inserted into the hole. The container is placed within an oven at a temperature between 60°C to 80°C for approximately 30 minutes to volatilize the ignitable liquid residues into the headspace. Immediately after removal from the oven the septum in the container lid is punctured with the SPME needle. The SPME fiber is inserted into the headspace allowing the ignitable liquid residues to adsorb onto the fiber. After one exposure of 5 to 15 minutes the SPME fiber is retracted into the needle and the SPME assembly removed

from the septum. Upon removal from the heated headspace, the SPME fiber is inserted into the heated injection port of a gas chromatograph.<sup>10</sup>

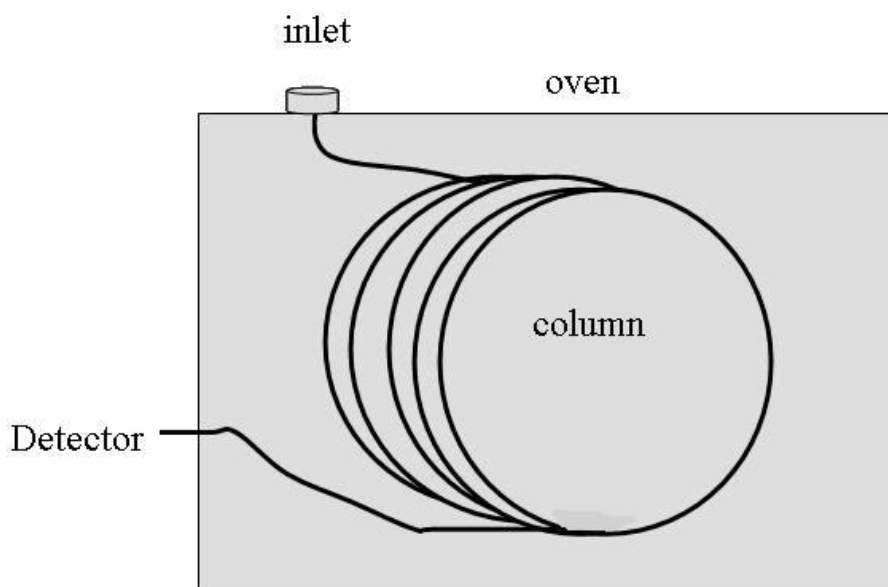
### *Detection of Ignitable Liquids*

Ignitable liquids are petroleum based liquids that are either flammable or combustible. Ignitable liquids are complex mixtures of hydrocarbons containing normal, branched, and cyclic alkanes as well as aromatics and polynuclear aromatics. An example is gasoline which is composed of over 400 compounds.<sup>11</sup> These petroleum based liquids are isolated from crude oil by a variety of chemical processes. The best methods for fire debris detection include gas chromatography, which separates the hydrocarbons within in the ignitable liquid residues before detection. There many detectors which may be used with the gas chromatograph. The choice of detector depends on the amount of chemical information or sensitivity required in the analytical method. These methods of detection include gas chromatography, gas chromatography-mass spectrometry (GC-MS), two dimensional gas chromatography - mass spectrometry (GC-GC-MS) and gas chromatography – mass spectrometry - mass spectrometry (GC-MS-MS).

### *Gas Chromatography*

Gas chromatography is the basis for the detection of ignitable liquid residues. An analyte is injected into a heated port to be vaporized, then is carried through a column by an inert gas such as helium. The column consists of a liquid phase immobilized on the surface of an inert solid where the analyte is partitioned between the mobile phase (inert carrier gas) and the stationary phase (liquid phase). Chromatographic columns are housed in an oven in which the temperature is controlled. Columns vary in length, internal diameter, type and thickness of liquid phase. Injector temperatures, columns, gas flow rates, and oven temperatures are modified

to achieve separation of the analyte compounds from one another before detection. Figure one is a schematic of a gas chromatograph. Common detectors of a gas chromatograph are flame ionization, thermal conductivity, electron capture detectors, and mass spectrometers. Data is presented as a chromatogram, a plot of retention time versus intensity which contains peaks corresponding to the separated compounds from the analyte.<sup>12, 13</sup> Gas chromatography is a natural match for ignitable liquid detection because of its capability to separate the complex mixture into its major components. Advances in chromatography such as capillary columns provided additional data for interpretation since better separation of the components was possible. Gas chromatography led to pattern recognition techniques for interpretation of the data and enabled an analyst to classify ignitable liquids into groups based on their physical properties.

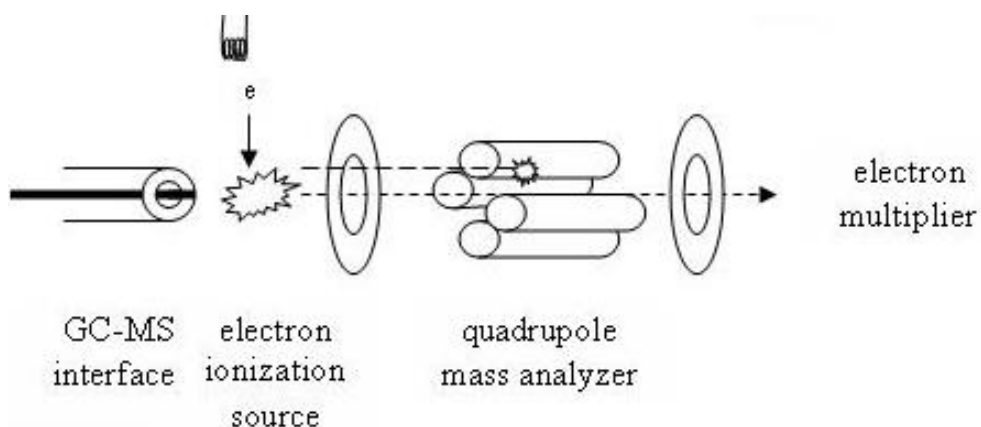


**Figure 1: Schematic of Gas Chromatograph**

## *Gas Chromatography – Mass Spectrometry*

Gas chromatography – mass spectrometry has superseded gas chromatography as the most widely used method for the detection of ignitable liquids. GC-MS still has the capability of separating the numerous compounds constituting an ignitable liquid, but with the incorporation of a mass spectrometer with electron ionization (EI) for detection it provides additional chemical information about the compounds. Mass spectrometers basically bombard the separated molecules being eluted from the gas chromatographic column with high-energy electrons. The field produced by the high energy electron passing near an analyte molecule can cause ionization of the analyte and impart large amounts of energy to the newly formed ions. The ion dissipates the energy through numerous processes, which may include fragmentation into lower mass ions. Electron ionization is the preferred ionization method for analysis of ignitable liquids due to its reproducibility. Some of the molecular fragments formed are ions that are accelerated within an electric field to pass into the mass analyzer which separates the ions according to their mass to charge ratio. Then the separated ions are detected by an electron multiplier which counts the number of ions striking it by producing a proportional electrical current. Figure 2 is a schematic of a mass spectrometer where the column enters the ionization source through the heated interface between the gas chromatograph and mass spectrometer. The ions travel to the mass analyzer with only selected ions allowed to proceed to the detector.





**Figure 2: Schematic of a Quadrupole Mass Spectrometer**

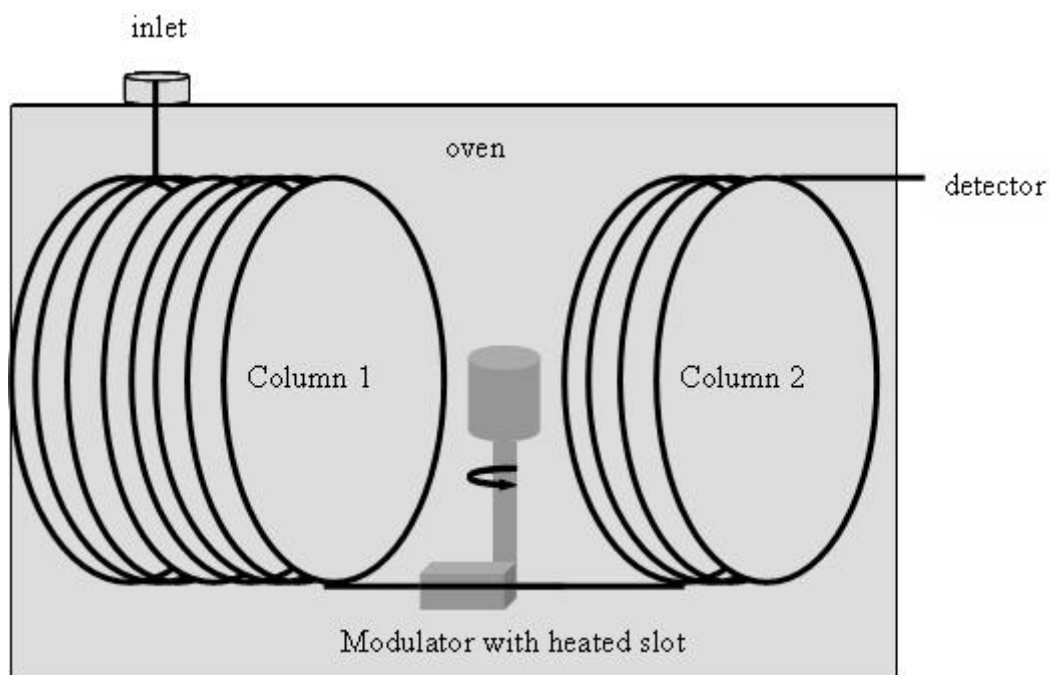
The data consists of perhaps thousands of mass spectra which are summed on a time axis producing a total ion chromatogram. The total ion chromatogram consists of peaks corresponding to the separated compounds plotted as retention time versus summed intensity. A mass spectrum of a peak within the TIC is a plot of ion abundance versus mass to charge ( $m/z$ ) ratio. The chromatogram still provides data for pattern recognition, but is now combined with the spectral data which provides structural information about each compound within the ignitable liquid.<sup>12, 14</sup>

### *Two Dimensional Gas Chromatography with Mass Spectrometry*

Gas chromatography is a one-dimensional separation technique. However, separation of the components can be improved by employing two dimensional separations techniques such as GC x GC or hyphenated methods such as GC-MS. Gas chromatography – mass spectrometry is considered a two-dimensional technique because it separates components chromatographically then separates and identifies them spectrometrically. However, spectrometric separation in the second dimension can be limited by the chromatographic separation in the first dimension.

Another separation technique employed combines GC x GC with GC – MS to create GC x GC-

MS, a three-dimensional separation technique which provides better chromatographic resolution. The differences in the method compared to GC and GC-MS are the inclusion of a second column and a focusing apparatus. Figure 3 is a schematic of the instrument showing a sample inlet connected to the first column which is connect serially to the second column by a focusing apparatus and terminating with a detector, which in this case is a mass spectrometer. Typically, the first column (dimension 1) is longer and has a larger internal diameter with a thicker film thickness than the second column (dimension 2). Also, the first column is relatively non-polar compared to the second column thus allowing compounds with similar boiling points but different functional groups to be further separated. The function of the focusing apparatus is to accumulate the analyte components after they elute from the first column then transfer them in their entirety onto the second column. There are multiple types of focusing apparatuses each with a different operating principal.



**Figure 3: Schematic of a Two Dimensional Gas Chromatograph**

One apparatus is the thermal modulator in which a modulator tube is the interface inserted between the two columns. The modulator tube is heated to desorb the analyte from the tube onto the second column. The other apparatus relies on cryogenic focusing of the analyte. The data is commonly plotted with the x-axis (minutes) reflecting the retention time of the first column and the y-axis (seconds) reflecting the retention time of the second column. The mass spectrum is summed to produce the total ion abundance for each point which is plotted in the third dimension (z-axis)<sup>15, 16</sup>

#### *Gas Chromatography – Mass Spectrometry – Mass Spectrometry*

Another method of separation and detection of ignitable liquids gaining some popularity is gas chromatography- mass spectrometry – mass spectrometry. This instrument couples a gas chromatograph with a mass spectrometer containing multiple quadrupole mass analyzers or one ion trap mass analyzer. The multiple quadrupole analyzers perform MS/MS in space whereas the ion trap performs MS/MS in time. Typically, chemical ionization rather than electron ionization is utilized in forming precursor ions since it is a softer ionization method usually producing ionic species such as  $[M+H]^+$ . A study on the detection of gasoline in fire debris by GC/MS/MS to overcome interfering pyrolysis products utilized an ion trap instrument.<sup>17</sup> Precursor ions were formed by electron ionization followed by ejection of all ions except the specified precursor ion. Product ions are formed from the precursor ions by collision-induced dissociation. A scan ejects the product ions allowing them to reach the detector resulting in a spectrum of product ions from the specified precursor ion.<sup>12</sup>

### *Analysis of Ignitable Liquids*

Typically, the ignitable liquids extracted from the fire debris are analyzed by gas chromatography or gas chromatography with mass spectrometry. The American Society for Testing and Materials (ASTM) publishes two testing methods for ignitable liquid residues. One testing method is the ASTM E 1387 Standard Test Method for Ignitable Liquid Residues in Extracts from Fire Debris Samples by Gas Chromatography which provides methods for the instrumental analysis and interpretation of the data by pattern recognition to classify the ignitable liquid residue.<sup>18</sup> The other testing method is the ASTM E 1618 Standard Test Method for Ignitable Liquid Residues in Extracts from Fire Debris Samples by Gas Chromatography-Mass Spectrometry which provides methods for the instrumental analysis and interpretation of the data by pattern recognition, extracted ion, and target ion analysis for the classification of ignitable liquid residues.<sup>19</sup>

#### *Pattern Recognition*


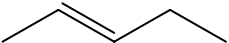
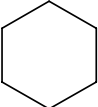
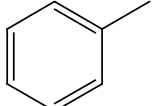
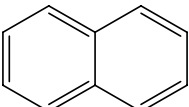
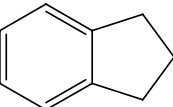
Pattern recognition techniques have been developed with the evolution of chromatographic methods of detection for fire debris. Both gas chromatography (GC) and gas chromatography mass spectrometry (GC-MS) produce chromatograms utilized in visual pattern recognition. Each peak within the chromatogram corresponds to a hydrocarbon in the ignitable liquid. The culmination of the peaks produces a pattern particular to a class of ignitable liquids. Groups of peaks composed of compounds of similar chemical composition and boiling points are examined to determine if the relative retention times and peak ratios are consistent with known ignitable liquids.<sup>20</sup> An example is the grouping of C<sub>2</sub> alkylbenzenes (o, m, p-xylenes) and C<sub>3</sub> alkylbenzenes within gasoline. Another example is the ratio of pristene to heptadecane and

phytane to octadecane within diesel fuel. The overall pattern is also examined and compared with the pattern of a known ignitable liquid. The criteria for classifying and identifying ignitable liquids by visual pattern recognition techniques are published in both ASTM standard methods E 1387 and E1618.

### *Extracted Ion Profiling*

Extracted ion profiling is the most commonly utilized method of detecting ignitable liquids by mass spectrometry in conjunction with gas chromatography. The mass spectrometer is capable of producing ion profiles by extracting ions from the total ion chromatogram as well as identifying specific compounds from their mass spectrum.. Petroleum derived ignitable liquids are generally comprised of compounds that can be classified into one of five general categories; alkanes, cycloalkanes, aromatics, indanes, and polynuclear aromatics. These classes of compounds with common chemical structures have common ions which are extracted to produce an extracted ion profile. Table 1 summarizes some of the important ions associated with classes of compounds found in ignitable liquids.<sup>19</sup>

**Table 1: Common Ions of Each Class of Compounds**

Class of Compound	Example Compound	Structure of Compound	Typical Ions of the Class (m/z)
Alkanes	Pentane		43, 57, 71, 85 (+14)
Alkenes	2-Pentene		55, 69, 83, (+14)
Cycloalkanes	Cyclohexane		55, 69, 83, (+14)
Aromatics	Toluene		91, 105, 119
Polynuclear Aromatics	Naphthalene		128, 142, 156, 170
Indanes	Indan		117, 131

Alkanes produce many ion fragments which are typically 14 mass to charge units apart corresponding to the loss of a methylene ( $\text{CH}_2$ ) group. Alkenes fragment in a similar fashion to the alkanes, but due to the double bonds in their chemical structure, the mass to charge ions are two less than those of the alkanes. Cycloalkanes have a predominant ion of 83 m/z corresponding to cyclohexyl. Smaller cycloalkanes or the fragmentation of larger cycloalkanes produces ions of 55 m/z and 69 m/z,  $[\text{C}_4\text{H}_7]^+$  and  $[\text{C}_5\text{H}_9]^+$  respectively. Aromatics have a ring structure which is more stable during the fragmentation process than the alkyl chains and therefore the molecular ion is usually seen in the mass spectrum. A common ion found in aromatic spectra has a mass to charge of 91 which is due to the formation of the tropylium ion,  $[\text{C}_7\text{H}_7]^+$ . The extracted ion profiles are compared to the ion profiles of known ignitable liquids by visual pattern recognition.<sup>19</sup> Extracted ion profiles are also utilized in determining the relative

abundance of certain classes of compounds within the ignitable liquid. This information assists in the classification of the ignitable liquid.

### *Target Ion Analysis*

Target compound analysis uses key specific compounds to characterize an ignitable liquid. Instead of separating the hydrocarbons into classes based on their fragmentation, target compound analysis seeks to identify specific analytes present as well as some selected isomers. A comparison of the relative peak heights for closely eluting aromatic and aliphatic compounds assist in ascertaining which class of ignitable liquid is present.<sup>21</sup> The hydrocarbons chosen for the peak ratios must be within one minute in retention time to minimize the effects of (weathering) evaporation.<sup>21</sup> Another consideration is that the hydrocarbons are solely present in the ignitable liquids and not from other contaminants from the fire debris. Table 2 contains a list of common hydrocarbon target compounds for medium petroleum distillates and gasoline. The relative ratios of the ions of the target compound from known ignitable liquids of particular classes are compared to the relative ratios of the ions of the same target compounds from the unknown ignitable liquid residue. The target compound data can be plotted as a target compound chromatogram that can be visually compared with other target compound chromatograms of known ignitable liquids.

**Table 2: Target Compounds in Gasoline and Medium Petroleum Distillates Found in the Standard Testing Method ASTM E1618-01.**

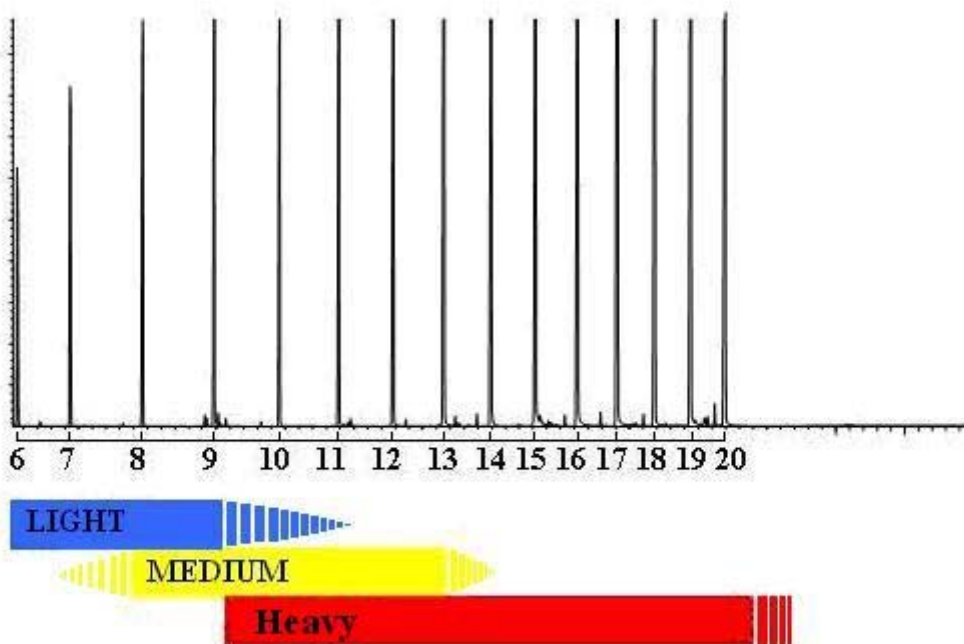
<b>Target Compounds</b>	
<b>Gasoline</b>	<b>Medium Petroleum Distillate</b>
1,3,5-Trimethylbenzene	Nonane
1,2,4-Trimethylbenzene	Propylcyclohexane
1,2,3-Treimethylbenzene	1,3,5-Trimethylbenzene
Indane	1,2,4-Trimethylbenzene
1,2,4,5-Tetramethylbenzene	Decane
1,2,3,5-Teetramethylbenzene	1,2,3-Trimethylbenzene
5-Methylindane	n-Butylcyclohexane
4-Methylindane	Trans-Decalin
Dodecane	Undecane
4,7-Dimethylindane	1,2,3,4-Tetramethylbenzene
2-Methylnaphthalene	n-Pentylcyclohexane
1-Methylnaphthalene	Dodecane
Ethyl-naphthalene (mixed)	n-Hexylcyclohexane
1,2-Dimethylnaphthalene	
2,3-Dimethylnaphthalene	

### *Classification*

Fire Debris analysts use pattern recognition, extracted ion profiling and target compound analysis for classification of ignitable liquids into classes which have similar physical and chemical characteristics. The same classification system is described in both the ASTM E1387 and the ASTM E1618 of eight characteristic classes and a miscellaneous class, each with three subclasses based on carbon range. The only class not sub-divided into carbon ranges is gasoline. Because some classes can not be distinguished without mass spectrometry ASTM E1618-01, the most common standard testing method used today, will be discussed here. The carbon number range is determined by comparing the chromatogram to a reference or test mixture containing known normal alkanes. Figure 4 is a total ion chromatogram on n-alkanes utilized as a



hydrocarbon ruler, it indicates the three carbon ranges described in ASTM E1618. The light range is between butane and nonane with no major peaks after dodecane. The medium range is between octane and tridecane with the majority of the pattern between heptane and tetradecane. The heavy range is between nonane and eicosane or a higher n-alkane and must encompass at least five consecutive n-alkanes. It may be necessary to characterize an ignitable liquid as “light to medium” or “medium to heavy” for those ignitable liquid patterns not fitting neatly into one of the previous carbon ranges. Gasoline has a carbon range between butane and dodecane and therefore does not fall into any of the carbon ranges described earlier. The eight classes are gasoline, petroleum distillates, isoparaffinic products, aromatic, products, naphthenic-paraffinic products, n-alkane products, de-aromatized products, and oxygenated products. If an ignitable liquid can not be characterized into one of these classes it is classified as miscellaneous.<sup>19</sup>

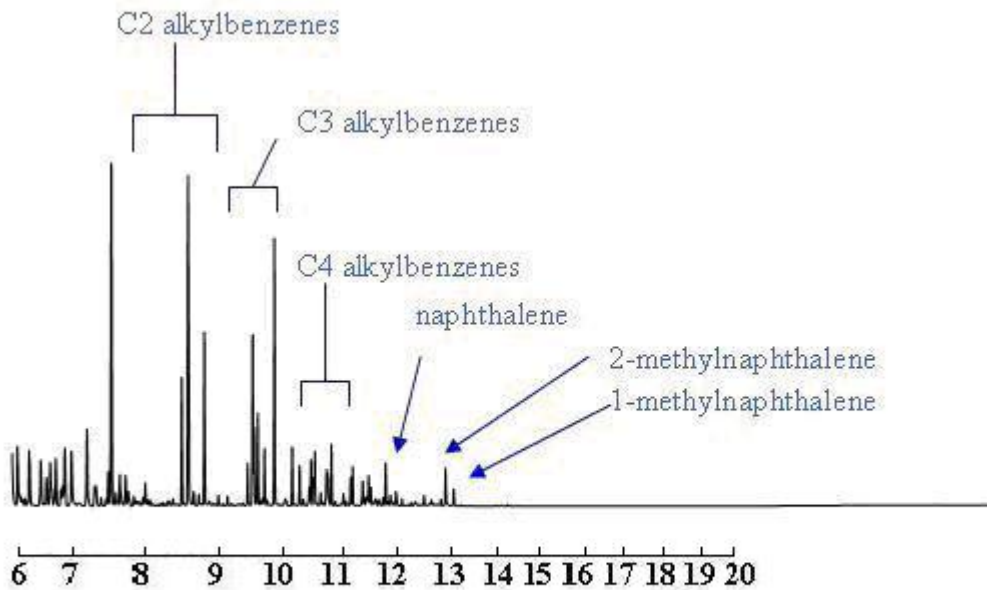


**Figure 4: Total Ion Chromatogram on n-Alkanes from n-Hexane to n-Eicosane**

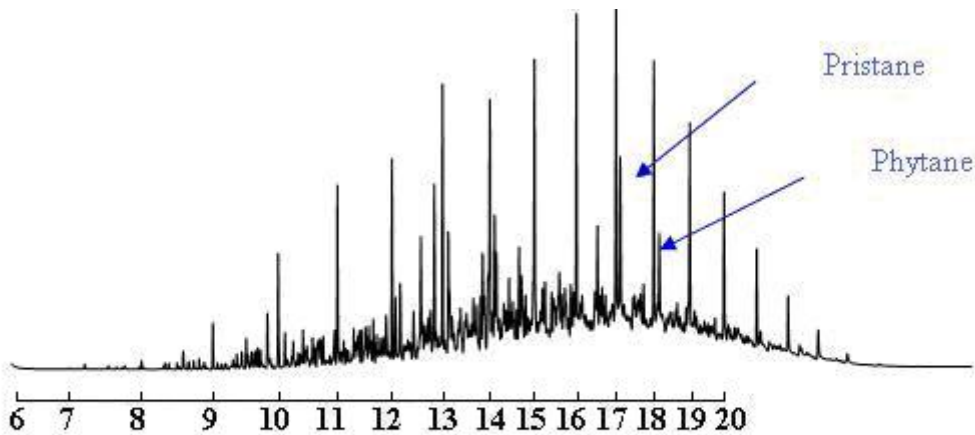
The characteristics and distinguishing features of the chromatographic patterns for each classification are described below along with examples.<sup>19, 20, 22, 23</sup>

A Gasoline chromatographic pattern is characterized by an abundance of aromatic compounds whose peaks cluster in specific patterns within a carbon range of C<sub>4</sub> to C<sub>13</sub> as demonstrated in Figure 5. Since the most prevalent species of compounds in gasoline are aromatics, the aromatic ion profile will be the most abundant. The chromatographic pattern will contain C<sub>2</sub>, C<sub>3</sub>, and C<sub>4</sub> alkyl benzenes in approximately the same relative concentrations of a known gasoline. Most gasoline contains naphthalene, 1- and 2- naphthalene, indan, and methyl indans.

A petroleum distillate chromatographic pattern has a Gaussian distribution of peaks with spiking n-alkanes and an unresolved baseline consisting of lower concentrations of aromatics, cycloalkanes and isoalkanes between the n-alkanes. Distillates in the heavy carbon range are characterized by the presence of pristane and phytane eluting after heptadecane and octadecane, respectively. For petroleum distillates the alkane ion profile is the most dominant as demonstrated in Figure 6.



**Figure 5: Total Ion Chromatogram of Gasoline**



**Figure 6: Total Ion Chromatogram of a Heavy Petroleum Distillate**

Isoparaffinic products are comprised almost exclusively of branched chain alkanes with minimal quantities of aromatics, normal alkanes or other species. The most abundant ion profile of isoparaffinic products are the alkanes with a similar but diminished ion profile of cycloalkanes

due to the fact that isoparaffins produce the same ions as alkanes and cycloalkanes. The chromatographic pattern is typically observed in the medium or heavy carbon range and is narrow (small carbon range) as demonstrated in Figure 7.

Aromatic products are comprised almost exclusively of aromatics and/or polynuclear aromatics. The chromatographic pattern of an aromatic product has a small carbon number range as demonstrated in Figure 8.

Naphthenic-paraffinic products are comprised mostly of branched alkanes and cycloalkanes with normal alkanes and aromatics not present or diminished. The alkane ion profile will be the most abundant of the ion profiles. The chromatographic pattern of a naphthenic – paraffinic product usually has a broad Gaussian distribution of peaks with an unresolved baseline as demonstrated in Figure 9. The chromatographic pattern is similar to that of a petroleum distillate minus the spiking n-alkanes.

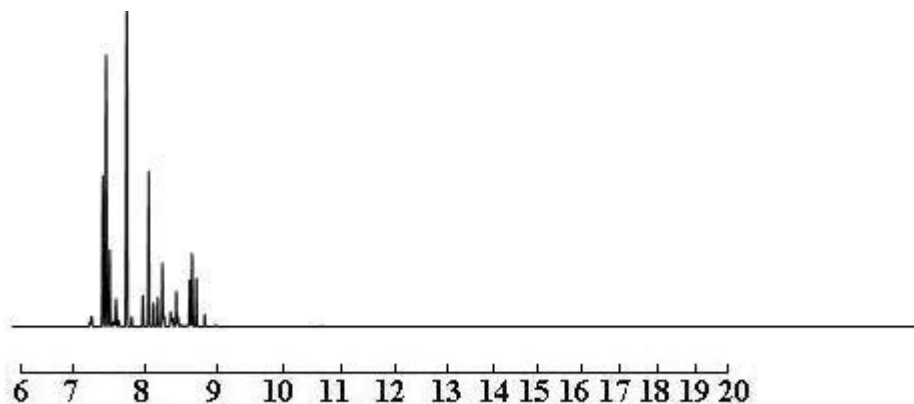
Normal alkanes are comprised almost exclusively of normal alkanes with no significant amounts of other species present. A typical chromatographic pattern is simple with only three to five peaks as demonstrated in Figure 10.

De-aromatized distillates are products characterized by the traditional petroleum distillate distribution with a notable absence of aromatic compounds as demonstrated in Figure 11.

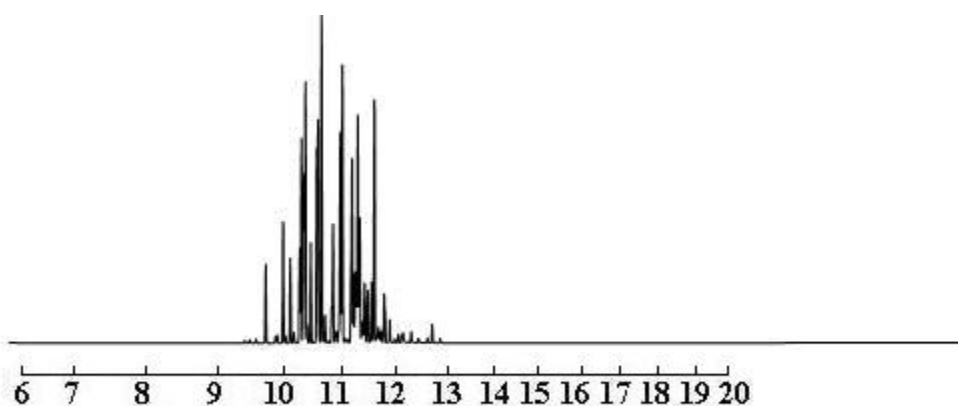
Alkanes are the most abundant ion profile. There is a notable reduction in the abundance of aromatics within the aromatic ion profile compared to the abundance of alkanes within the alkane ion profile for a de-aromatized distillate.

Oxygenated products contain a significant amount of an oxygenated product or products. ASTM E1618-01 suggests at least one order of magnitude above the other peaks within the chromatogram. Oxygenated products usually contain a small number of compounds which

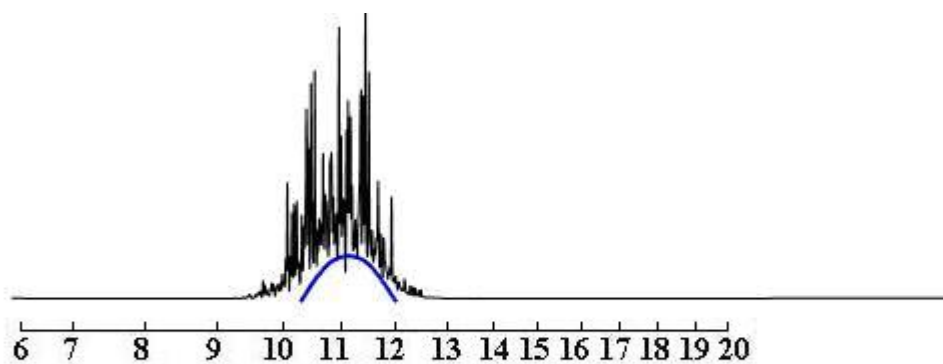
produce a chromatogram with no particular chromatographic pattern as demonstrated in Figure 12. Oxygenated compounds within the ignitable liquid must be identified with gas chromatography-mass spectrometry.



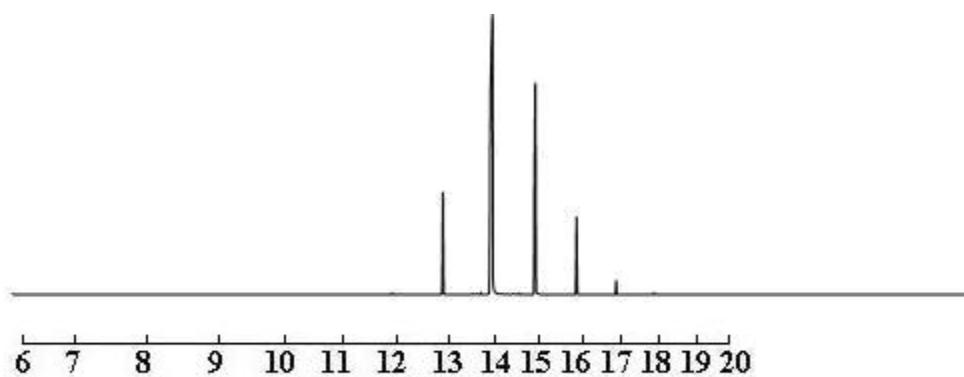
**Figure 7: Total Ion Chromatogram of an Isoparaffinic Product**



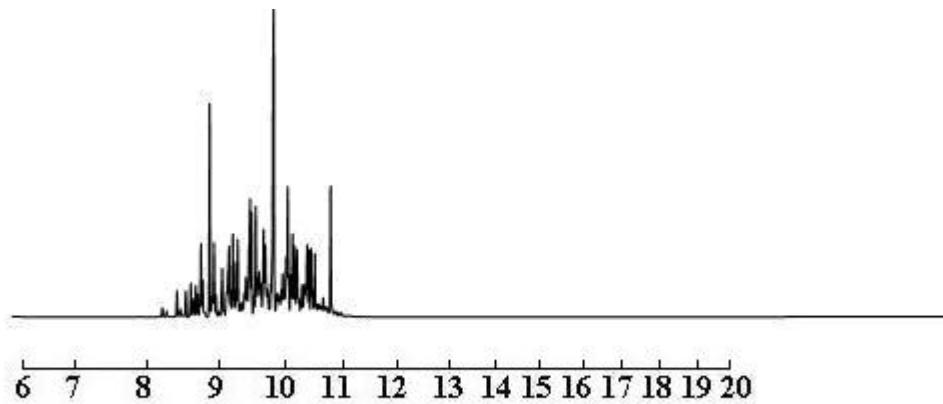
**Figure 8: Total Ion Chromatogram of an Aromatic Product**



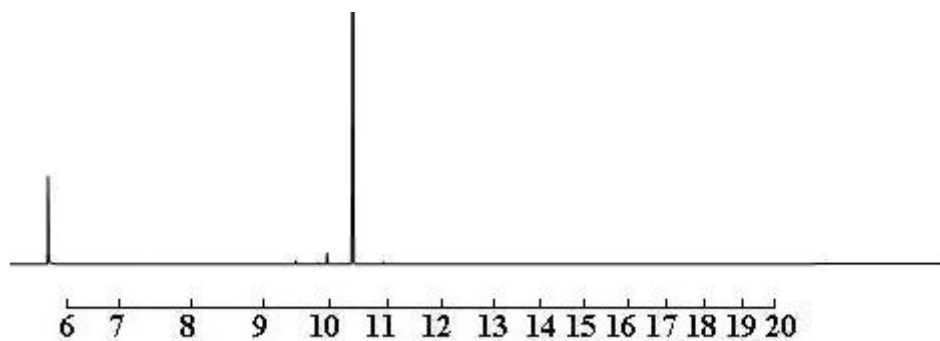
**Figure 9: Total Ion Chromatogram of a Naphthenic Paraffinic Product**



**Figure 10: Total Ion Chromatogram of a Normal Alkane Product**



**Figure 11: Total Ion Chromatogram of a De-aromatized Product**



**Figure 12: Total Ion Chromatogram of an Oxygenated Product**

The analysis of fire debris evidence encompasses four major aspects; collection of physical evidence at the point of origin, extraction of the ignitable liquid residue from the fire debris, detection of the ignitable liquid residue, and data interpretation to classify the ignitable liquid residue. Each aspect relies on the previous one to ultimately provide the fire investigator with useful information in determining the cause of the fire. There are challenges within each step of the process from preventing the loss of the physical evidence through evaporation, extracting a representative sample of the ignitable liquid from the fire debris, increasing the

selectivity and sensitivity of instrumentation, and providing a robust data analysis method for the identification of an ignitable liquid. The methods of collection, extraction, detection and interpretation of fire debris evidence within this chapter summarize the current practices and published methods utilized in fire debris evidence analysis. Advances on each aspect of fire debris analysis based on scientific principles forms the basis for this research.



## **CHAPTER THREE: EXTRACTION OF IGNITABLE LIQUIDS FROM FIRE DEBRIS BY PASSIVE HEADSPACE SAMPLING WITH ACTIVATED CARBON**

### *Introduction*

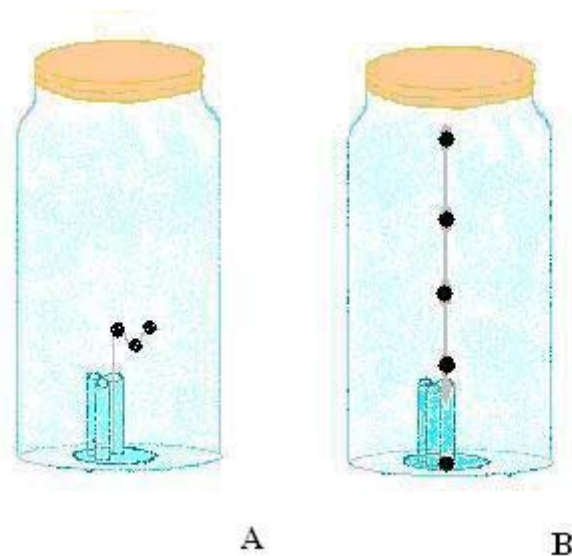
The American Society of Testing and Materials standard practice E 1412-00 covers the procedure for removing ignitable liquid residues from fire debris by adsorption onto activated carbon suspended in the static headspace above the sample then desorbing the residue from the adsorbent with a solvent. The extraction of ignitable liquid residues from fire debris by passive headspace sampling with activated carbon is the most commonly used method for separating ignitable liquids from fire debris.<sup>24</sup> The effects of adsorption time, temperature, carbon size, and sample concentration of common ignitable liquids using activated carbon have been published with a recommended analysis scheme. The study presented here follows the recommendations of the standard practice, but encompasses a more thorough investigation into the adsorption process. Hydrocarbon molecule interaction with the activated carbon was studied for the determination of the activated carbon surface area, substitution by other hydrocarbon molecules on to the activated carbon and the loss of hydrocarbon molecules from the activated carbon. An activated carbon size and ignitable liquid volume were demonstrated to affect the chromatographic profile of ignitable liquids due to saturation of the activated carbon. A modification of the extraction method incorporating a sub-sampling technique reduced the effects of saturation on the chromatographic profiles.

### *Methods and Materials*

Two hydrocarbon stock solutions were prepared with five hydrocarbons in an equimolar ratio (i.e. each hydrocarbon in the solution had a mole fraction of 0.20). Hydrocarbon **Solution 1** consists of heptane, toluene, octane, nonane and decane. Hydrocarbon **Solution 2** consists of heptane-d<sub>16</sub>, toluene-d<sub>8</sub>, octane, nonane, and decane-d<sub>22</sub>. All of the hydrocarbons as well as xylene were purchased from Aldrich Chemical Company and used without further purification. Carbon disulfide used in desorbing the hydrocarbons from the activated carbon and toluene were purchased from Fisher Scientific. Activated carbon strips were purchased from Albrayco then cut into pieces of various areas by utilizing a hole - punch or razor blade. A hydrocarbon liquid container was constructed from vial inserts super-glued together onto the underside of an evaporating dish. A metal rod with four male quick disconnects attached every 2.5 cm and an alligator clip was designed to hold the activated carbon above the hydrocarbon liquid container. The activated carbon pieces were attached to the quick disconnects with double sided tape. A second method perforated the activated carbon pieces onto a paperclip which stood upright inside an empty vial insert. The liquid containers and activated carbons were placed inside Ball<sup>®</sup> glass mason jars and fitted with a standard pressure-canning flat and band as shown in Figure 13.

All extractions of the hydrocarbons from the activated carbon were performed in accordance with ASTM E1412-00 Standard Practice for Separation of Ignitable Liquid Residues from Fire Debris Samples by Passive Headspace Concentration with Activated Charcoal. The glass jars containing the liquid containers with activated carbon were placed in a 66°C oven for approximately 16 to 24 hours, then removed and allowed to cool down to room temperature.

The activated carbon pieces were removed then placed into half dram vials with 1.0 ml of carbon disulfide.



**Figure 13: Experimental Setup**

Analysis of the hydrocarbons was performed on an Agilent 6890 gas chromatograph with a 5973 mass selective detector and a 7683 auto-sampler. Samples were chromatographed on a HP-1 methylsiloxane column 25m in length with an internal diameter of 0.2mm and a film thickness of 0.50  $\mu\text{m}$ . Sample volumes of 1.0  $\mu\text{l}$  were injected through a 250°C split/splitless injector with a 50:1 split ratio. The initial oven temperature was 50°C which was held for 3 minutes, then ramped at a rate of 10°C/min to a final temperature of 100°C and held for 2 minutes for experiments performed with the simple hydrocarbon solution. For experiments with gasoline, the initial oven temperature was 50°C which was held for 3 minutes, then ramped at a rate of 10°C/min to a final temperature of 280°C and held for 4 minutes. The mass spectrometer was tuned according to the manufacturer's specifications at a source temperature of 230°C. The spectra were collected over a scan range of 30-350 m/z units. Calibration curves were created to

quantify the hydrocarbons recovered from the activated carbon by an external standard method. Identification of the protonated species and deuterated species of both hydrocarbon solutions was accomplished by comparing retention times and spectra with standards.

The van der Waals calculations used to determine the surface area occupied by each hydrocarbon adsorbed onto the activated carbon was performed with Hyperchem 7 molecular modeling software.

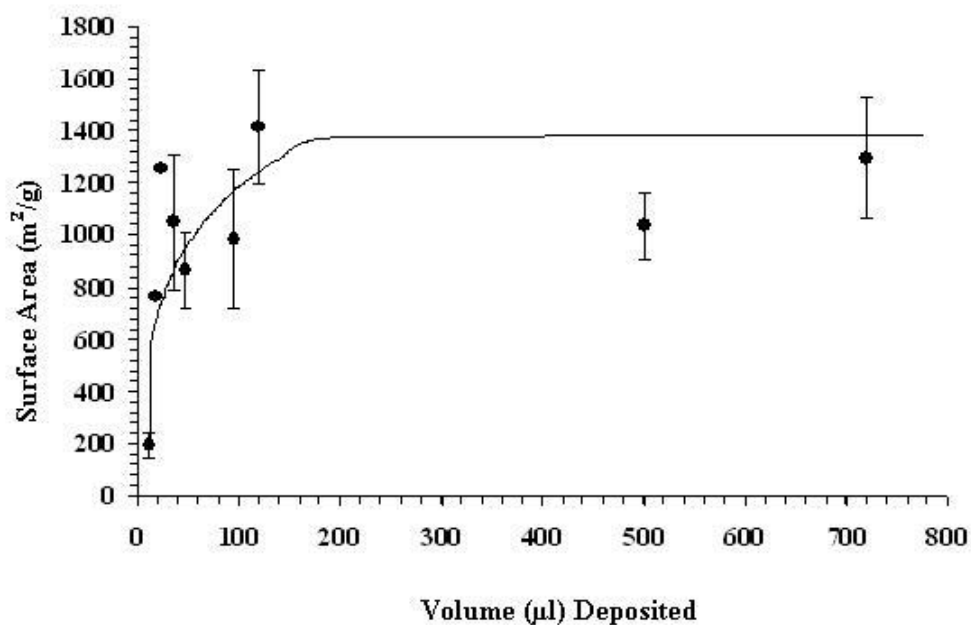
## *Results*

### *Hydrocarbon Molecule Interactions with Activated Carbon*

#### *Determination of Activated Carbon Surface Area*

Hydrocarbon **Solution 1** was deposited in volumes of 12 $\mu$ l, 18 $\mu$ l, 24 $\mu$ l, 36 $\mu$ l, 48 $\mu$ l, 96 $\mu$ l, 120 $\mu$ l, 500 $\mu$ l, and 720 $\mu$ l which correspond respectively to  $1.52 \times 10^{-5}$ ,  $2.28 \times 10^{-5}$ ,  $3.04 \times 10^{-5}$ ,  $4.56 \times 10^{-5}$ ,  $6.09 \times 10^{-5}$ ,  $1.22 \times 10^{-4}$ ,  $1.52 \times 10^{-4}$ ,  $6.34 \times 10^{-4}$ ,  $9.13 \times 10^{-4}$  moles of each hydrocarbon into vial insert(s) within each of nine glass jars. The geometric area of the activated carbon disks created with the hole punch was 33.2 mm<sup>2</sup>. The total number of hydrocarbon moles extracted from the activated carbon disks increased significantly from the lowest volume of 12 $\mu$ l up to 18 $\mu$ l, however further significant increases were not observed for the larger volumes of hydrocarbon liquid being deposited into the system. The distribution of hydrocarbon moles per gram for volumes from 24 $\mu$ l through 720 $\mu$ l varied even though the surface area of the activated carbon discs remained constant. The estimated surface area available for adsorption was based on the moles of each hydrocarbon recovered and one half of the van der Waals surface area for each hydrocarbon molecule. Only one side (i.e.  $\frac{1}{2}$  of the van der Waals surface area) of each hydrocarbon molecule was assumed to lie on the activated carbon surface in an extended

conformation. The total van der Waals surface areas calculated for heptane, toluene, octane, nonane, and decane were 173.26, 128.56, 194.00, 214.97, and 235.69 Å<sup>2</sup>/molecule respectively. An overall surface area average of 1128 ± 197 m<sup>2</sup>/g was determined by calculating the average surface areas for the 24µl through 720µl volumes of hydrocarbon molecules adsorbed onto the activated carbon. Surface area measurements by nitrogen adsorption for Sorbonorit B activated carbon of 1,100 – 1,200 m<sup>2</sup>/g are similar to those calculated from these experiments.<sup>25</sup> Figure 14 shows a plot of the surface area corresponding to the volumes of hydrocarbon liquid.



**Figure 14: Activated Carbon Surface Area Covered by Adsorbed Hydrocarbons as Calculated from the van der Waals Area of Each Hydrocarbon**

*Hydrocarbon Molecule Substitutions on Activated Carbon*

Three sets of three activated carbon disks with an area of 33.2 mm<sup>2</sup> were designated as sets A, B and C. Each set of disks was perforated onto a paperclip which was placed in a vial

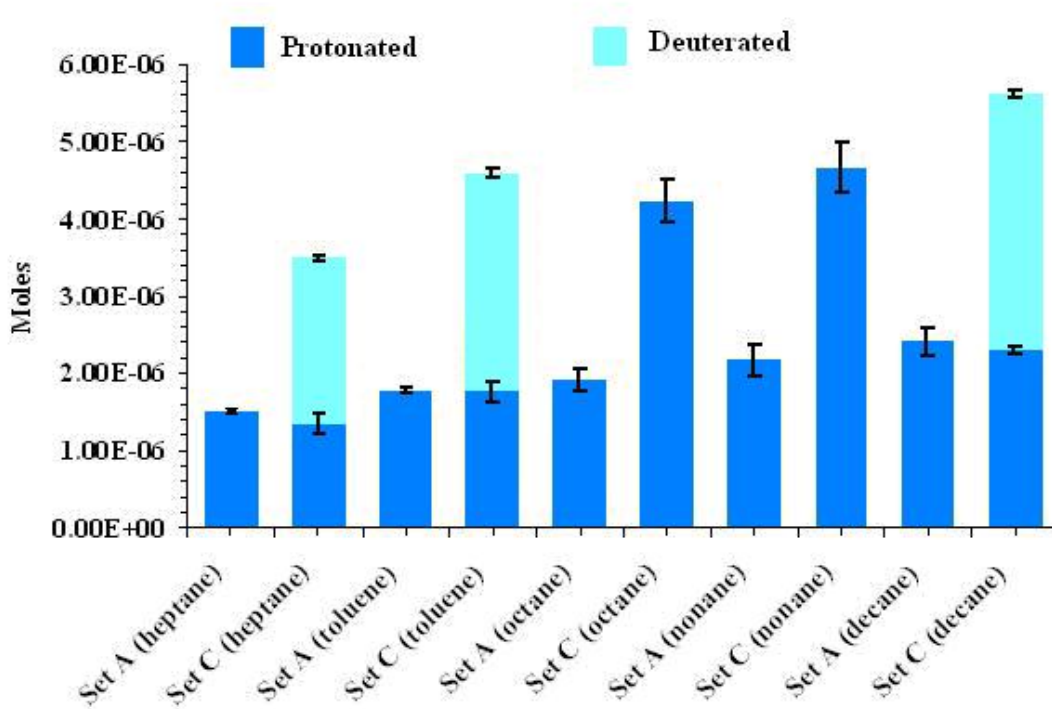
insert of a glass mason jar with 10  $\mu\text{l}$  of hydrocarbon **Solution 1** (heptane, toluene, octane, nonane and decane) as shown in Figure 13. The containers were placed in a 66°C oven for 16 hours. After the containers were removed from the oven and allowed to cool, set A was analyzed while sets B and C were each placed into a clean unused jar. Set B had an additional 10  $\mu\text{l}$  of hydrocarbon **Solution 1** (heptane, toluene, octane, nonane and decane) deposited into the new jar and set C had a 10  $\mu\text{l}$  of hydrocarbon **Solution 2** (heptane-d<sub>16</sub>, toluene-d<sub>8</sub>, octane, nonane, and decane-d<sub>22</sub>) deposited into its new jar. The jars were returned to the 66°C oven for an additional 16 hours. After the jars were removed from the oven and cooled to room temperature both sets of activated carbon disks were analyzed. This experiment was repeated with 18 $\mu\text{l}$  of hydrocarbon solutions rather than the 10  $\mu\text{l}$  of hydrocarbon solutions and the activated carbon disks were designated as sets D, E, and F. Set D corresponded to set A with only one exposure to hydrocarbon **Solution 1**, set E corresponded to set B with the double exposure to hydrocarbon **Solution 1**, and set F corresponded to set C with the first exposure to hydrocarbon **Solution 1** and the second exposure to hydrocarbon **Solution 2**. Table 3 summarizes the experimental conditions for each container.

**Table 3: Summary of Experimental Conditions for each Container**

10 $\mu\text{l}$ aliquot samples	18 $\mu\text{l}$ aliquot samples	Solution	Heating
A	D	Solution 1	Once
B	E	Solution 1 twice	Twice
C	F	Solution 1 then Solution 2	Twice

The hydrocarbons extracted from the activated carbon disks in set A had an average number of  $9.71 \times 10^{-6}$  moles. The hydrocarbons extracted from the disks in set C which were exposed twice to 10  $\mu\text{l}$  of hydrocarbon **Solution 1** had an average number of  $1.82 \times 10^{-5}$  moles.

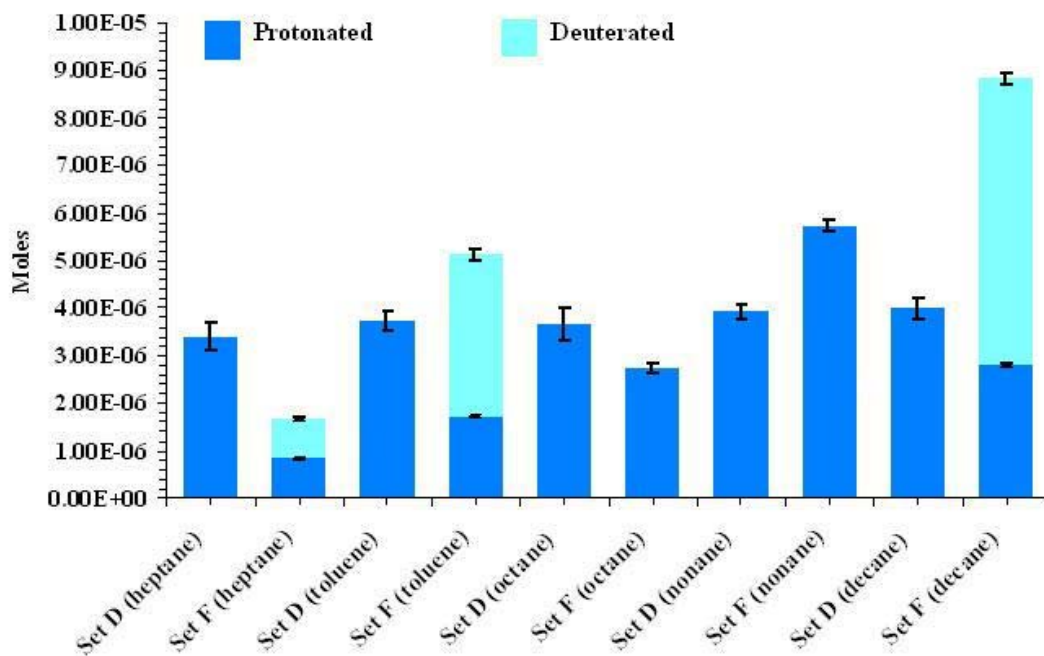
The total number of moles of hydrocarbons extracted from the activated carbons doubled upon the second exposure to the hydrocarbon solution as shown in Figure 15. The number of protonated heptane, toluene, and decane moles from set A were the same as those from set C with only the addition of heptane-d<sub>16</sub>, toluene-d<sub>8</sub>, octane, nonane, and decane-d<sub>22</sub> after the second exposure. The experiment demonstrates additional adsorption and no desorptive loss of hydrocarbons at sub-monolayer coverage on activated carbon of this geometric area and hydrocarbon liquids of this composition and volume.



**Figure 15: Additional Adsorption of Hydrocarbon Molecules onto Activated Carbon**

The hydrocarbons extracted from the activated carbon disks of set D had an average number of  $1.87 \times 10^{-5}$  moles. The hydrocarbons extracted from the disks of set F which was exposed twice to 18  $\mu$ l of hydrocarbon solution had an average number of  $2.12 \times 10^{-5}$  moles.

The total number of moles of hydrocarbons extracted from the activated carbons did not increase significantly upon the second exposure to the hydrocarbon solution as shown in Figure 16. The average number of moles of hydrocarbons extracted after one exposure of 18  $\mu\text{l}$  is almost double the average number of moles of hydrocarbons extracted after one exposure of 10  $\mu\text{l}$ . There was a loss of heptane, toluene, octane and decane which were initially adsorbed onto the activated carbon (set D), but after the addition of more hydrocarbon solution the number of moles of each hydrocarbon decreased (set F). The experiment demonstrates desorptive loss as well as a change in the relative number of the protonated hydrocarbon moles upon the second exposure of 18  $\mu\text{l}$  of hydrocarbon solution.



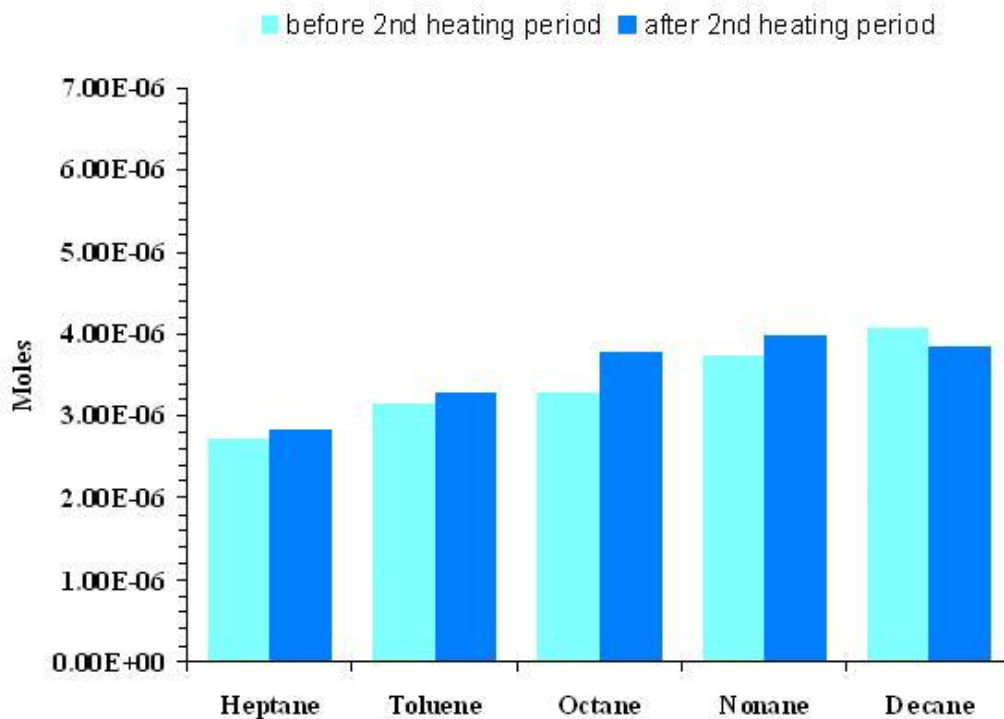
**Figure 16: Displacement and Loss of Hydrocarbon Molecules Previously Adsorbed onto Activated Carbon**



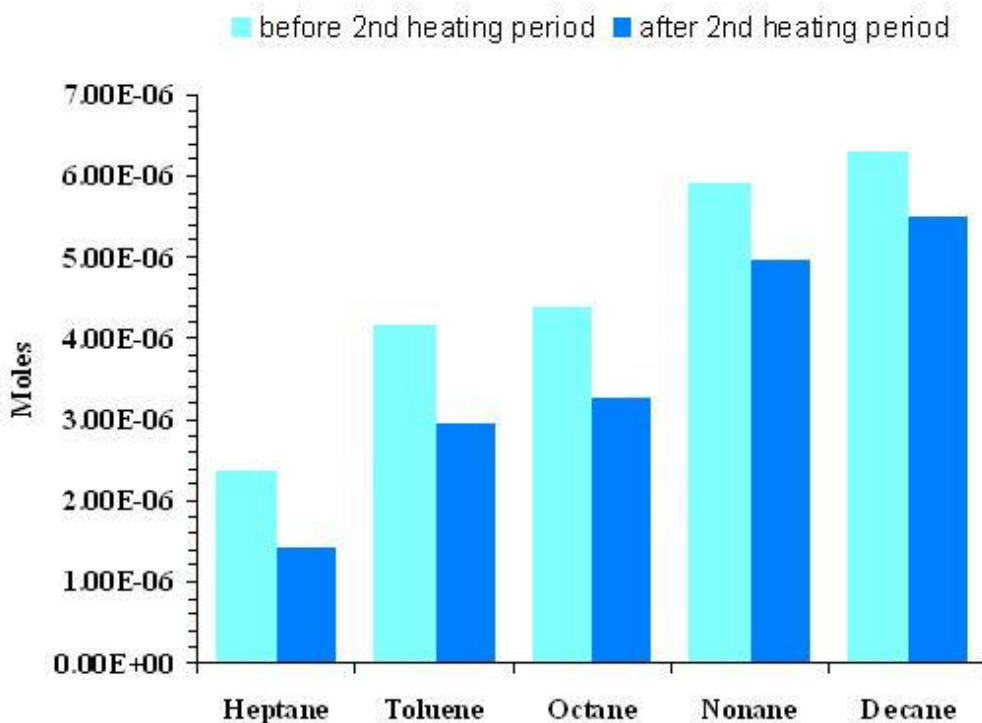
### *Hydrocarbon Loss from Activated Carbon*

The following experiments were performed to further demonstrate and explain the cause of hydrocarbon loss from activated carbon. Two sets of three activated carbon disks with geometric areas of  $33.2 \text{ mm}^2$  were perforated onto paperclips, one set was placed into a glass jar with  $10 \text{ }\mu\text{l}$  of hydrocarbon **Solution 1** (set G) and the other set was placed into a glass jar with  $18 \text{ }\mu\text{l}$  of hydrocarbon **Solution 1** (set H). The containers were placed in a  $66^\circ\text{C}$  oven for 16 hours. After the jars were removed from the oven and cooled to room temperature, one disk from each set was removed from the paperclip and analyzed. The two paperclips holding the remaining carbon disks from each set were placed into clean unused empty jars and returned to the oven for another period of heating. After the jars were removed from the oven and cooled to room temperature the remaining activated carbon disks were analyzed. The moles of adsorbed hydrocarbons extracted from the activated carbon disks of set G indicate there was no loss of the adsorbed hydrocarbons from the activated carbon as seen in Figure 17. The mole fractions of the recovered hydrocarbons before and after the second heating period are approximately 0.20, the mole fractions of the hydrocarbons in the hydrocarbon solution deposited into the system. However, the moles of adsorbed hydrocarbons from set H do indicate there was a loss of hydrocarbons from the activated carbon after the second heating period as seen in Figure 18. The sets of activated carbon disks from set H (before and after second heating period) exhibit a deviation in mole fraction from the hydrocarbon solution deposited into the system. The mole fraction of heptane decreases to approximately 0.10 and decane increases to approximately 0.30 with a small increase for nonane and small decreases for both toluene and octane. The results demonstrate no loss of adsorbed hydrocarbon molecules from the activated carbon and no change in the mole fraction of the hydrocarbons from that of the original hydrocarbon solution

when low volumes (i.e. 10  $\mu\text{l}$ ) were deposited into the system. Whereas both loss of the hydrocarbon molecules from the activated carbon and differences in mole fractions from the original hydrocarbon solution were observed when higher volumes (i.e. 18  $\mu\text{l}$ ) were deposited into the system.



**Figure 17: Adsorbed Hydrocarbon Molecules Remaining on Activated Carbon after a Second Heating Period**



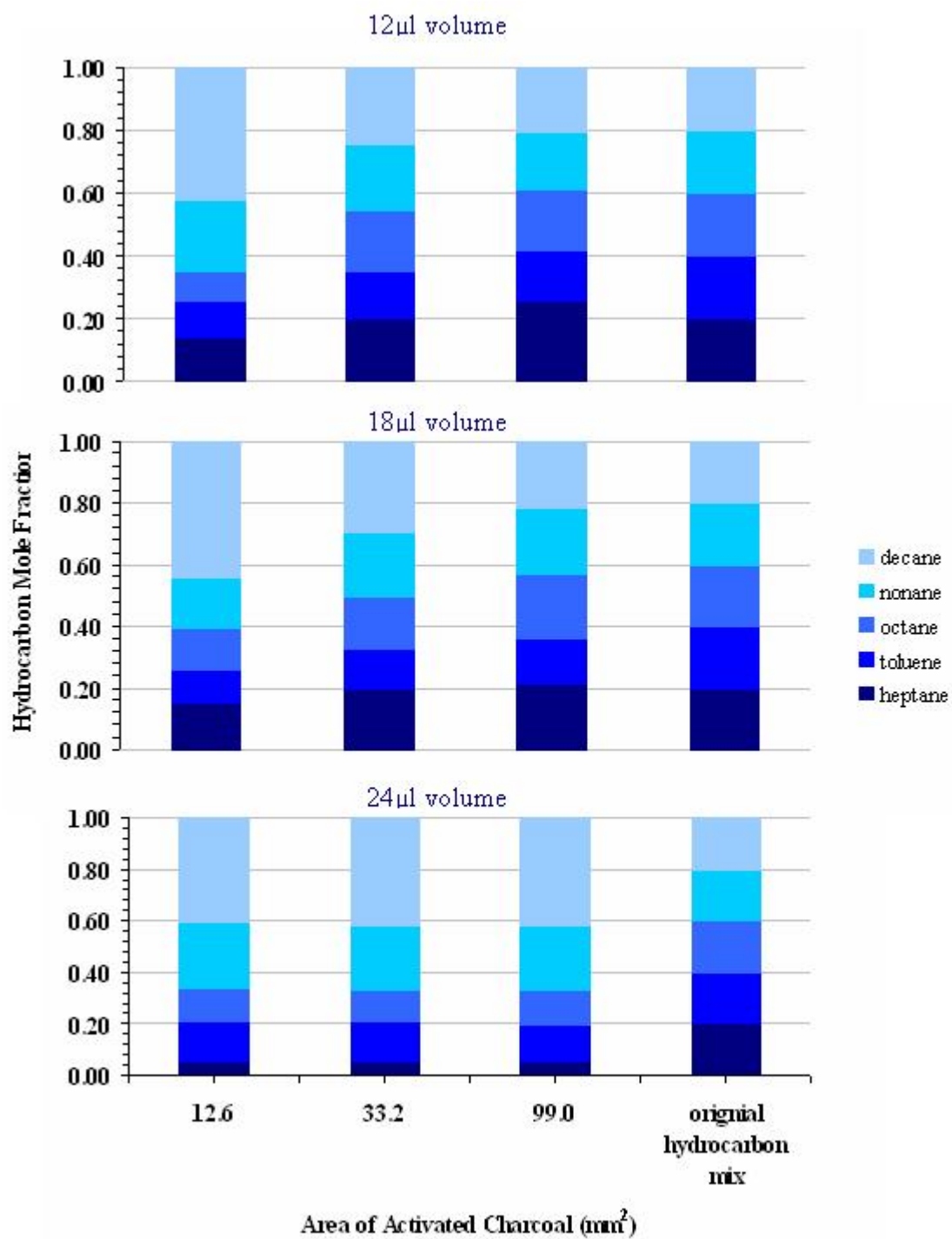
**Figure 18: Hydrocarbon Molecule Loss from Activated Carbon after a Second Heating Period**

*Effects of Adsorbent Size and Liquid Volume on Hydrocarbon Recovery*

*Effect of activated carbon size*

The physical size of the activated carbon piece has been addressed in the ASTM E1412-00 Standard Practice for Separation of Ignitable Liquid Residues from Fire Debris Samples by Passive Headspace Concentration with Activated Charcoal.<sup>9</sup> and by Newman, Dietz, and Lothridge, therefore three activated carbons with varying geometric areas (physical sizes) were used in these experiments.<sup>26</sup> The surface area of the activated carbon significantly impacts the distribution of hydrocarbon mole fraction recovered and thus the chromatographic profile. Three

activated carbon pieces with geometric areas of 12.6 mm<sup>2</sup>, 33.2 mm<sup>2</sup>, and 99.0 mm<sup>2</sup> weighing 0.006 g, .020 g, and 0.060 g respectively have surface areas of 6.8 m<sup>2</sup>, 22.6 m<sup>2</sup>, and 68.8 m<sup>2</sup>. The surface areas were calculated based on the previously determined average surface area of 1128 m<sup>2</sup>/g. Volumes of 12 μl, 18 μl, and 24 μl of hydrocarbon **Solution 1** were deposited into quart glass jars each containing an individual activated carbon piece for a total of nine jars (3 volumes x 3 activated carbon sizes). At the lowest volume, a significant deviation was observed between the hydrocarbon mole fractions of the deposited liquid and the hydrocarbon mole fractions recovered from the 12.6 mm<sup>2</sup> activated carbon. This effect was not observed for the 33.2 mm<sup>2</sup>, 99.0 mm<sup>2</sup> carbons. At a volume of 18μl, a significant deviation from the 0.20 mole fraction of each hydrocarbon of the deposited liquid was observed for both the 12.6 mm<sup>2</sup> and 33.2 mm<sup>2</sup> activated carbons, but not the 99.0 mm<sup>2</sup> carbon. At a volume of 24μl significant deviations from the 0.20 mole fractions of each hydrocarbon of the deposited liquid was observed for all of the carbons. The distributions of the hydrocarbon mole fractions recovered from all three activated carbons were the same as shown in Figure 19.



**Figure 19: Distribution of Mole Fractions of Hydrocarbons Adsorbed on Various Sizes of Activated Carbon**

### *Effects of hydrocarbon liquid volume*

The mole fraction of the adsorbed hydrocarbons extracted from the activated carbon at the 7.5 cm depth was compared to the mole fractions of the hydrocarbons in the original equal molar solution (Solution 1). After the glass jars containing volumes of 12  $\mu\text{l}$ , 36  $\mu\text{l}$ , 48  $\mu\text{l}$ , 96  $\mu\text{l}$ , 120  $\mu\text{l}$ , 500  $\mu\text{l}$ , and 720  $\mu\text{l}$  were removed from the oven and cooled to room temperature residual hydrocarbon solution was observed in the vial inserts in which the solution was deposited for volumes of 120  $\mu\text{l}$ , 500  $\mu\text{l}$ , and 720  $\mu\text{l}$  hydrocarbon solution whereas the vial inserts of hydrocarbon solution volumes 12  $\mu\text{l}$ , 36  $\mu\text{l}$ , 48  $\mu\text{l}$ , and 96  $\mu\text{l}$  were empty of hydrocarbon solution. The liquid volumes recovered from the jars with volumes of 120  $\mu\text{l}$ , 500  $\mu\text{l}$ , and 720  $\mu\text{l}$  hydrocarbon solutions with their respective mole fractions are given in Table 4.

**Table 4: Hydrocarbon Mole Fractions from Recovered Liquid**

Hydrocarbon Mole Fractions from Recovered Liquid					
Volume Deposited ( $\mu\text{l}$ )	Heptane	Toluene	Octane	Nonane	Decane
120	0.01	0.01	0.02	0.19	0.77
500	0.04	0.02	0.1	0.26	0.58
720	0.05	0.03	0.11	0.27	0.54

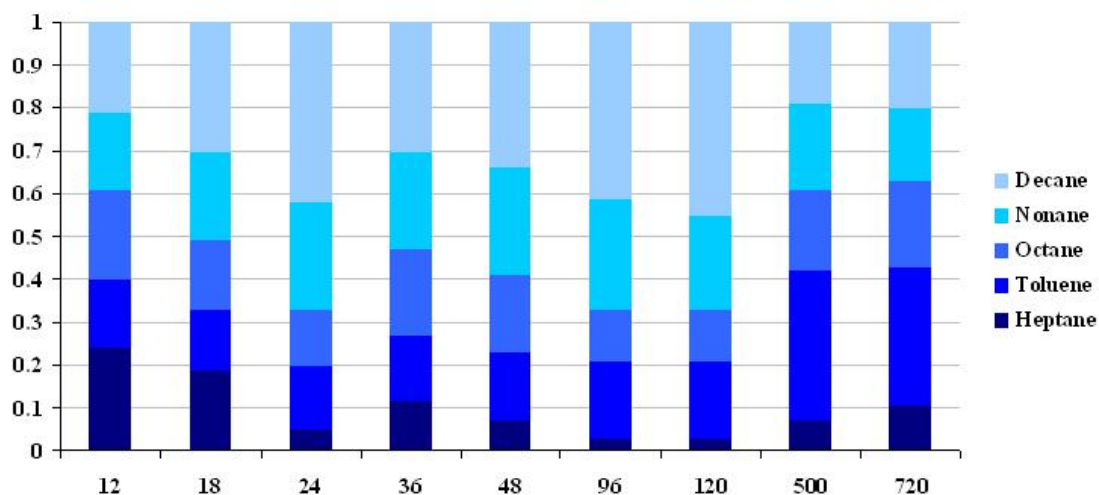
The recovery of significant amounts of hydrocarbon liquid from the inserts reveals that not all of the hydrocarbon solution went into the vapor phase of the quart size containers at oven temperatures of 66°C for durations of approximately 20 hours. Mole fractions of each hydrocarbon in the vapor phase were calculated for all of the hydrocarbon solution volumes, the results are given in Table 5. The mole fractions of the adsorbed hydrocarbons extracted from the activated carbons at each volume of hydrocarbon solution are shown in Figure 20 demonstrating the variation in distribution of the mole fractions for the various volumes of hydrocarbon solution deposited into the systems. At the lowest volume of 12  $\mu\text{l}$ , all the mole fractions of

hydrocarbons recovered from the activated carbons were similar to those of the original hydrocarbon solution. However, as the volume of hydrocarbon solution increased from 24  $\mu\text{l}$  to 120  $\mu\text{l}$  a higher mole fraction of decane and a lower mole fraction of heptane were recovered from the activated carbon with the most extreme augmentation occurring at the 96  $\mu\text{l}$  and 120  $\mu\text{l}$  volumes. For the volumes of hydrocarbon solution greater than 120  $\mu\text{l}$ , the mole fractions of the hydrocarbons recovered from the activated carbon appear to return to amounts approximating those of the original hydrocarbon solution which coincides with the emergence of residual liquid in the vial inserts. The exceptions are toluene and heptane which were comprised of mole fractions of 0.32 and 0.11 respectively for volumes 96  $\mu\text{l}$  and 120  $\mu\text{l}$ .

**Table 5: Hydrocarbon Mole Fraction of Vapor Phase**

<b>Hydrocarbon Mole Fractions of Vapor Phase</b>					
<b>Volume Deposited (<math>\mu\text{l}</math>)</b>	<b>Heptane</b>	<b>Toluene</b>	<b>Octane</b>	<b>Nonane</b>	<b>Decane</b>
12	0.20	0.20	0.20	0.20	0.20
36	0.20	0.20	0.20	0.20	0.20
48	0.20	0.20	0.20	0.20	0.20
96	0.20	0.20	0.20	0.20	0.20
120 *	0.22	0.22	0.22	0.20	0.13
500 *	0.26	0.27	0.24	0.18	0.06
720 *	0.28	0.30	0.25	0.16	0.01

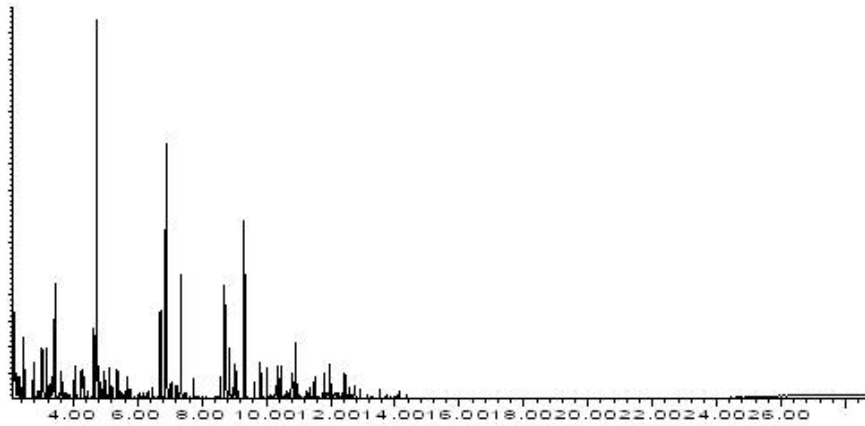
\* calculated from recovered liquid composition



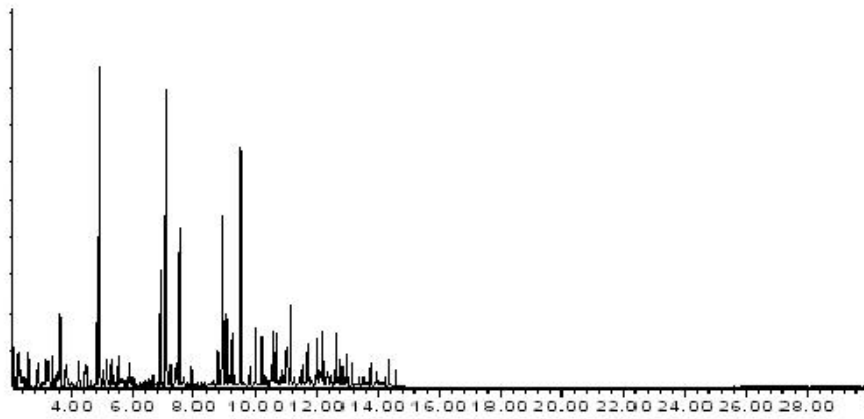
**Figure 20: Mole Fraction Distribution of Hydrocarbons Recovered from Activated Carbon**  
*Modifications to the Extraction Method*

The first experiment presented here was conducted to determine the effect of activated carbon saturation on the chromatographic profile of gasoline. Two volumes of un-weathered (un-evaporated) gasoline, 12 $\mu$ l and 96 $\mu$ l were deposited into quart glass jars with 33.2 mm<sup>2</sup> activated carbon disks then extracted following the ASTM E 1412-00 standard testing method. Two diluted neat solutions of the same gasoline were analyzed, one un-weathered and the other 75% weathered (by volume). The chromatographic profile of the recovered hydrocarbons from the 12 $\mu$ l gasoline sample shown in Figure 21 resembles the chromatographic profile of the same un-weathered gasoline in Figure 22. The chromatographic profile of the recovered hydrocarbons from the 96 $\mu$ l gasoline sample shown in Figure 24 resembles the chromatographic profile of the 75% weathered gasoline in Figure 25.

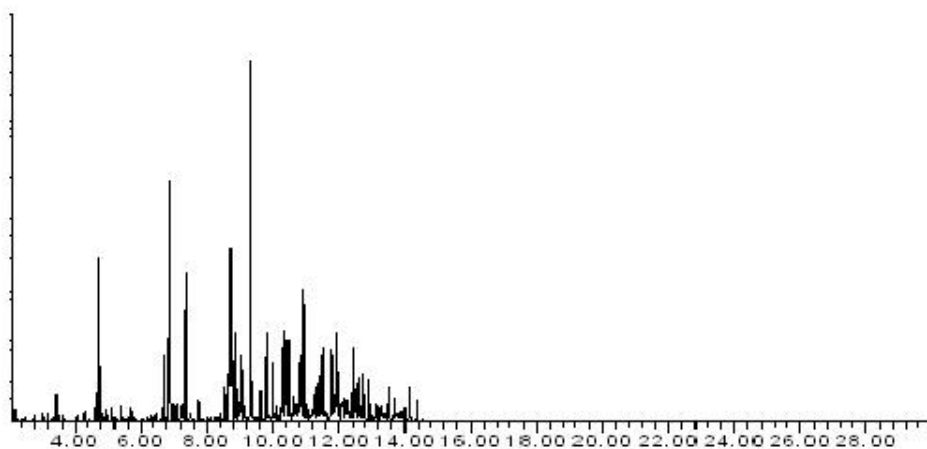




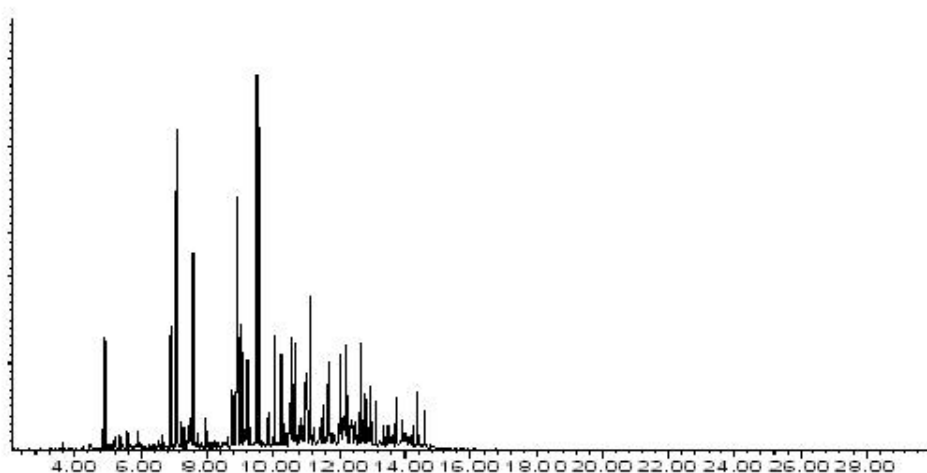
**Figure 21: Chromatogram of 12µl of Gasoline after Extraction from Activated Carbon**



**Figure 22: Chromatogram of 0% Weathered Gasoline**



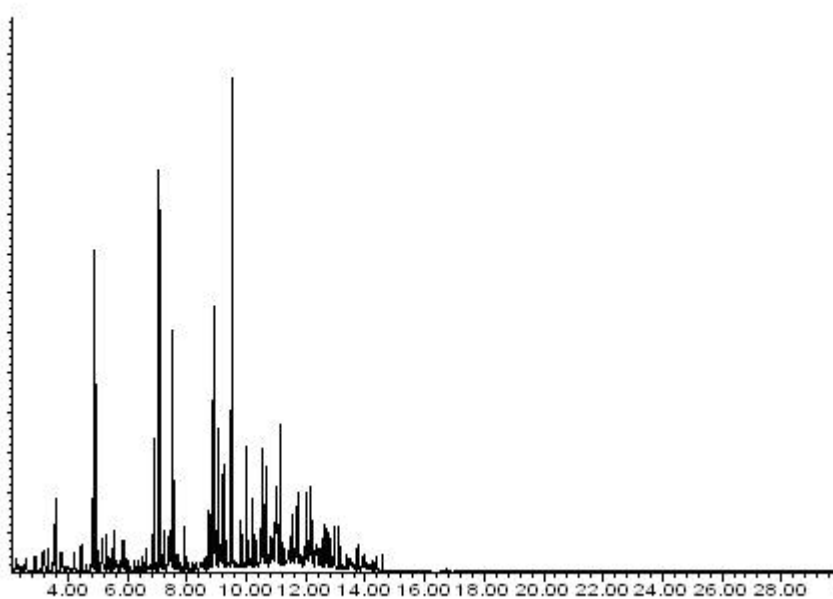
**Figure 23: Chromatogram of 96µl of Gasoline after Extraction from Activated Carbon**



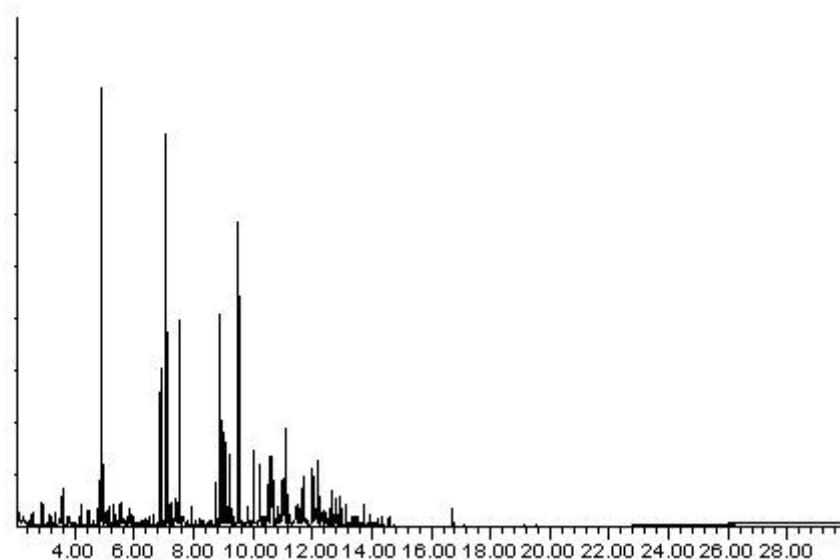
**Figure 24: Chromatogram of 75% Weathered Gasoline**

The second experiment alters the standard extraction method to avoid the saturation of the activated carbon and thus reducing distortion of the chromatographic profile. Two pieces of carpet with carpet padding were cut into 3.8 cm X 7.6 cm pieces then placed inside glass jars designated A and B. In the center of each piece of carpet 96 µl of un-weathered gasoline was deposited with jar A containing a 99.0 mm<sup>2</sup> piece of activated carbon. Both jars were sealed and placed in a 66°C oven for 16 hours. The carbon strip from jar A was eluted with carbon disulfide

and analyzed resulting in the chromatogram shown in Figure 25. The purpose of heating jar B was to obtain homogenous and representative sub-samples. After cooling jar B, two 1.9 cm X 1.9 cm sections of the carpet/padding sample were removed from the outer edge of the sample away from the site of gasoline deposition. The remainder of the extraction proceeded according to the ASTM E 1412-00 standard testing method. The chromatographic profiles of the two sub-samples from jar B in Figure 26 were similar to one another however they differed significantly from the chromatographic profile of jar A.



**Figure 25: Chromatogram of Hydrocarbons Recovered from 96  $\mu$ l of 0% Weathered Gasoline Deposited onto Carpet**



**Figure 26: Chromatogram of Hydrocarbons Recovered from a Sub-sample of Carpet Spiked with 96  $\mu$ l of 0% Weathered Gasoline**

*Discussion*

The number of moles of hydrocarbon adsorbed per gram of activated carbon for a geometric area of 33.2 mm<sup>2</sup> increased significantly as the volume of hydrocarbon liquid deposited into the system increased from 12  $\mu$ l to 24  $\mu$ l. The moles adsorbed per gram of activated carbon for hydrocarbon liquid volumes greater than 24  $\mu$ l remained reasonably constant even though the volumes increased substantially. The physical adsorption of the hydrocarbon molecules onto the activated carbon is due to the van der Waals interactions between the surface and the adsorbed molecules.<sup>27</sup> At equilibrium, the rate of hydrocarbons being adsorbed and the rate of hydrocarbons being desorbed are equal; therefore the relative concentration of each hydrocarbon extracted from the activated carbon is dictated by the concentrations of each hydrocarbon in the vapor phase. The relatively constant number of adsorbed moles per gram for volumes of 24  $\mu$ l to 720  $\mu$ l indicates that all of the adsorption sites

of the activated carbon have been filled. An estimate of the activated carbon surface area available for adsorption was calculated utilizing the data collected from the activated carbon disks exposed to liquid volumes greater than 24  $\mu\text{l}$ . A surface area of  $1128 \pm 197 \text{ m}^2/\text{g}$  was based on the number of moles of each hydrocarbon in **Solution 1** adsorbed onto the activated carbon with the assumption that each hydrocarbon molecule was in an extended conformation and only one side of the molecule was exposed to the surface. The calculated value agrees with surface areas of 1,100 – 1,200  $\text{m}^2/\text{g}$  determined by nitrogen adsorption on other activated carbons. The adsorption capacity of an activated carbon disk with a 33.2  $\text{mm}^2$  geometrical area weighing 0.020 g, which corresponds to a surface area of 22.6  $\text{m}^2$ , is reached when 24  $\mu\text{l}$  of vaporized hydrocarbon liquid resides in a headspace volume of approximately one quart.

The adsorptive and desorptive interactions between hydrocarbon molecules and activated carbon were demonstrated at volumes of 10  $\mu\text{l}$  and 18  $\mu\text{l}$  of hydrocarbon liquid and activated carbon disks with surface areas of 22.6  $\text{m}^2$  (33.2  $\text{mm}^2$  geometric area). Activated carbon disks of this geometric area have adsorption sites still available when exposed to low volumes (i.e. 10 $\mu\text{l}$ ) of hydrocarbon liquid within quart volume containers. This was demonstrated when the average moles of adsorbed hydrocarbons doubled after the set of activated carbon disks were exposed to an additional 10  $\mu\text{l}$  of hydrocarbon solution. The number of hydrocarbon moles adsorbed at sub-monolayer coverage remained relatively constant with no desorptive losses after subsequent addition of another 10  $\mu\text{l}$  of hydrocarbon liquid. Under similar conditions, the hydrocarbon molecules were retained on the activated carbon disks after a second heating period in the absence of additional hydrocarbons. Activated carbon disks with surface areas of 22.6  $\text{m}^2$  (33.2  $\text{mm}^2$  geometric area) exposed to higher volumes (i.e. greater than 18 $\mu\text{l}$ ) of hydrocarbon liquid within quart volume containers became saturated. This was demonstrated when the average

moles of adsorbed hydrocarbons did not increase significantly after the set of activated carbon disks were exposed to an additional 18  $\mu\text{l}$  of hydrocarbon liquid. Under similar conditions adsorbed hydrocarbon molecules in excess of the monolayer were not retained onto the activated carbon after a second heating period. Desorptive losses of the hydrocarbon molecules were observed and the relative molar distribution of the hydrocarbons departed from the equimolar concentrations of the original solution. The results can be explained by the hydrocarbon molecules first filling the available adsorption sites of the activated carbon forming a monolayer with additional adsorption into successive layers. Heating leads to a loss of all hydrocarbons not adsorbed within the monolayer. Subsequent addition of hydrocarbon molecules leads to desorptive displacement of less strongly adsorbed hydrocarbon molecules by more strongly adsorbing molecules which have stronger dispersion interactions with activated carbon. The adsorption of each hydrocarbon is dependent on the concentration of the hydrocarbon in the vapor phase and the number of available adsorption sites on the activated carbon.

The variation in hydrocarbon molar distribution upon saturation of the activated carbon surface area is reflected as a distortion in the chromatographic profile. The size of the activated carbon and consequently the available surface area is an important factor in the adsorption of hydrocarbons onto activated carbon in any efforts to avoid distortion of the chromatographic profile. Smaller geometrical sizes (weights) have less surface area, thus fewer adsorption sites onto which the hydrocarbon molecules can adsorb leading to activated carbon saturation. Larger geometrical sizes (weights) have the capacity to adsorb hydrocarbon molecules of the same concentration without hydrocarbon loss and displacement thus chromatographic distortions are not observed. ASTM E 1412-00, a standard test method for the extraction of ignitable liquid residues from fire debris recommends using activated carbons with a 100  $\text{mm}^2$  geometrical area.

The experiments reported here have shown activated carbon of a 99.0 mm<sup>2</sup> geometrical area can be saturated with a hydrocarbon liquid volume 24 μl which is evident in the deviation from the equimolar distribution of the liquid deposited into the container. Notice the molar distribution of the hydrocarbons recovered from all three activated carbons where 24 μl of hydrocarbon solution was deposited into the container, see Figure 19.

The effect of chromatographic distortion when decreasing the geometric area of the activated carbon has been demonstrated. Another factor which causes distortion and thus affects the chromatographic profile is the volume of liquid deposited into the container. If the surface area remains constant, but the concentration of hydrocarbon molecules in the vapor phase increases, the activated carbon eventually achieves its absorption capacity. Displacement of the lower molecular weight hydrocarbons by the higher molecular weight hydrocarbons reached a maximum at 96 μl of hydrocarbon solution deposition. Figures 19 and 20 indicate that the mole fractions of toluene at various activated carbon geometric areas and hydrocarbon liquid volumes remains moderately constant compared to the other hydrocarbons. Toluene and other aromatics are known to retain on activated carbon more effectively than aliphatic hydrocarbons.<sup>28</sup> The extent of the molar distribution distortion of adsorbed hydrocarbons is controlled by the vapor phase concentration of the hydrocarbons and the strength of the hydrocarbon interactions with the activated carbon surface upon physical adsorption as described by Polanyi's theory of adsorption.<sup>29, 30, 31</sup> The hydrocarbon molecules are adsorbed onto the activated carbon by van der Waals intermolecular forces primarily through London dispersion forces. The strength of the dispersion interactions is proportional to the square of the molecular polarizability,  $\alpha^2$ . The molecular polarizability has been used in several quantitative structure activity relationships for the prediction of hydrocarbon adsorption properties on activated carbon.<sup>32, 33, 34</sup> The

experimental data of hydrocarbons recovered from the 99.0 mm<sup>2</sup> activated carbon in which 24 μl of equimolar hydrocarbon solution was deposited into the quart container presents conditions where the activated carbon is saturated while the entire 24 μl is in the vapor phase at equimolar concentrations. Under these conditions the adsorbed mole fraction of each hydrocarbon becomes a linear function of the square of the polarizability as shown in Figure 27 where  $n = 9$  and  $r = 0.998$ .

The 96 μl volume of hydrocarbon solution deposited into the jar was the largest volume in which a liquid phase was not observed within the vial inserts at 66°C. An estimation of the vapor pressure of each hydrocarbon component at 66°C based on their heats of vaporization and the Clausius –Clapeyron equation predicts vapor pressures at the elevated temperature that would allow complete vaporization of all the hydrocarbons at each volume.

$$p = p^* \exp \left\{ \frac{\Delta H_{vap,m}}{R} \left( \frac{1}{T} - \frac{1}{T^*} \right) \right\}$$

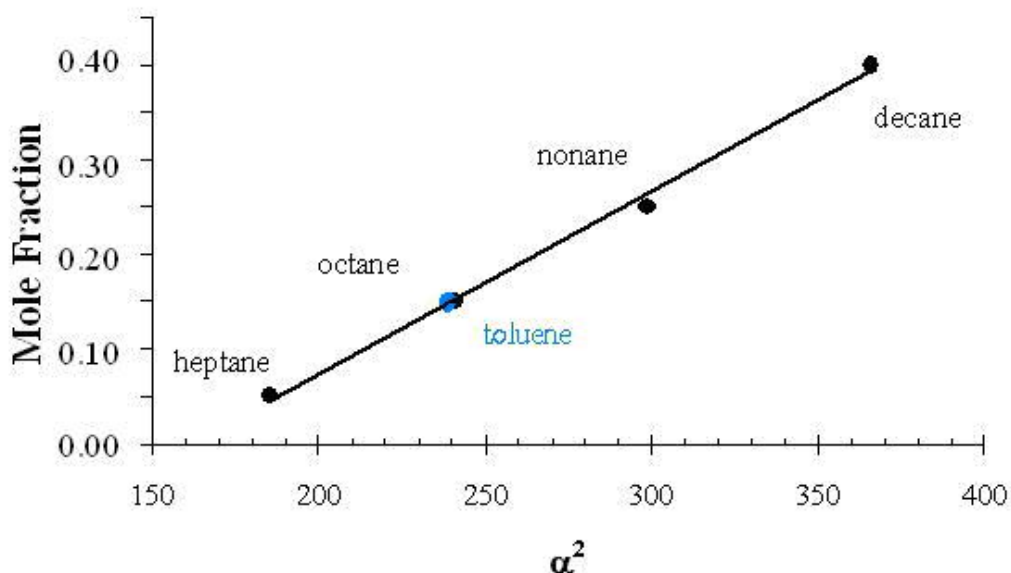
Where  $p^*$  is the vapor pressure at some temperature  $T^*$

(1)

The exception is the 720 μl volume where a trace amount of decane would still remain in the liquid phase. In these experiments, hydrocarbon liquid solution was recovered from the inserts of the 120 μl, 500 μl and 720 μl volumes indicating the vapor phase had been saturated at 66 °C and not all of the hydrocarbon liquid evaporated. This behavior deviates negatively from ideality; the vapor pressures for the hydrocarbon components are lower than expected. The hydrocarbon mole fractions in the gas phase of the 720 μl volume containing heptane, toluene, octane, nonane, and decane, calculated from the liquid recovered from the vial inserts were 0.28, 0.30, 0.25, 0.16, and 0.01 respectively, assuming all of the missing liquid from the insert was in



the vapor phase at 66°C. The mole fractions in the vapor phase calculated for ideal behavior at 25 °C from the 720 µl volume would be 0.32, 0.32, 0.25, 0.08, and 0.03 for heptane, toluene, octane, nonane and decane respectively. The similarity of the calculated results for ideal behavior at 25 °C and the experimental results at 66 °C suggests the hydrocarbon solution exhibited a negative deviation from ideal behavior and that all of the hydrocarbons were affected alike.



**Figure 27: Mole Fractions of Adsorbed Hydrocarbons on Activated Carbon Plotted as a Function of the Square of the Molecular Polarizability ( $\alpha^2$ )**

The effects of adsorbent saturation were demonstrated with a sample of gasoline as shown in Figures 21-24 where the recovered hydrocarbons of an un-weathered gasoline from 33.2 mm<sup>2</sup> geometrical area activated carbons with volumes of 12µl and 96 µl are compared to neat diluted solutions of 0% weathered and 75% weathered (by volume) gasoline respectively. When the volume of gasoline was low, the activated carbon surface did not become saturated and the chromatographic profile was not distorted from that of the neat solution of 0% weathered

gasoline. However, the chromatographic profile became distorted, resembling the 75% weathered gasoline, when the activated carbon was saturated by the larger volume of gasoline. Since the chromatographic effects of gasoline adsorption onto activated carbon recovered from carpet and vial inserts are similar as shown in Figures 23 and 25 it can be assumed the adsorption of the gasoline onto the carpet has no influence on the chromatographic profile. The amount of ignitable liquid within fire debris cannot be controlled and the prohibitive expense of increasing the size of the activated carbon requires an alternative approach to sampling the fire debris. The approach taken in this study was to limit the sample size, thus reducing the ignitable liquid concentration. Two steps preceding the extraction procedure; heating the sample and removing a sub-sample produced a representative fraction of the original sample. The passive headspace concentration extraction procedure was performed on the sub-sample. The ignitable liquid residue concentration of the sub-sample did not saturate the activated carbon therefore the chromatographic profile resembled the original ignitable liquid as seen in Figure 26.

## CHAPTER FOUR: COLLECTION AND STORAGE OF FIRE DEBRIS EVIDENCE

### *Introduction*

An effective fire debris evidence container must be contaminant free and vapor-tight. The need for a vapor-tight evidence container is critical for retaining the ignitable liquid residues collected at a fire scene for subsequent analysis. Ignitable liquid residues mostly consist of volatile hydrocarbons. Containers recommended for fire debris evidence include metal “paint” cans with compression lids, glass mason jars with standard pressure-canning flats and bands, and special polymer sample bags.<sup>4, 35, 36</sup> The advantages and disadvantages of each type of container are discussed in the second edition of “*Practical Fire and Arson Investigation*”. Past investigations on the suitability of various commercial containers for the collection and preservation of fire debris evidence have been conducted.<sup>37, 38, 39</sup> Most of these investigations compared a specific type of container to an existing acceptable container to determine the container’s suitability for the collection and storage of fire debris evidence. The main objective of this study was to determine which type of container (metal can, glass jar, or polymer bag) retains ignitable liquid vapors most effectively.

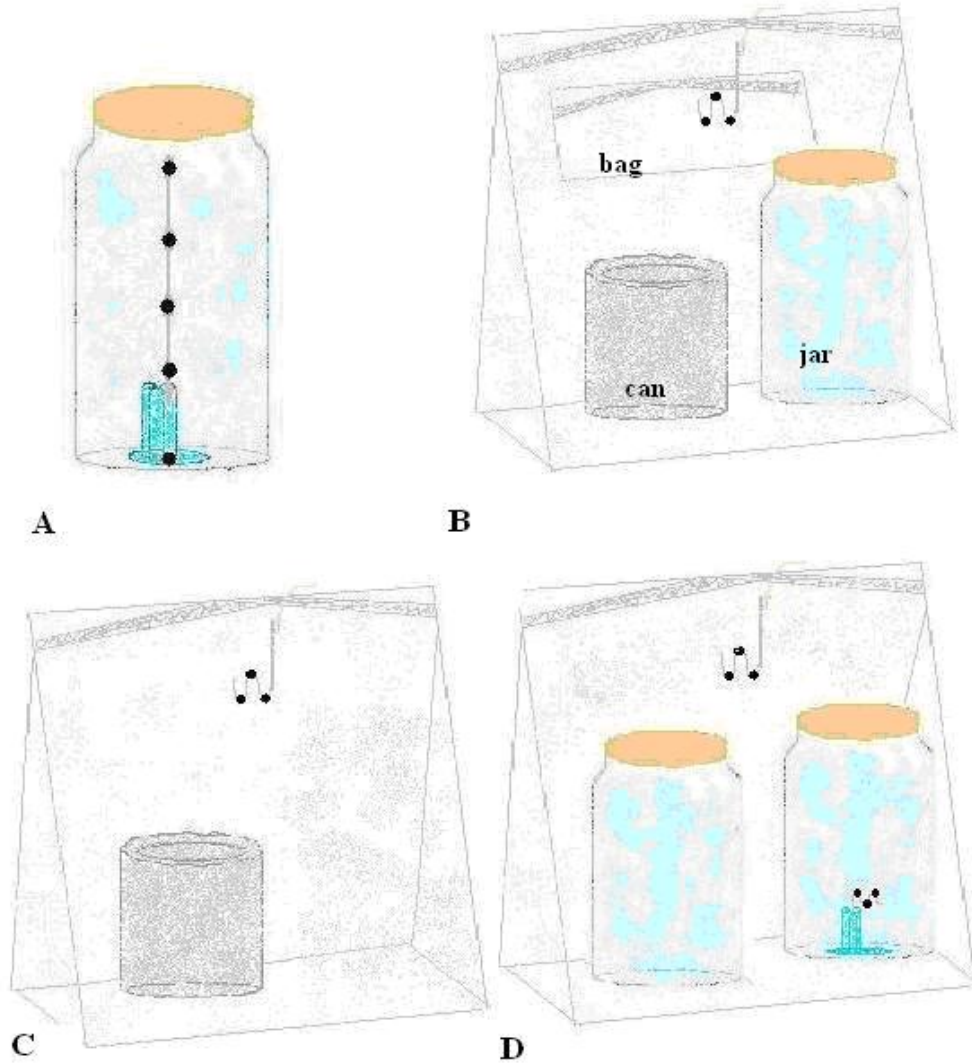
The study utilized the method of passive headspace concentration of ignitable liquids onto activated carbon for all experiments. Activated carbon disks were placed throughout the volume of a glass jar to determine if the hydrocarbon vapor was uniform throughout the container and whether placement of the activated carbons was critical for obtaining unbiased results. Leak rates for metal “paint” cans, glass mason jars, and Kapak polymer bags were determined under carefully specified conditions. Deviations of the recovered hydrocarbon mole fractions from the initial equimolar values were observed for containers which were determined

to have leaked. Hydrocarbons from the immediate environment penetrating a closed container was observed as well as hydrocarbon transfer between two closed containers.

### *Methods and Materials*

A stock solution of hydrocarbons consisting of heptane, toluene, octane, nonane, and decane was prepared in an equimolar ratio of each hydrocarbon (i.e. the mole fraction of each hydrocarbon in the mixture was 0.20). Toluene was purchased from Fisher Scientific the other hydrocarbons as well as p-xylene and toluene-d<sub>8</sub> were purchased from Aldrich Chemical Co. Low benzene carbon disulfide was purchased from Fisher Scientific for desorbing hydrocarbons from the activated carbon. Activated carbon strips were purchased from Albrayco then cut into 33.2mm<sup>2</sup> area circular pieces using a hole-punch. A hydrocarbon liquid container was constructed from GC auto sampler vial inserts super-glued together onto the underside of an evaporating dish. A metal rod with four male quick disconnects attached every 2.5 cm and an alligator clip at one end was designed to hold the activated carbon pieces with double sided tape above the hydrocarbon liquid container. A second method perforated the activated carbon disks onto a paperclip which was placed into an empty vial insert. A third method perforated the activated carbon disks onto a paperclip which hung from the sealed opening of the container by dental floss. The containers studied were quart metal paint cans, Ball<sup>®</sup> quart mason jars, and Kapak Fire DebrisPAK<sup>®</sup> (cast nylon, acrylonitrile/ methacrylate co-polymer) bags. The DebrisPAK<sup>®</sup> bags were cut into quart size volumes. Large binder clips were inserted inside the bags to prevent collapsing then the bags were heat sealed with the Kapak Corporation's pouch sealer following the manufacturer's recommendations. The metal cans were sealed with compression lids and the mason jars fitted with standard pressure-canning flats and bands.

The experiments investigating the effects of carbon placement utilized a metal rod with five activated carbon disks spaced 2.5 cm apart from each other throughout the depth of the glass jar as shown in Figure 28 A. The equimolar solution of hydrocarbons was deposited into the vial inserts within the glass jar. The set of experiments investigating commercial container leak rates, placed a metal can, a glass mason jar, and a DebrisPAK<sup>®</sup> bag of quart volume (as described above) inside a full sized DebrisPAK<sup>®</sup> bag. The full sized bag also contained a paperclip with three activated charcoal disks suspended by dental floss from the heat seal, as shown in Figure 28 B. The set of experiments investigating the effect of a leaking container's closing mechanism on the hydrocarbon composition, placed a single container inside a full sized DebrisPAK<sup>®</sup> bag along with three activated carbon disks on a paperclip suspended by dental floss from the heat seal at the top of the bag, as shown in Figure 28 C. The set of experiments investigating cross contamination of adjacent containers, placed two glass mason jars inside a full sized DebrisPAK<sup>®</sup> bag with three activated carbon disks inside one jar and three more activated carbon disks on a paperclip suspended from the top of the bag, as shown in Figure 28 D.



**Figure 28: Experiment Setup**

All extractions of the hydrocarbons from the activated carbon were performed in accordance with ASTM E1412-00 Standard Practice for Separation of Ignitable Liquid Residues from Fire Debris Samples by Passive Headspace Concentration with Activated Charcoal. In the experiments investigating the effects of activated carbon placement, the glass jars with activated carbon were heated in a 66°C oven for 16 to 24 hours, then removed and allowed to cool. The experiments investigating the container leak rates entailed keeping the containers in the heated oven for 20, 50, 100, and 150 hours. The experiments investigating the effect of a leaking

container's closing mechanism on the hydrocarbon composition required heating the systems in the oven for 146 hours. The experiments investigating cross contamination of adjacent containers involved keeping the systems in the oven for 163 hours. All of the activated carbon pieces were placed into half dram vials containing 1.0 ml of carbons disulfide. Each activated carbon disk extract was analyzed in triplicate.

Control experiments demonstrated that 90-95% of the extractable hydrocarbons were eluted from the carbon with a single CS<sub>2</sub> elution. Control experiments utilized concentrations of hydrocarbon solution which would not saturate the vapor phase and activated carbon, thereby eliminating concerns of chromatographic distortion and skewing of analytical results. The activated carbons were sequentially eluted with CS<sub>2</sub> twice, following the protocols used for the experiments described previously. Control experiments in which empty, un-used bags containing activated carbon strips were heated at 66°C for 16 hours, demonstrated that the bags did not contribute any interfering compounds to the chromatograms. Control experiments in which an 8 cm<sup>2</sup> piece of DebrisPAK<sup>®</sup> bag were exposed to the equimolar hydrocarbon vapor at levels replicating the experiments described herein, with subsequent CS<sub>2</sub> extraction of the material, showed no retention of the hydrocarbons by the bag material.

Detection of the hydrocarbons was performed on an Agilent 6890 gas chromatograph with a 5973 mass selective detector and a 7683 auto-sampler. Samples were chromatographed on a HP-1 methylsiloxane column 25m in length with an internal diameter of 0.2mm and a film thickness of 0.50 µm. Sample volumes of 1.0 µl were injected through a 250°C split/splitless injector with a 50:1 split ratio. The initial oven temperature was 50°C which was held for 3 minutes, then ramped at a rate of 10°C/min to a final temperature of 100°C and held for 2 minutes. The mass spectrometer was tuned according to the manufacturer's specifications at a

source temperature of 230°C. The spectra collected were over a scan range of 30-350 m/z units. Calibration curves were created to quantify the hydrocarbons recovered from the activated carbon by an external standard method.

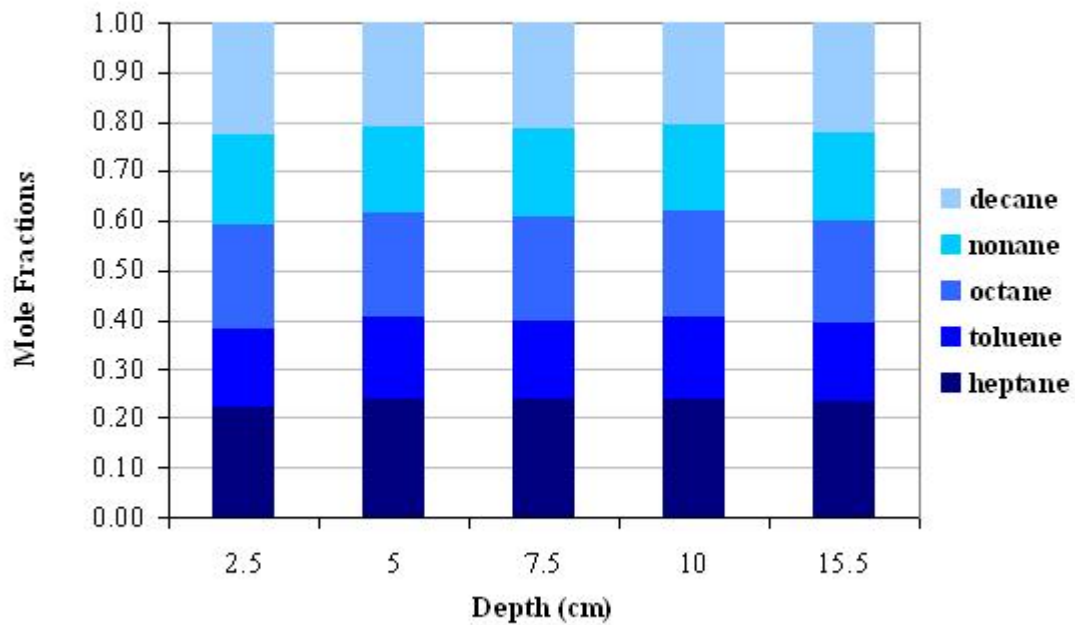
## *Results*

### *Commercial Container Leak Rates*

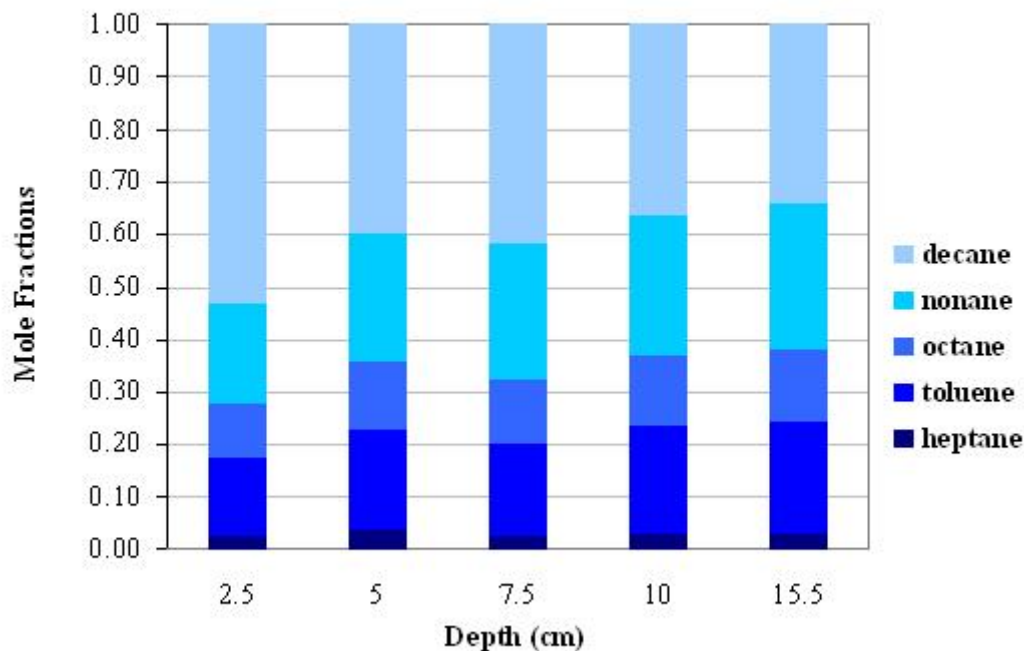
#### *Placement of Activated Carbon*

Five activated carbon disks of 33.2mm<sup>2</sup> geometric areas were adhered to a metal rod every 2.5 cm from the top of the glass jar to the bottom as shown in Figure 28 A. Two volumes of hydrocarbon solution, 12 µl and 96 µl volumes were deposited into a vial insert within one of the glass jars. The mole fractions of the hydrocarbons were calculated for each activated carbon disk placed at various depths within the glass jar. The variability of the mole fractions of each hydrocarbon recovered from the activated carbons in the glass jar containing 12 µl of hydrocarbon solution varied by approximately one percent. The actual mole fractions recovered from the activated carbon were close to 0.20, which corresponds to the mole fractions of each hydrocarbon in the solution deposited into the jar as shown in Figure 29. The variability of the mole fractions of each hydrocarbon recovered from the activated carbon disks at various depths within the jar containing a 96µl volume of hydrocarbon solution also remained low, but the mole fractions between the hydrocarbons varied from 0.02 for heptane to 0.40 for decane as shown in Figure 30.





**Figure 29: Mole Fractions of Recovered Hydrocarbons from Activated Carbon Disks at Various Depths within the Container with a Volume 12  $\mu$ l Hydrocarbon Solution**

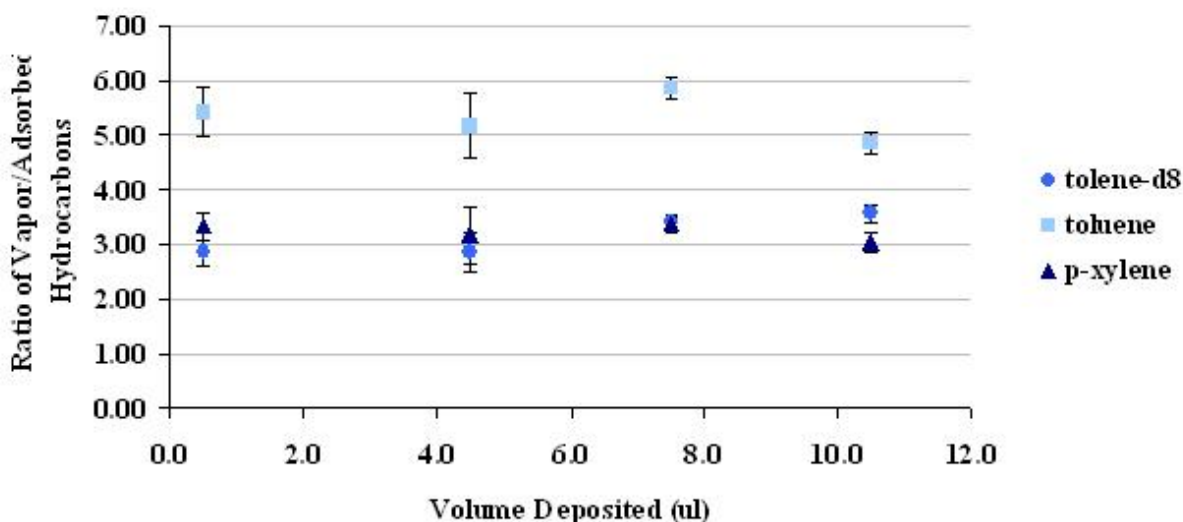


**Figure 30: Mole Fractions of Recovered Hydrocarbons from Activated Carbon Disks at Various Depths within the Container with a Volume 96  $\mu$ l Hydrocarbon Solution**

*Leak Rates*

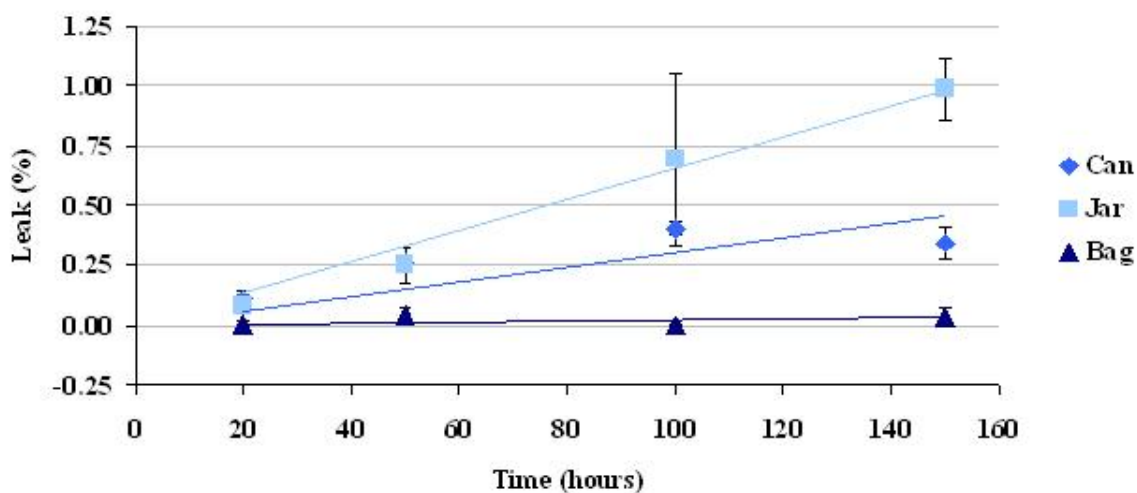
Based on the evaluation of nylon bags performed by the Centre of Forensic Sciences and the recommendation from the manufacturer, the DebrisPAK<sup>®</sup> bags used in this study were heat sealed.<sup>40</sup> Preliminary experiments indicated the heat sealed DebrisPAK<sup>®</sup> bag leaked less than the metal can and glass jar, so heat sealed bags were utilized as the outer secondary container in the experiments, as shown in Figure 28 B. The concentration of each hydrocarbon in the headspace of the secondary container was calculated from experiments correlating the amount of each hydrocarbon eluted from the activated carbons to the hydrocarbon concentration in the vapor phase. Vapor phase concentrations were calculated from the complete vaporization of

known volumes of hydrocarbon solution deposited into the secondary container. A solution of toluene, toluene-d<sub>8</sub>, and p-xylene, which have similar molecular weights (92.13 g/mol, 100.19 g/mol, and 106.17 g/mol, respectively), densities (0.865 g/ml, 0.943 g/ml, and 0.866 g/ml, respectively) and molecular structures, was prepared by mixing equal volumes of each hydrocarbon. Volumes of 0.5, 4.5, 7.5, and 10.5 µl of the solution were deposited into individual full size DebrisPAK<sup>®</sup> bags (secondary containers) each containing an empty quart sized metal can, an empty glass quart jar, and an empty quart volume DebrisPAK<sup>®</sup> bag with 3 carbon disks suspended from the heat seal of the outer full size bags. The four bags were all placed into a 66°C oven for 20 hours, then the hydrocarbons desorbed from the carbon disks with carbon disulfide. After analysis, the weight ratio of each hydrocarbon (in nanograms) deposited into the outer DebrisPAK<sup>®</sup> bags was calculated relative to the amount of hydrocarbon (ng) eluted from the carbon disks. This ratio describes the relationship between the concentrations of each hydrocarbon in the vapor phase within in the secondary container to the hydrocarbons eluted from the carbon disks as shown in Figure 31. The results demonstrate that the ratio of adsorbed hydrocarbon to vapor phase hydrocarbon is independent of the hydrocarbon volume when complete evaporation has occurred and the activated carbon remains unsaturated.



**Figure 31: Ratio of Hydrocarbons in the Vapor Phase to Hydrocarbons Adsorbed**

To determine container leak rates at 66°C, 5 $\mu$ l of toluene-d<sub>8</sub>, 5 $\mu$ l of toluene, and 5 $\mu$ l of p-xylene were deposited into a metal quart can, a glass quart jar, and a quart volume DebrisPAK<sup>®</sup> bag, respectively. Each type of container with its corresponding hydrocarbon was placed into a secondary container with 3 carbon disks constituting a system. Triplicate systems were placed in the oven for 20, 50, 100, and 150 hours for a total of 12 systems. The amount of hydrocarbon leaking from each container was ascertained based upon the ratios calculated from results in Figure 31. The percent leak in moles per hour for each type of container was determined to be an approximate linear function of time, i.e. zero order kinetic behavior. The observed leak rates for the metal cans, glass jars, and DebrisPAK<sup>®</sup> bags were  $3.0 \times 10^{-3}$  mol %/h,  $6.5 \times 10^{-3}$  mol %/h, and  $2.0 \times 10^{-4}$  mol %/h, respectively as shown in Figure 32.



**Figure 32: Container Leak Rates**

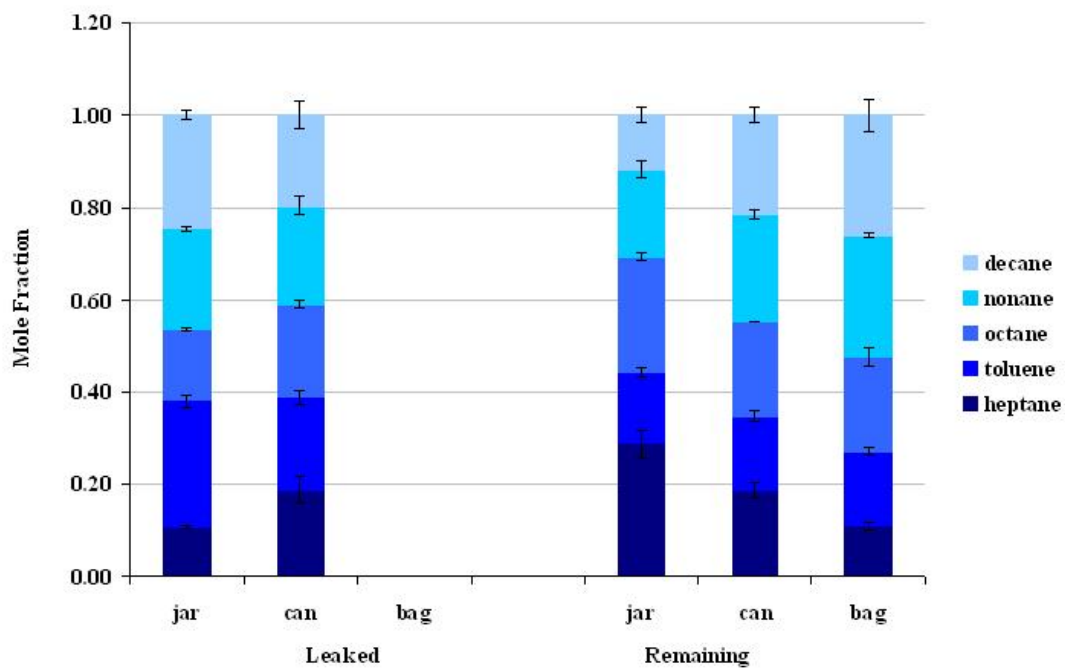
The glass mason jars exhibited the fastest leak followed by the metal paint cans then the DebrisPAK<sup>®</sup> bags. When properly heat sealed the DebrisPAK<sup>®</sup> bags did not leak significantly, but when sealed incorrectly the leak rate increased substantially. Only one bag out of twelve bags used in the experiments did not seal properly clearly creating anomalous results.

### *Effects of Container Leaks*

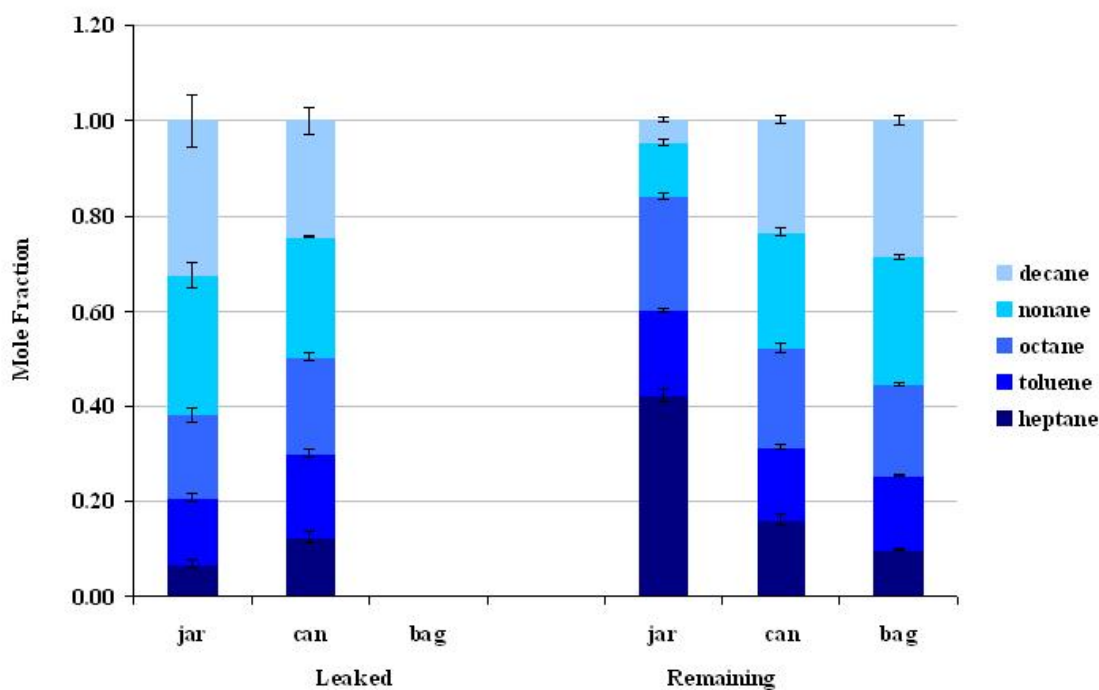
#### *Effect Container Leaks have on the Hydrocarbon Molecular Distribution*

The following experiment was performed to determine if a leaking container effects the distribution of a hydrocarbon remaining inside the container. A 10  $\mu$ l volume of an equimolar hydrocarbon solution containing heptane, toluene, octane, nonane, and decane was deposited into a jar, can, and bag of quart size volumes then the containers were properly sealed. Each of these containers was placed inside an individual full sized DebrisPAK<sup>®</sup> bag containing three activated carbon disks suspended from the top of the bag by a paperclip and dental floss as shown in

Figure 28 C. Each of the three container systems were replicated with an 18  $\mu\text{l}$  volume of the same equimolar hydrocarbon solution. The systems were placed in a 66°C oven for 146 hours, removed then cooled to room temperature. The mole fractions of each hydrocarbon which leaked from each of the three containers (can, jar, and bag) were calculated after analysis of the activated carbon disks. Subsequently, each container was placed inside a new individual DebrisPAK<sup>®</sup> bag containing a new set of three activated carbon disks. Prior to heat sealing the outer bag each of the containers was opened. The new systems were placed inside a 66°C oven for 20 hours to facilitate the remaining hydrocarbon molecules to enter the vapor phase then the systems were removed from the oven and allowed to cool to room temperature. The mole fractions of each hydrocarbon remaining inside the containers during the first 146 hour heating period were calculated after analysis of the activated carbon disks. The DebrisPAK<sup>®</sup> bag did not leak, while the glass jar and metal paint can did leak as demonstrated by the hydrocarbon mole fractions extracted from the activated carbon disks shown in Figures 33 and 34 for the 10 $\mu\text{l}$  and 18  $\mu\text{l}$  volumes respectively.



**Figure 33: Hydrocarbon Mole Fractions from the 10 $\mu$ l Volume Deposited into Each Container Type of Hydrocarbons that Leaked from the Container and Hydrocarbons that Remained in the Container**



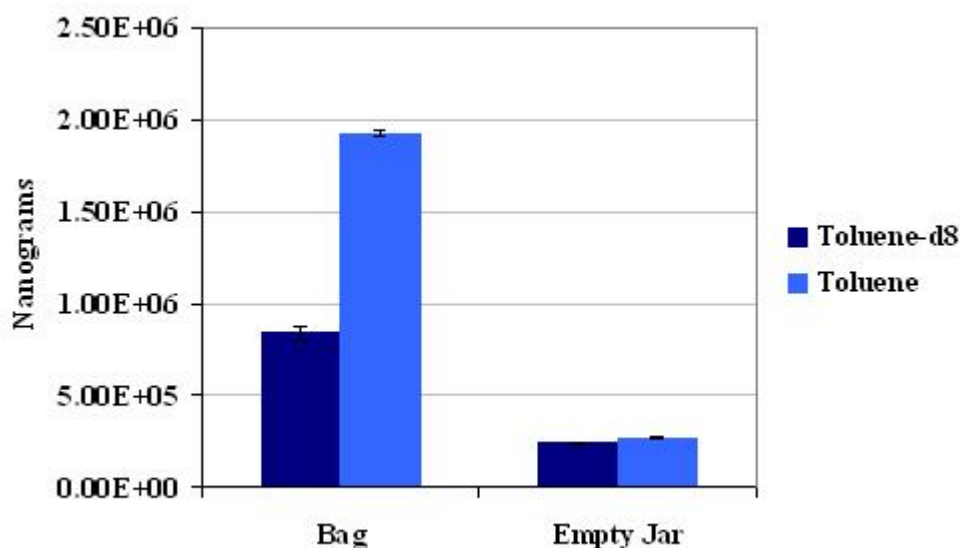
**Figure 34: Hydrocarbon Mole Fractions from the 18 $\mu$ l Volume Deposited into Each Container Type of Hydrocarbons that Leaked from the Container and Hydrocarbons that Remained in the Container**

*Contamination of Containers from the Environment*

Since it has been determined that glass mason jars leak, this type of container was used in the following experiment to determine if hydrocarbons from the environment can cause contamination within the container. A full size DebrisPAK<sup>®</sup> bag contained two glass mason jars, a set of three activated carbon disks suspended from the heat seal by dental floss and a paperclip and 10  $\mu$ l of toluene-d<sub>8</sub> deposited into the bag. One of the jars contained three activated carbon disks perforated onto a paperclip and no hydrocarbon liquid and the other jar contained 50  $\mu$ l of toluene deposited into a vial insert as shown in Figure 28 D. The bag was placed in a 66°C oven for 163 hours, removed then allowed to cool to room temperature. The analyses of the activated



carbon disks from the DebrisPAK<sup>®</sup> bag revealed that toluene constituted seventy percent of the hydrocarbons recovered. Furthermore, the activated carbon disks from the jar originally containing no hydrocarbon liquid now contained an equal quantity of both toluene-d<sub>8</sub> from the bag and toluene from the other glass jar as shown in Figure 35.

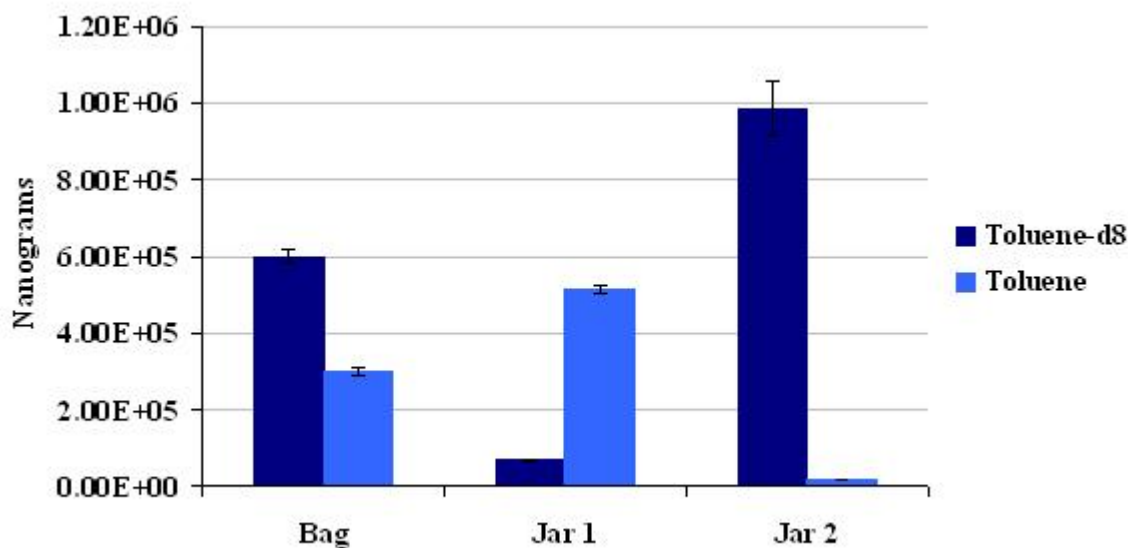


**Figure 35: Demonstration of Hydrocarbon Transfer from Environment into Empty Jar**

*Cross Contamination of Containers from Adjacent Containers*

In the previous experiment, a sealed glass jar containing toluene-d<sub>8</sub> leaked and was detected in the adjacent sealed jar. To determine whether the sealed glass jars are capable of cross contaminating each other the following experiment was conducted. The experiment was constructed similarly to the experiment described in the previous paragraph with two exceptions. First, 50 µl of toluene was deposited into jar 1 and 50 µl of toluene-d<sub>8</sub> was deposited into jar 2 with no toluene or toluene-d<sub>8</sub> deposited into the outer bag. Secondly, both jars and the outer bag each contained a set of three activated carbon disks. The bag was placed in a 66°C oven for 192 hours. Analyses of the activated carbon disks revealed all of the disks had adsorbed both toluene

and toluene-d<sub>8</sub>. The major constituent in each jar was the hydrocarbon originally deposited inside the jar as a liquid (i.e. toluene in jar 1 and toluene-d<sub>8</sub> in jar 2) as shown in Figure 36.



**Figure 36: Demonstration of Cross Contamination**

*Discussion*

Vapor densities of the hydrocarbons in the solution used for determining whether placement (depth) of the activated carbons within the container have an effect ranged from 3.5 (heptane) to 4.9 (decane) times the density of air. The results shown in Figure 29 reveal no significant change in the molar distribution of the hydrocarbons recovered from the activated carbons placed at various depths within the container to the molar distribution of the hydrocarbons from the 12  $\mu\text{l}$  volume deposited into the container. The results shown in Figure 30 reveal a significant change in the molar distribution of the hydrocarbons recovered from the activated carbons placed at various depths within the container to the molar distribution of the hydrocarbons from the 96  $\mu\text{l}$  volume deposited into the container. However, the molar distribution of the hydrocarbons recovered from the activated carbon disks at each of the five

depths within the container show minimal variation. The results from both sample volumes (12  $\mu\text{l}$  and 96  $\mu\text{l}$ ) contain no evidence of hydrocarbon vapor stratification within the closed containers indicated by the lack of variation in the molar distribution of hydrocarbons recovered from the activated carbon disks. The hydrocarbon molecules were evenly distributed throughout the system for a narrow range of C7-C10, but a larger molecular size range of hydrocarbons may be expected to display unequal distributions within the container.

At 66°C the glass jar had the fastest leak while the DebrisPAK<sup>®</sup> bag had the slowest leak indicated by their respective leak rates. The leak rates of the glass mason jars and metal paint cans were indistinguishable within the first 50 hours, however, subsequent monitoring showed the mason jars leak at a faster rate than the metal paint cans. The glass jar leaked 98% of the hydrocarbon after six days at 66°C. The heat sealed DebrisPAK<sup>®</sup> bags did not leak significantly with only one exception being a single bag which had been improperly sealed.

An examination of the hydrocarbon mole fractions recovered from activated carbons within each type of container exposed to an equimolar hydrocarbon solution over a period of several days demonstrated dissimilar leaking mechanisms. Typically a 10  $\mu\text{l}$  volume of hydrocarbon solution does not saturate a 33.2  $\text{mm}^2$  activated carbon disk inside a quart volume container at 66°C for a 20 hour period. Mole fractions from both sets of activated carbon disks reveal the relative composition of hydrocarbons which leaked from the sealed container and those which remained within the container. Hydrocarbons within the glass jar did not leak equally; those with the smallest collision diameters leaked faster than those with larger collision diameters. According to the USDA Complete Guide to Home Canning, “the lid gasket softens and flows slightly when heated to cover the jar-sealing surface, yet allows air to escape from the jar”.<sup>41</sup> Hydrocarbons within the metal can leaked equally, thus the remaining hydrocarbons

within the can were equimolar in distribution. The DebrisPAK<sup>®</sup> bag did not leak; therefore all of the hydrocarbons remained inside the bag. However, the mole fractions of the recovered hydrocarbons were not equal as expected, perhaps a result of the extended period of heating and surface/vapor equilibration leading to some distortion. Typically an 18  $\mu\text{l}$  volume of hydrocarbon solution does saturate a 33.2  $\text{mm}^2$  activated carbon disk inside a quart volume container at 66°C for a 20 hour period resulting in a non-uniform distribution of the hydrocarbon mole fractions and thus a distortion of the chromatographic hydrocarbon profile. The effect of activated carbon saturation on the molar distribution of the hydrocarbons under similar conditions appears to have been reduced for the metal paint cans possibly due to the equal loss of each hydrocarbon from the container. The leaking of the hydrocarbons from the sealed metal can reduced the total volume of hydrocarbons, thereby preventing saturation of the activated carbon disk.

Over a period of several days a glass jar at 66°C will leak. Subsequently hydrocarbons which leaked from one container as well as hydrocarbons from the surrounding environment may penetrate into an empty glass jar. The performance of the glass jar flats and bands may vary from container to container as shown in Figure 36.

In the present study, properly heat sealed co-polymer bags retained all of the hydrocarbons. The other two containers leaked at different rates with the glass jars having the fastest leak. Depending on the container closing mechanism, the hydrocarbons from glass jars leaked in different proportions compared to the hydrocarbons of the metal cans imparting hydrocarbon molar distributions distinctly different from one another. Over time, leaking jars containing hydrocarbons are capable of cross contaminating other jars stored in close proximity to one another as well as hydrocarbons from the immediate environment.

## CHAPTER FIVE: ANALYSIS OF FIRE DEBRIS EVIDENCE BY COVARIANCE MAPPING

### *Introduction*

Fire debris analysts utilize pattern recognition, extracted ion profiling, and target ion profiling techniques to classify an unknown ignitable liquid extracted from fire debris into a group or type of ignitable liquid by comparing the relative ratios of the components (peaks) observed in the total ion and extracted ion profiles. The data from an unknown sample is compared to similar data obtained from reference ignitable liquids of known classes. ASTM E1618-01 describes how to use these techniques for class determination of the ignitable liquid. Various methods for improving detection and alternative methods for data analysis and interpretation have been studied. Parallel –column gas chromatography, GC X GC/MS, and GC/MS/MS methods have been introduced to improve resolution of the components within these complex mixtures thus aiding in the identification of the ignitable liquid components.<sup>15, 16, 42</sup> Automated comparisons of GC/MS data of complex mixtures have been utilized through advanced software, but still rely on visual pattern recognition for data interpretation.<sup>43</sup> Statistical methods for comparison of GC/MS data have been applied for classification of ignitable liquids as well as identification of gasoline but have not provided a method of common source estimation with a known statistical certainty.<sup>44, 45, 46, 47, 48</sup>

Covariance mapping and coincidence measurements have been applied to time-of-flight mass spectrometry to resolve correlated events.<sup>49, 50, 51, 52, 53</sup> Covariance mapping has not previously been applied to the analysis of complex GC/MS data sets. Advantages of the covariance mapping method are that it requires no additional equipment and can be used with existing GC/MS data for automation of ignitable liquid comparisons. Current ignitable liquid

databases containing GC/MS data sets remain valuable tools. The use of covariance mapping with a distance measurement has been utilized to characterize ignitable liquids according to the ASTM class, carbon range, and percent evaporation. The additional application of a t-test has been able to distinguish 10 un-evaporated gasoline samples as having come from different sources and identified a gasoline with a statistical certainty.

### *Methods and Materials*

The gas chromatographic – mass spectral data sets utilized in the present study on the analysis of fire debris evidence were gathered from the Ignitable Liquid Reference Collection (ILRC) or from the GC-MS analyses of 10 gasoline samples obtained at retail stations in the geographical area around Orlando, FL. Gasoline samples were collected in new unused clear glass vials fitted with Teflon-lined screw caps. The gasoline samples listed in Table 5 were not altered (i.e. evaporated) and the diluted gasoline samples were analyzed in triplicate. All samples were prepared by dilution of 20  $\mu$ L of liquid into 1 ml of carbon disulfide for GC-MS analysis. GC-MS analyses were conducted on an Agilent 6890 gas chromatograph with a 5973 mass selective detector and a 7683 auto-injector. Sample volumes of 1.0  $\mu$ l were injected through a Merlin septumless system into a 250°C split/splitless inlet with a 50:1 split ratio. Helium carrier gas was maintained at a constant flow of 0.8 ml/min on the column, corresponding to a linear velocity of 33 cm/sec. The sample components were separated on a HP-1 methylsiloxane column 25m in length with an internal diameter of 0.2mm and a film thickness of 0.50  $\mu$ m. The initial oven temperature was 50°C which was held for 3 minutes, then ramped at a rate of 10°C/min to a final temperature of 280°C and held for 4 minutes. The mass spectrometer transfer line was maintained at 280 °C and the source temperature was 230 °C. The mass

spectrometer was tuned according to the manufacturer’s specifications at a source temperature of 230°C. The spectra were collected over a scan range of 30-350 m/z units.

**Table 6: Gasoline Sources and Octane Ratings**

<b>Gasoline Number</b>	<b>Source</b>	<b>Octane Rating</b>
1	Racetrack	87
2	Chevron	89
3	Mobil	87
4	Hess	87
5	76	87
6	Costco	87
7	Mobil	93
8	Cumberland Farms	87
9	BP	87
10	Shell	87

Thirteen ignitable liquids representing six of the nine classes described in the ASTM E1618-01 were chosen for comparison. The classification and carbon range of each ignitable liquid chosen was ascertained from the ILRC database. The database classification information is provided by a committee consisting of several fire debris analysts from local, state and federal crime laboratories. The committee members review the data sets and then determine the classification, predominant ion profile, carbon range, and major peaks for each ignitable liquid. The sample reference numbers with their associated ASTM classification and carbon range are shown in Table 6

**Table 7: Samples from Ignitable Liquid Reference Collection**

<b>Sample Reference Number</b>	<b>Product Name</b>	<b>Condition</b>	<b>Carbon Range</b>	<b>ASTM Classification</b>
301	Hess Gasoline	0 % weathered	6-14	Gasoline
303	Hess Gasoline	75% weathered	7-14	Gasoline
96	BP Gasoline	25% weathered	6-14	Gasoline
98	BP Gasoline	75% weathered	6-16	Gasoline
105	Phillips 66 Gasoline	0 % weathered	6-14	Gasoline
224	Ace VM&P Naphtha	0 % weathered	6-11	Distillate
227	Ace Paint Thinner	0 % weathered	8-13	Distillate
226	Ace odorless grade 1 Kerosene	0 % weathered	8-16	Distillate
81	Exxon Varsol 1	0 % weathered	8-13	Distillate
164	BBQ Pro Charcoal Starter	0 % weathered	8-11	De-aromatized Distillate
119	Exxon Isopar H	0 % weathered	9-12	Isoparaffinic Product
252	DEFT Fabric/Furniture Protector	0 % weathered	6-11	Oxygenated Product
140	Lamplight Farms Citronella Torch Fuel	0 % weathered	10-14	Naphthenic Paraffinic Product

The Agilent Chemstation 3D-Export option was used to export spectral data into comma-separated values (CSV) format ASCII files. The ion range exported was 30 – 200 m/z corresponding to the first 2000 consecutive scans which was considered to be sufficient since the range included all eluting peaks. The CSV files were imported into Excel (Microsoft Inc.) then condensed by selecting only m/z versus scan number data. The new data sets were converted back to a CSV file format before being exported to Mathematica (Wolfram Inc.) for all matrix manipulations. All matrix visualization graphics were produced with Sigma Plot (Systat Software Inc.). All manipulations of the covariance matrices (i.e. normalization) were performed in Excel.



## Results

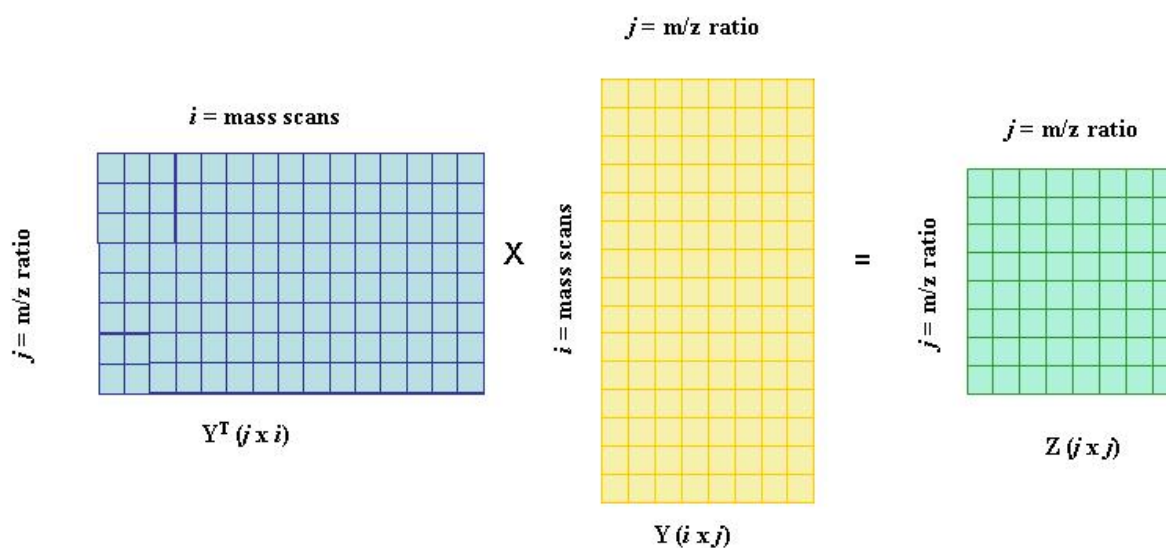
### Covariance Mapping

#### Covariance Matrix

A total ion chromatogram consists of ions with m/z ratios and retention times corresponding to the mass scan number. Each ignitable liquid data set contains a matrix  $\mathbf{Y}$  composed of  $i$  rows corresponding to the mass scan numbers (1 – 2000) designated as  $s_i$  and  $j$  columns corresponding to a m/z ratio (30-200 m/z) designated as  $r_j$ . The matrix value  $y(s_i, r_j)$  corresponds to the ion abundance of a m/z ratio at a single mass scan number. The covariance matrix  $\mathbf{Z}$  is generated by multiplying the transpose matrix  $\mathbf{Y}^T$  by the matrix  $\mathbf{Y}$  as in equation 2.

$$\mathbf{Z} = \mathbf{Y}^T \cdot \mathbf{Y} \quad (2)$$

The covariance matrix is a table listing the variances (diagonal) and the co-variances (off diagonal) of two or more variables; each ignitable liquid matrix contains 197 variables.<sup>54</sup> The generation of a covariance matrix  $\mathbf{Z}$  from the data matrix  $\mathbf{Y}$  is graphically represented in Figure 37. The generated covariance matrix  $\mathbf{Z}$  is a symmetric matrix with each element  $z_{ij}$  representing the similarity between the measured intensities of the variables (abundances of the m/z ratios). Since the values in the  $\mathbf{Y}$  matrix were not normalized before the calculation of  $\mathbf{Z}$ , the values for the  $\mathbf{Z}$  matrix are weighted in proportion to the absolute magnitude of the ion abundances of  $\mathbf{Y}$ .<sup>55</sup> The ion abundances of the  $\mathbf{Y}$  matrix are concentration dependent therefore the elements of  $\mathbf{Z}$  are also concentration dependent. To remove any sample concentration dependence each covariance matrix  $\mathbf{Z}$  was normalized such that the sum of all the elements within the matrix equaled a value of 1.0 and was designated  $\mathbf{Z}_N$ . Normalization of the covariance matrices was required for comparison calculations between two ignitable liquids.



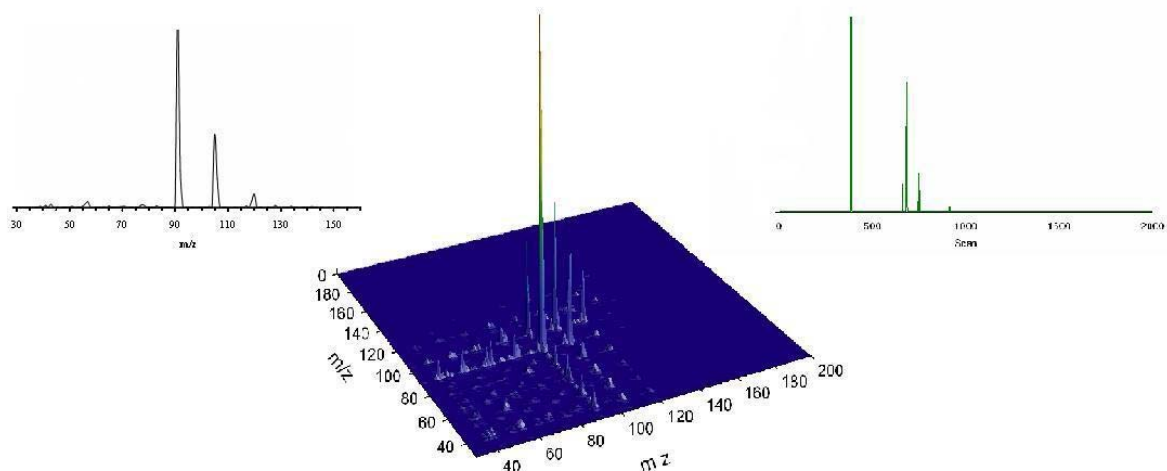
**Figure 37: A Graphical Representation of a Covariance Matrix being generated from a GC-MS data set**

*Covariance Map*

The normalized covariance matrix  $\mathbf{Z}_N$  eliminates concentration and time dependence from the original data set becoming a potential method for rapidly comparing complex samples such as ignitable liquids. A covariance map (B) is a 3D visual representation of the ignitable liquid  $\mathbf{Z}_N$  matrix as shown in Figure 38. The variance of the m/z ratios lie on the diagonal of the covariance map corresponding to the sum of the squared ion intensities (A). The covariance of the ion intensities lie on the off-diagonal and express the relationship between two different m/z ratio ions within the data set (C). The diagonal components reflect the intensity of each extracted ion chromatogram multiplied by its self and summed over all scan events (i.e. each time point in the chromatogram). The off-diagonal components reflect the product of two extracted ion chromatograms summed over all scan events.

(A) A Sum of the squared ion intensities corresponding to the diagonal of the covariance map shown in (B) of the figure.

(C) Extracted ion profile for m/z 91



(B) Covariance Map

The large intensity at m/z 91 on the diagonal corresponds to the sum of the square of the intensities of the corresponding extracted ion chromatogram shown in (C) of the figure.

### Figure 38: Covariance Map of Gasoline

#### *Distance between Covariance Matrices*

A distance between two  $\mathbf{Z}_N$  matrices was calculated to facilitate an analytical comparison of two ignitable liquids. A Manhattan distance  $D$  was calculated on an element to element basis as the absolute difference between the matrix elements. The distance  $D$  of each element was summed over all of the elements then divided by two for an absolute difference between the two matrices. The distance  $D$  between two matrices designated  $\mathbf{Z}_{N1(ij)}$  and  $\mathbf{Z}_{N2(ij)}$ , is calculated by equation 3.

$$D = \frac{\sum_i \sum_j |z_{M1}(i, j) - z_{M2}(i, j)|}{2} \quad (3)$$

The values of  $D$  lie between 0 and 1, where two identical  $\mathbf{Z}_N$  matrices have a minimum distance  $D$  of 0 and two non related  $\mathbf{Z}_N$  matrices have a maximum distance  $D$  of 1. Alternatively, a similarity index,  $S$ , can be calculated based on  $D$  which is defined by equation 4.  $D$  is defined so that  $D_{\max}$  equals 1 and lies between 0 and 1. Therefore, the similarity equals 1 minus  $D$ .

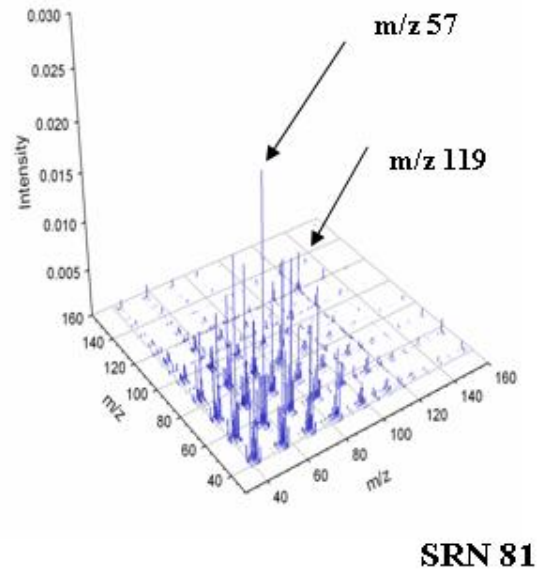
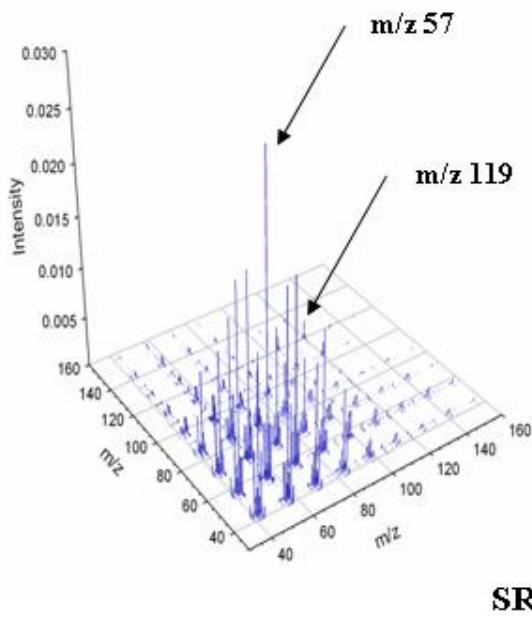
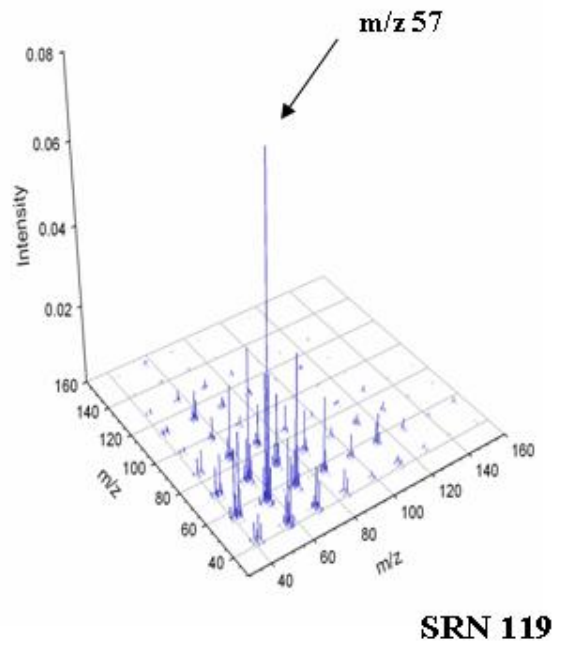
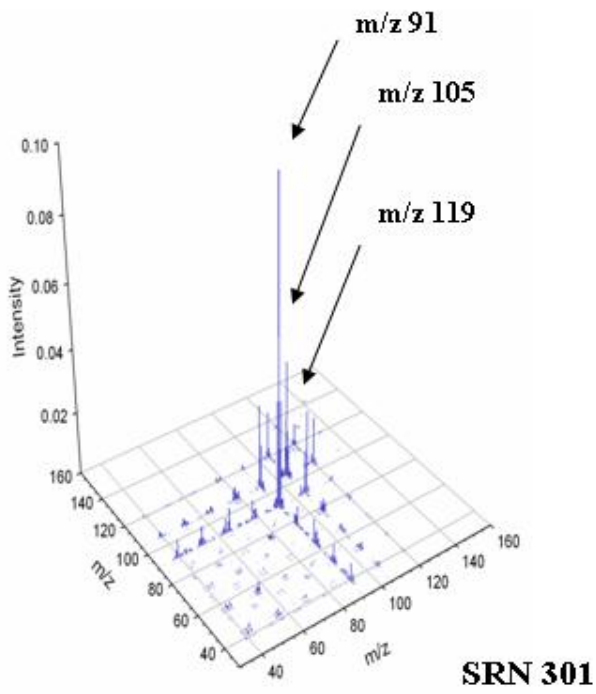
$$S = 1 - \frac{D}{D_{\max}} \quad \mathbf{S} = 1 - \mathbf{D} \quad (4)$$

### *Characterization of Ignitable Liquids*

#### *Covariance Maps of Ignitable Liquids*

Hydrocarbons with specific functional groups within their molecular structure typically fragment in the electron ionization source in a particular manner producing a set of diagnostic ions. Extracted ion profiles of the  $m/z$  ratio constituting five various molecular structures aid in the classification of ignitable liquids according to ASTM E 1618-01 and are listed in Table 1. The  $m/z$  ratios of a  $\mathbf{Z}_N$  matrix are easily observed on the covariance map along with their relative intensities. The  $\mathbf{Z}_N$  map for SRN 226 a heavy petroleum distillate clearly shows ions indicative of alkanes ( $m/z$  43, 57, 71), cycloalkanes and alkenes ( $m/z$  41, 55), aromatics ( $m/z$  91, 105), and indanes ( $m/z$  131, 132) with the alkane ions most predominate. The  $\mathbf{Z}_N$  map for SRN 119 an isoparaffinic product clearly shows ions indicative of alkanes ( $m/z$  43, 57, 71) being the most predominant, cycloalkanes and alkenes ( $m/z$  41, 55) reduced in relative abundance to the alkanes

with no ion contribution from any of the aromatic species. Since isoparaffinic products are comprised almost exclusively of branched chain alkanes the ions produced should be the same ions as those produced for alkanes. The  $Z_N$  map for SRN 301 a gasoline clearly shows the most predominant ions being  $m/z$  91, 105, and 119 which are indicative of aromatics with substantially lesser contributions from the alkanes ( $m/z$  43, 57, 71). The  $Z_N$  map for SRN 81 a medium petroleum distillate is not visually distinguishable from SRN 226 a heavy petroleum distillate. The covariance maps of the other  $Z_N$  matrices are visually distinguishable as liquids of different classes.



**Figure 39: Covariance Maps of Ignitable Liquids**

*Distances between Covariance Matrices of Ignitable Liquids*

The distances  $D$  calculated between all thirteen ignitable liquid samples are given in Table 7. All of the distances  $D$  fall over a range of 0 to 1 with a maximum and minimum values observed of 0.975 and 0.084, respectively. The maximum distance observed was between SRN 119 an isoparaffinic product and SRN 303 a 75% weathered gasoline reflects the striking difference between isoparaffins consisting primarily of branched alkanes and gasoline consisting primarily of aromatics. The minimum distance observed was between SRN 301 and SRN 105 which are 0% weathered gasolines.

**Table 8: Distances between Ignitable Liquid Samples**

SRN	301	303	96	98	105	224	227	226	81	164	119	252
301	0.00											
303	0.307	0.00										
96	0.137	0.356	0.00									
98	0.353	0.103	0.385	0.00								
105	0.084	.308	0.113	0.357	0.00							
224	0.897	0.971	0.824	0.962	0.849	0.00						
227	0.763	0.810	0.688	0.790	0.709	0.429	0.00					
226	0.826	0.874	0.753	0.859	0.772	0.456	0.152	0.00				
81	0.789	0.834	0.710	0.813	0.736	0.423	0.105	0.155	0.00			
164	0.897	0.968	0.823	0.960	0.848	0.277	0.257	0.285	0.265	0.00		
119	0.910	0.975	0.844	0.969	0.857	0.511	0.406	0.400	0.443	0.382	0.00	
252	0.722	0.789	0.645	0.777	0.666	0.568	0.463	0.494	0.478	0.525	0.566	0.00
140	0.890	0.955	0.825	0.944	0.848	0.497	0.486	0.422	0.428	0.383	0.569	0.638

The distance between the two 0% weathered gasoline samples was 0.084 and the distance between the two 75% weathered gasoline samples was 0.103. However, a comparison of the distances between 75% weathered gasoline samples and 0% weathered gasoline samples gave an average distance of  $0.336 \pm 0.0262$  thus distinguishing a 0% weathered gasoline sample from a 75% weathered gasoline sample. The average distance between the two 0% weathered gasoline samples and the single 25% weathered gasoline sample was  $0.125 \pm 0.0170$  which may indicate

that it is possible to distinguish the 25% weathered gasoline from 0% weathered gasoline after more comparisons are completed. A comparison of the distances between the petroleum distillates suggests the light (LPD), medium (MPD), and heavy distillates (HPD) can be differentiated from one another, especially the light petroleum distillate. The distance between the two MPD was 0.105 while the average distance between the two MPD and the single HPD was 0.153. The LPD average distance with the two MPD was 0.426 and the distance between the LPD and the HPD was 0.456. Most of the remaining  $Z_N$  matrix distance comparisons demonstrate significant differences between the major classes designated by ASTM E 1618-01 of ignitable liquids.

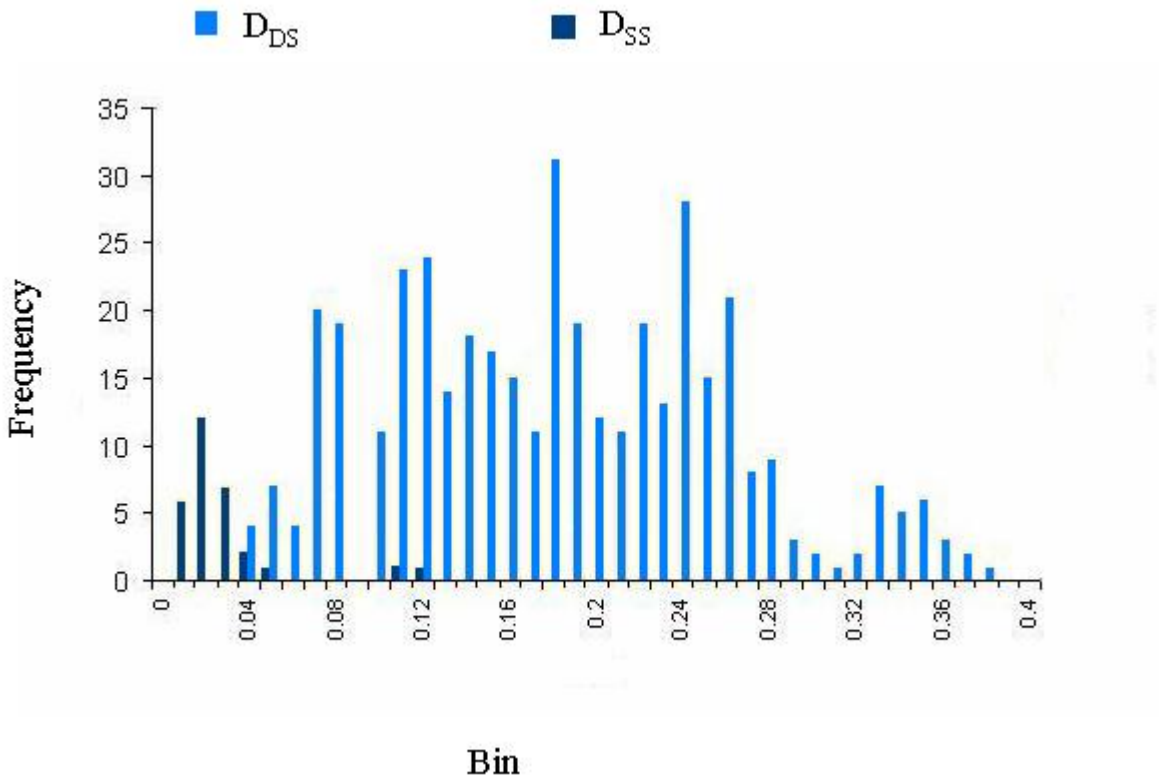
#### *Comparison of Gasoline Samples by Covariance Mapping*

##### *Discrimination of gasoline samples*

Each gasoline sample in Table 5 was analyzed in triplicate back to back runs on the same instrument and analytical method. The GC/MS data sets were converted into covariance matrices and normalized. Distances were calculated between the three replicate analyses of the same gasoline sample for three pair wise comparisons designated  $D_{SS}$ . Distances were calculated between each replicate analysis of every gasoline sample to each replicate analysis of every other gasoline sample giving nine pair-wise comparisons designated  $D_{DS}$ . The average  $D_{SS}$  value and standard deviation of the set of 30 values was  $0.024 \pm 0.024$  (i.e. the covariance maps varied by 2.4%). The number of  $D_{SS}$  values and  $D_{DS}$  values falling into bins of 0.01 increments were plotted in Figure 40. The distribution of  $D_{SS}$  values contained two values 0.11 and 0.12 which were approximately three standard deviations greater than the average for the set. These two  $D_{SS}$  values of 0.103 and 0.110 resulted from a single analysis of gasoline 1 which was the first



analysis performed in the set of 30 and was likely due to not preconditioning the column with solvent prior to analysis.



**Figure 40: Frequency Distribution Plot of 30 same sample distances ( $D_{SS}$ ) and 405 different sample distances ( $D_{DS}$ ).**

The Dixon's  $r_{12}$  statistic, a discordance test for an upper outlier pair was used to test the two large  $D_{SS}$  values as possible outliers using Equation 5.<sup>56</sup>

$$T = \frac{D_{ss(n)} - D_{ss(n-2)}}{D_{ss(n)} - D_{ss(2)}}$$

(5)

The calculated test statistic had a value of 0.652 which exceeded the 1% significance bound of 0.433 for 30 values. The calculation allowed the null hypothesis that all of the  $D_{SS}$  values originated from the same normal distribution to be rejected. Once the two large  $D_{SS}$  values resulting from the single analysis of gasoline 1 were discarded the distribution of  $D_{SS}$  values was more normal with an average the two large  $D_{SS}$  of 0.018 and a standard deviation of 0.010. The average  $D_{DS}$  value and standard deviation of 0.177 and 0.077 respectively were calculated from the 405 pair-wise comparisons of  $D_{DS}$  values, the distances between the 10  $Z_N$  matrices of gasoline samples (9  $D_{DS}$  values for each of the 45 pair-wise sample comparisons). The average of the  $D_{DS}$  values and the standard deviation for the values are considerably different from the average and standard deviation of the  $D_{SS}$  values.

A t-test for data sets where the number of data points are not equal ( $n_{SS} \neq n_{DS}$ ) and unknown population variances that are possibly unequal is given in Equation 6, where  $\bar{D}_{DS}$  and  $\bar{D}_{SS}$  are the average distances and  $S_{DS}$  and  $S_{SS}$  are the standard deviations.<sup>57</sup>

$$t' = \frac{|\bar{D}_{DS} - \bar{D}_{SS}|}{\sqrt{\frac{S_{DS}^2}{n_{DS}} + \frac{S_{SS}^2}{n_{SS}}}} \quad (6)$$

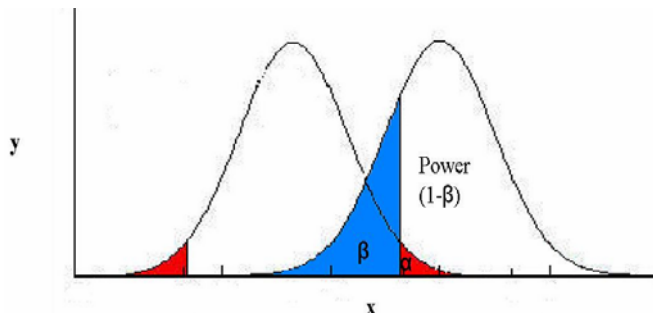
The number of degrees of freedom is approximated by Equation 7 which will lie between the smaller number of points  $n_{DS}-1$  and  $n_{SS}-1$  and their sum.

$$DF = \frac{\left( \frac{S_{DS}^2}{n_{DS}} + \frac{S_{SS}^2}{n_{SS}} \right)^2}{\frac{\left( \frac{S_{DS}^2}{n_{DS}} \right)^2}{n_{DS} - 1} + \frac{\left( \frac{S_{SS}^2}{n_{SS}} \right)^2}{n_{SS} - 1}} \quad (7)$$

When the t-test comparing the entire set of 30  $D_{SS}$  values and the set of 405  $D_{DS}$  values was performed, the test statistic  $t'$  equalled 37.648. The calculated  $t'$  from equation 6 was significantly larger than the critical  $t$  of 1.967 where the  $DF$  equalled 336 and the significance level  $\alpha$  was 0.05. The null hypothesis that the two populations  $D_{SS}$  and  $D_{DS}$  have the same mean values ( $\bar{D}_{SS} = \bar{D}_{DS}$ ) was rejected.

A common statistical approach to differentiating two samples with a known level of statistical certainty is to hypothesize that the two samples come from the same population and therefore have the same value for some measurable parameter. The hypothesis is referred to as the null hypothesis where statistical tests are employed to determine whether the null hypothesis should be accepted or rejected. If the null hypothesis is rejected the alternative hypothesis is accepted, i.e. the two samples come from different populations. The statistical test (t-test) is conducted at some significance level  $\alpha$  which controls the risk of making an error when accepting or rejecting the null hypothesis. The error of incorrectly rejecting the null hypothesis is a Type I error which is controlled by the significance level  $\alpha$ . The error of incorrectly accepting the null hypothesis is a Type II error and the probability of making a Type II error is given by  $\beta$ . Figure 41 depicts two probability distributions with different means and equal

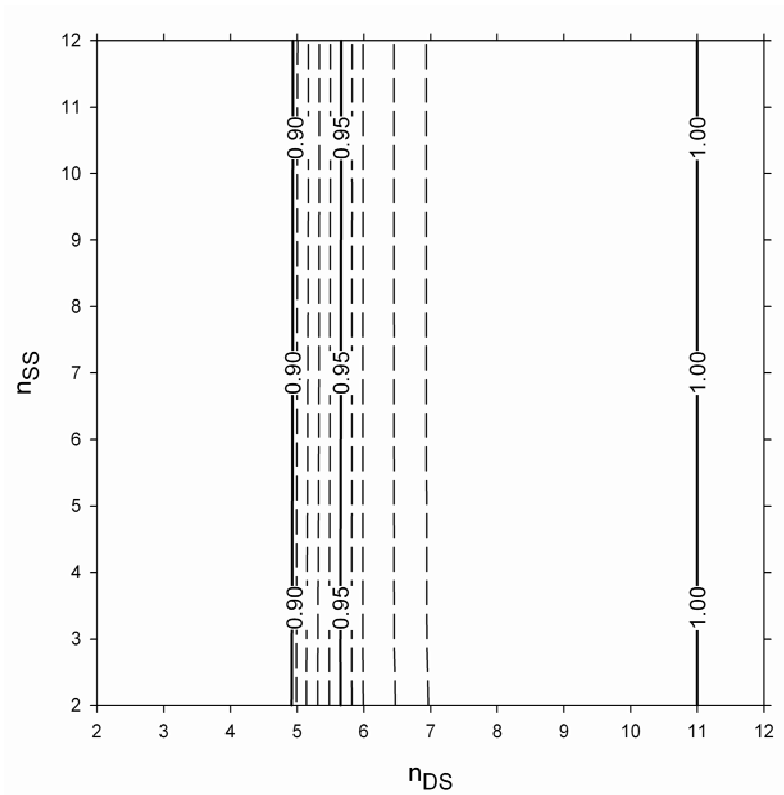
standard deviations depicting two populations. The power of a test corresponds to  $1-\beta$  and represents the probability of making a correct decision when the null hypothesis is false.



**Figure 41: Depiction of Two Probability Distributions**

For two given distributions,  $\beta$  is determined when  $\alpha$  (significance level) and  $n$  (number of measurements for each sample) are set. A smaller  $\alpha$  leads to a greater  $\beta$  hence a lower power for the test. In practice the significance level is set  $\alpha = 0.01$  when a Type I error is most costly whereas  $\alpha = 0.05$  is commonly used when a Type II error is most costly.

When comparing the individual gasoline samples, the number of replicate measurements must be determined to provide statistically reliable results which protect against Type II errors. An analysis of the power of the two-sided t-test for the given  $\bar{D}_{DS}$  and  $\bar{D}_{SS}$  with their associated standard deviations was performed for the varying sample sizes  $n_{SS}$  and  $n_{DS}$  at a significance level  $\alpha$  of 0.05.<sup>58</sup> The result of the power analysis is shown in Figure 41 indicating for  $\alpha = 0.05$  at least 7  $D_{DS}$  values are required to achieve 99% probability of making a correct decision when the null hypothesis is false. The result suggests that the triplicate GC-MS analyses of each gasoline should be able to discriminate gasoline samples from different sources with a 1% or less chance of making a Type II error.



**Figure 42: The Calculated Power for  $n_{SS}$  and  $n_{DS}$  at a significance level  $\alpha$  of 0.05**

A comparison of two individual gasoline samples was conducted by a t-test to determine if  $\bar{D}_{DS}$  and  $\bar{D}_{SS}$  arise from the same populations, i.e. if the two samples share a common origin. The six  $D_{SS}$  values for each pair-wise comparison of the replicate analyses for the same sample allowed the  $\bar{D}_{SS}$  calculation. The nine  $D_{DS}$  values for each pair-wise comparison of the replicate analyses for different samples allowed the calculation of  $\bar{D}_{DS}$ . The set of  $\bar{D}_{DS}$  values calculated for each of the 45 unique pair-wise comparisons are shown in Table 8. The t-test was conducted as described in the previous paragraph comparing  $\bar{D}_{DS}$  and  $\bar{D}_{SS}$  with the associated standard deviations and number of data points at a significance level  $\alpha = 0.05$ . The results of the t-test conclude that 100% of the gasoline samples could be distinguished from one another hence

having come from different sources with no Type II errors. Gasoline samples 7 and 9 had the smallest  $\bar{D}_{DS}$  value of 0.042 for all pair-wise comparisons. Statistical tests as discussed here can rule out a common source with a known risk of Type I error, but can not prove the existence of a common source.

**Table 9: Average Distances between Gasoline Samples**

Gas	1	2	3	4	5	6	7	8	9
2	0.182								
3	0.150	0.222							
4	0.315	0.259	0.260						
5	0.140	0.217	0.069	0.241					
6	0.179	0.241	0.149	0.149	0.115				
7	0.168	0.187	0.132	0.166	0.104	0.069			
8	0.275	0.336	0.247	0.142	0.216	0.111	0.176		
9	0.161	0.198	0.098	0.187	0.072	0.069	0.042	0.177	
10	0.287	0.342	0.251	0.117	0.226	0.117	0.179	0.058	0.181

*Identification of Two Unknown Gasoline Samples*

Two blind tests were performed to evaluate whether the covariance method which was able to discriminate the 10 gasoline samples could correctly identify unknown gasoline sample within a set of possible sources. Aliquots of two gasoline samples from Table 5 were chosen and presented as unknown A and unknown B. The unknown samples were analyzed in triplicate and the  $D_{SS}$  values calculated, then  $D_{DS}$  values were calculated between each unknown and the 10 gasoline samples. Comparisons of the unknowns against each of the 10 gasoline samples were conducted by the t-test described previously. The null hypothesis  $H_0: \bar{D}_{DS} = \bar{D}_{SS}$  is accepted if the calculated t' is less than the critical t value. If the calculated t' is greater than the critical t value then the null hypothesis is rejected and the alternative hypothesis  $H_a: \bar{D}_{DS} \neq \bar{D}_{SS}$  is

accepted. The average distances, DF,  $t'$ , critical  $t$  and hypothesis test results are given in Tables 9 and 10. The results illustrate that the  $t$ -test correctly identified Unknown A as gasoline 8, however the test failed to identify Unknown B. A Type I error occurred by incorrectly rejecting the null hypothesis  $H_0: \bar{D}_{DS} = \bar{D}_{SS}$  for Unknown B and gasoline 4. The smallest  $\bar{D}_{DS}$  between Unknown B and each of the ten gasoline samples was gasoline 4, which was significantly smaller than the other average distances. Unfortunately, it was significantly different from  $\bar{D}_{SS}$  of gasoline 4 as proven by the  $t$ -test.

**Table 10: Unknown A Comparison to Ten Gasoline Samples**

Gas	$\bar{D}_{DS}$	$\bar{D}_{SS}$	DF	$t'$	t critical	Accept $H_0$
1	0.2441	0.0346	10	12.8648	2.2281	No
2	0.3154	0.0341	10	27.8234	2.2281	No
3	0.2378	0.0340	6	29.1167	2.4469	No
4	0.1679	0.0246	9	13.5863	2.2622	No
5	0.1933	0.0256	6	19.3374	2.4469	No
6	0.1002	0.0266	5	8.6094	2.5706	No
7	0.1602	0.0269	7	14.3471	2.3646	No
8	0.0425	0.0293	13	1.1116	2.1604	Yes
9	0.1658	0.0258	5	16.2873	2.5706	No
10	0.0944	0.0280	13	5.6634	2.1604	No

**Table 11: Unknown B Comparison to Ten Gasoline Samples**

Gas	$\bar{D}_{DS}$	$\bar{D}_{SS}$	DF	$t'$	t critical	Accept $H_0$
1	.2912	.0185	9	19.3383	2.2622	No
2	.2355	.0234	10	28.8626	2.2281	No
3	.2403	.0233	12	40.7474	2.1788	No
4	.0294	.0138	12	4.5599	2.1788	No
5	.2189	.0149	13	55.5377	2.1604	No
6	.1273	.0159	11	28.5921	2.2010	No
7	.1435	.0162	13	26.8374	2.1604	No
8	.1378	.0186	9	43.6475	2.2622	No
9	.1643	.0151	13	33.4558	2.1604	No
10	.1286	.0172	11	32.3314	2.2010	No

## *Discussion*

Covariance mapping with subsequent comparisons by distance measurements could be used in rapidly comparing an unknown ignitable liquid to a database of reference ignitable liquids. A database search between  $Z_N$  matrix of an unknown ignitable liquid and the  $Z_N$  matrices of ignitable liquids from a database would generate a list of best matches based on the distances calculated. The distance measurement between covariance matrices of ignitable liquids can distinguish between various classes of ignitable liquids as well as the sub-classifications of light, medium, and heavy. The method was able to distinguish the relative amounts of weathering (evaporation) between gasoline samples.

Covariance mapping with subsequent comparisons by distance measurements and t-tests has distinguished 10 gasoline samples as having come from different sources. GC-MS 3D data has been converted to a covariance matrix then sample comparisons have been made by calculating a distance between the normalized matrices of the two samples. To determine if the distance is significant a t-test was performed while keeping a Type II error low. Blind tests were conducted to determine if an unknown gasoline sample could be correctly identified with the method. No Type II errors (incorrectly accepting the null hypothesis) were made, but a Type I error (incorrectly rejecting the null hypothesis) was made for Unknown B.

The distance measurement of sample covariance matrices with a subsequent t-test is an applicable method for comparative analysis of complex mixtures. The study used neat dilute solutions of ignitable liquids analyzed with the same analytical method and performed almost exclusively on the same instrument. Identification of ignitable liquids collected from a fire scene becomes more complicated with the addition of pyrolysis and combustion products from building materials and furnishing within the structure as well as volatiles remaining from the



manufacturing process.<sup>59</sup> Other complications in identification of an ignitable liquid arise from weathering, biological degradation,<sup>60</sup> chromatographic distortion due to the extraction procedure, and inter laboratory differences in analytical methods. These complications are valid with current methods of characterization and identification of ignitable liquids by pattern recognition. The method presented was not tested with fire debris samples, but has the capability of removing a covariance matrix of substrate compounds from the fire debris sample covariance matrix for an improvement in ignitable liquid comparison with the fire debris sample. The covariance mapping with a distance measurement provides a rapid method to characterize an ignitable liquid by class, carbon range and percent evaporation and as a direct comparison between two liquids with a known statistical certainty

## CHAPTER SIX: DISCUSSION

There are four major aspects in the analysis of fire debris beginning at the fire scene with the collection of fire debris evidence from the point of origin, the extraction of ignitable liquid residues from the fire debris, the detection of the ignitable liquid residue, and the interpretation of the data leading to the classification or identification of the ignitable liquid. Valuable information is obtained through the analysis of the fire debris allowing the fire investigator to determine the cause of the fire thus assisting in assigning responsibility and culpability. Current practices for the collection and preservation of the fire debris evidence recommend that evidence containers be vapor-tight and contaminant free. The American Society of Testing and Materials has published six standard practices for the extraction of ignitable liquid residues from fire debris. ASTM has also published two standard practices for the detection of ignitable liquid residues by GC and GC/MS methods. Besides the recommended analytical method for GC/MS, the practice describes three tools for the interpretation of the data for classification of the ignitable liquid residue into a group of ignitable liquid products with similar chemical and physical properties. The standard practices are reviewed and updated every five years by a committee consisting of practicing fire debris analysts.

The ASTM standard practice for separation of ignitable liquid residues from fire debris samples by passive headspace concentration with activated charcoal is a sensitive and nondestructive method of extraction. The main limitation of the method is saturation of the activated carbon which results in hydrocarbons with stronger dispersion interactions with the activated carbon displacing hydrocarbons with weaker dispersion interactions. The effect of hydrocarbon displacement is a distortion of the ignitable liquid chromatographic profiles applied

in data interpretation. An estimation of the activated carbon surface area available for adsorption was calculated at  $1128 \pm 197 \text{ m}^2/\text{g}$  based on the van der Waals interactions between five hydrocarbons (heptane, toluene, octane, nonane and decane) and the activated carbon. The results indicate the ASTM E1412-00 recommended activated carbon size of  $100 \text{ mm}^2$  could be saturated with a hydrocarbon concentration of  $24 \text{ }\mu\text{l}$  within a one quart volume. Consequently the molar distribution of extracted hydrocarbons from the activated carbon does not resemble the hydrocarbon molar distribution of the ignitable liquid residue. Adsorption of additional hydrocarbon molecules continued when coverage of the activated carbon was sub-monolayer along with no desorptive losses of previously adsorbed hydrocarbon molecules. Once all of the adsorption sites of the activated carbon surface area were filled, uniform desorptive hydrocarbon molecule losses occurred when heat alone was applied. However, upon subsequent addition of hydrocarbon molecules preferential adsorption was demonstrated by molecules with stronger dispersion forces. When liquid phase concentrations of ignitable liquid residues are present within fire debris ASTM E1412-00 standard practice is not the recommended due to complications which arise from the adsorption interactions of hydrocarbon molecules with activated carbon. The ASTM E1412-00 standard practice is best used with fire debris containing low concentrations of ignitable liquid residues. Since liquid residue concentrations are unknown incorporation of two simple steps prior to the application of the method prevents saturation of the activated carbon. A sub-sample created by the two steps in which the ignitable liquid residue is uniformly distributed throughout the fire debris is selected for extraction hence avoiding saturation of the activated carbon.

A major concern in fire investigations is the collection and preservation of ignitable liquid residues obtained from fire debris at the point of fire origination. The physical evidence

container must be vapor-tight due to the volatile nature of ignitable liquid residues and contaminant free. Metal paint cans, glass mason jars and co-polymer bags are typical fire debris evidence containers. Activated carbon positioned throughout the depth of a glass jar container revealed no significant variation in the hydrocarbon molar distribution hence placement of the activated carbon within the container was not critical in the experiment. Leak rates of the three container types were calculated and compared to one another followed by demonstrations of the possible ramifications. After six days, the glass jar lost 98 percent of the hydrocarbons originally deposited into the container. The fastest leak rate was obtained by the glass jars followed by the metal cans with the co-polymer bags not leaking at all when properly sealed. Molar distributions of the recovered hydrocarbons were affected by the closing mechanisms of the glass jar and metal can. Hydrocarbons with smaller collision diameters leaked from the jars preferentially to those with larger collision diameters. However, the hydrocarbons from the metal can leaked the container at equal rates.

Interpretation of GC/MS data by pattern recognition of chromatographic profiles, extracted ion profiles, and target ion analysis rare described in ASTM E1618-01 with a classification scheme designed to group ignitable liquids together based on their chemical and physical properties. The classification scheme relies on comparing the unknown ignitable liquid residue to a known reference ignitable liquid. The method relies heavily upon the analyst's interpretation of the data and the standard practice. Covariance mapping with subsequent comparisons by distance measurements was able to distinguish between various classes of ignitable liquids and sub-classify by boiling point ranges established by the ASTM E1618-01 classification scheme. States of gasoline evaporation could be ascertained by comparison of covariance matrices of known evaporated gasoline. Ten gasoline samples were compared to one

another by calculating a distance between the normalized covariance matrices of two gasoline samples. To determine if the distance (difference) between the covariance matrices was significant a t-test was performed. All gasoline samples were determined to have originated from different sources with no Type I or Type II errors occurring. Two blind tests were conducted to determine if an unknown gasoline could be identified with a gasoline from a known source. One gasoline sample was correctly identified from the 10 gasoline samples. However, the other gasoline sample could not be identified with a known statistical certainty and by rejecting the null hypothesis a Type I error occurred. The combination of covariance mapping with a distance measurement and t-test has the potential to characterize, distinguish and possibly identify ignitable liquids from existing GC/MS data with a known statistical certainty.

A covariance mapping method combined with a distance measurement allows for quick searching of a large database of ignitable liquid GC/MS data. It does not require the analyst to perform pattern recognition, ion profiling, nor target ion analysis to compare the ignitable liquid samples thus saving time. The results in the study of the study are compatible with the ASTM classification system and do not rely on the subjective interpretation of the analyst. Comparisons between GC/MS data sets originating from different laboratories may be possible since during the formation of the covariance matrix the time element (scan number) is removed.

Future studies for software development using covariance mapping with distance measurements would enable an analyst to search a database containing GC/MS data collected from multiple laboratories of ignitable liquid samples. Inter-laboratory comparisons involved further refinements to the method. Other complications with developing software for database searching are weathering (evaporation) of samples which alters the composition, and interfering products from the fire scene. The method has proven to be an excellent tool in comparing

ignitable liquids from neat solutions. However, most ignitable liquid samples encountered in a crime laboratory have been weathered and contain interfering products all produced from the fire and fire scene.

**APPENDIX: PERMISSION LETTER**

PERMISSION REQUEST FORM

Date: 3/5/07

To: Copyright Office  
Publications Division  
American Chemical Society  
1155 Sixteenth Street, N.W.  
Washington, DC 20036

FAX: 202-776-8112

From: Mary R.

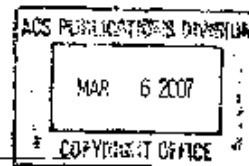
Williams

P.O. Box 162367

Orlando FL 32816-2367

Your Phone No. 407-823-6038

Your Fax No. 407 823-3162



I am preparing a paper entitled:

Advances in Fire Debris Analysis

to appear in a (circle one) book, magazine, journal, proceedings, other thesis  
entitled: \_\_\_\_\_

to be published by: University of Central Florida

I would appreciate your permission to use the following ACS material in print and other formats with the understanding that the required ACS copyright credit line will appear with each item and that this permission is for only the requested work listed above:

From ACS journals or magazines (for ACS magazines, also include issue no.):

ACS Publication Title Issue Date Vol. No. Page(s) Material to be used\*

Analytical Chemistry manuscript ID ac062230n accepted 2/27/07 Figure 3

From ACS books: include ACS book title, series name and number, year, page(s), book editor's name(s), chapter author's name(s), and material to be used, such as Figs. 2 & 3, full text, etc.\*

PERMISSION TO REPRINT IS GRANTED BY  
THE AMERICAN CHEMICAL SOCIETY

\* If you use more than three figures/tables will also be required.  
Questions? Please call Arleen Courtney

ACS CREDIT LINE REQUIRED. Please follow this sample:  
Reprinted with permission from (reference citation). Copyright (year) American Chemical Society.

This space is reserved for  
ACS Copyright Office Use

APPROVED BY: C. Arleen Courtney 3/6/07  
ACS Copyright Office

If box is checked, author permission is also required. See original article for address.



## REFERENCES

- 
- <sup>1</sup> U.S. Fire Administration December 2006.  
<http://www.usfa.dhs.gov/statitics/quickstats/index.shtm>. Accessed March 3, 2007.
- <sup>2</sup> Redsicker DR, O'Connor JJ. Practical Fire and Arson Investigation. 2nd ed. Boca Raton: CRC Press; 1997.
- <sup>3</sup> NFPA 921: Guide for Fire and Explosions Investigations. National Fire Protection Association; 1998.
- <sup>4</sup> Hine GA. Fire Scene Investigation: An Introduction for Chemists: Analysis and Interpretation of Fire Scene Evidence. Boca Raton: CRC Press; 2004.
- <sup>5</sup> ASTM E1385-00 Standard Practice for Separation and Concentration of Ignitable Liquid Residues from Fire Debris Samples by Steam Distillation: ASTM Annual Book of Standards. West Conshohocken: ASTM International; 2002. Vol. 14.02.
- <sup>6</sup> ASTM E1386-00 Standard Practice for Separation and Concentration of Ignitable Liquid Residues from Fire Debris Samples by Solvent Extraction: ASTM Annual Book of Standards. West Conshohocken: ASTM International; 2002. Vol. 14.02.
- <sup>7</sup> ASTM E1388-00 Standard Practice for Sampling Headspace Vapors from Fire Debris Samples: ASTM Annual Book of Standards. West Conshohocken: ASTM International; 2002. Vol. 14.02.
- <sup>8</sup> ASTM E1413-00 Standard Practice for Separation and Concentration of Ignitable Liquid Residues from Fire Debris Samples by Dynamic Headspace Concentration: ASTM Annual Book of Standards. West Conshohocken : ASTM International; 2002. Vol. 14.02.
- <sup>9</sup> ASTM E1412-00 Standard Practice for Separation of Ignitable Liquid Residues from Fire Debris Samples by Passive Headspace Concentration with Activated Charcoal: ASTM Annual Book of Standards. West Conshohocken: ASTM International; 2002. Vol. 14.02.
- <sup>10</sup> ASTM E2154-01 Standard Practice for Separation and Concentration of Ignitable Liquid Residues from Fire Debris Samples by Passive Headspace Concentration with Solid Phase Microextraction (SPME): ASTM Annual Book of Standards. West Conshohocken: ASTM International; 2002. Vol. 14.02.
- <sup>11</sup> Kelly RL, Martz RM. Accelerant Identification in Fire Debris by Gas Chromatography/Mass Spectrometry Techniques. Journal of Forensic Sciences 1984; 29(3):714-722.
- <sup>12</sup> Skoog, Holler, Nieman. Principles of Instrumental Analysis. 5th ed. Philadelphia: Harcourt Brace & Co.; 1998.

- 
- <sup>13</sup> Grob RL. *Modern Practice of Gas Chromatography*. 3<sup>rd</sup> ed. New York: John Wiley & Sons; 1995.
- <sup>14</sup> Pavia DL, Lampman GM, Kriz GS. *Introduction to Spectroscopy: A Guide for Students of Organic Chemistry*. 2<sup>nd</sup> ed. Fort Worth: Harcourt Brace College Publishers; 1996.
- <sup>15</sup> Bertsch W. Two-Dimensional Gas Chromatography. Concepts, Instrumentation, and Applications – Part 2: *Comprehensive Two-Dimensional Gas Chromatography*. *J High Resol Chromatography* 2000; 23(3):167-181.
- <sup>16</sup> Frysinger GS, Gainers RB. *Comprehensive Two-Dimensional Gas Chromatography with Mass Spectrometric Detection (GC x GC/MS) Applied to the Analysis of Petroleum*. *J. High Resol Chromatography* 1999; 22(5):251-255.
- <sup>17</sup> deVos BJ, Froneman M, Rohwer E, Sutherland DA. Detection of Petrol (Gasoline) in Fire Debris by Gas Chromatography/Mass Spectrometry/Mass Spectrometry (GC/MS/MS). *Journal of Forensic Sciences* 2002; 47(4):1-21.
- <sup>18</sup> ASTM E1387-01 Standard Test Method for Ignitable Liquid Residues in Extracts from Fire Debris Samples by Gas Chromatography: *ASTM Annual Book of Standards*. West Conshohocken: ASTM International; 2002. Vol. 14.02.
- <sup>19</sup> ASTM E1618-01 Standard Test Method for Ignitable Liquid Residues in Extracts from Fire Debris Samples by Gas Chromatography-Mass Spectrometry: *ASTM Annual Book of Standards*. West Conshohocken: ASTM International; 2002. Vol. 14.02.
- <sup>20</sup> Dolan J. *Detection and Characterization of Ignitable Liquid Residues: Analysis and Interpretation of Fire Scene Evidence*. Boca Raton: CRC Press; 2004.
- <sup>21</sup> Keto RO. GC/MS Data Interpretation for Petroleum Distillate Identification in Contaminated Arson Debris. *Journal of Forensic Sciences* 1995; 40(3):412-423.
- <sup>22</sup> Mann D. Comparison of Automotive Gasolines Using Capillary Gas Chromatography I: Comparison Methodology. *Journal of Forensic Sciences* 1987; 32(3):606-615.
- <sup>23</sup> Nowicki J. An Accelerant Classification Scheme Based on Analysis by Gas Chromatography/Mass Spectrometry (GC/MS). *Journal of Forensic Sciences* 1990; 35(5):1064-1086.
- <sup>24</sup> Newman R. *ASTM Approach to Fire Debris Analysis: Analysis and Interpretation of Fire Scene Evidence*. Boca Ration: CRC Press; 2004.
- <sup>25</sup> Yun JH, Choi DK, Kim SH. Equilibria and dynamics for mixed vapors of BTX in an activated carbon bed. *AIChE Journal* 1999; 45(4):751-60.

- 
- <sup>26</sup> Newman RT, Dietz WR, Lothridge K. The Use of Activated Charcoal Strips for Fire Debris Extractions by Passive Diffusion. Part 1: The Effects of Time, Temperature, Strip Size, and Sample Concentration. *Journal of Forensic Sciences* 1996; 41(3):361-370.
- <sup>27</sup> Atkins PW. *Physical Chemistry*. 2<sup>nd</sup> Ed. New York: W.H. Freeman and Co.; 1982.
- <sup>28</sup> Buckleton JS, Bettany BL, Walsh KAJ. A Problem of Hydrocarbon Profile Modification by Charcoal. *Journal of Forensic Sciences* 1989; 34(2):449-453.
- <sup>29</sup> Ouellette RJ, Rawn JD. *Organic Chemistry*. Upper Sadle River: Prentice Hall; 1996.
- <sup>30</sup> Glasstone S, Lewis D. *Elements of Physical Chemistry*. 2<sup>nd</sup> ed. Princeton: Van Nostrand Co. Inc.; 1960.
- <sup>31</sup> Wood GO. Affinity coefficients of the Polanyi/Dubin adsorption isotherm equations. A review with compilation and correlations. *Carbon* 2001; 39:343-356.
- <sup>32</sup> Pre' P, Delage F, Faur-Brasquet C, Le Cloirec P. Quantitative structure-activity relationships for the prediction of VOCs adsorption and desorption energies onto activated carbon. *Fuel Processing Technology* 2002; 77-78:345-351.
- <sup>33</sup> Selim MM, El-Nabarawy TA. A general relationship between adsorption of hydrocarbons and their polarizabilities on activated carbon. *Carbon* 1980; 18:287-290.
- <sup>34</sup> Selim MM, El-Nabarawy TA. The relation between the adsorption of hydrocarbons and their polarizabilities on activated carbon. *Surface Technology* 1980; 10:65-72.
- <sup>35</sup> U.S. Department of Justice. *Fire and Arson Scene Evidence; A Guide for Public Safety Personnel*. Washington, DC: U.S. Department of Justice, 2000.
- <sup>36</sup> International Association of Arson Investigators. *A Pocket Guide to Accelerant Evidence Collection*. 2nd ed. Brimfield: IAAI Massachusetts chapter; 1999.
- <sup>37</sup> Tontarski R. Evaluation of Polyethylene Containers Used to Collect Evidence for Accelerant Detection. *Journal of Forensic Science* 1983; 28(2):440-445.
- <sup>38</sup> Kinard W, Midkiff M. Arson Evidence Container Evaluation: II "New Generation" Kapak Bags. *Journal of Forensic Sciences* 1991; 36(6):1714-1721.
- <sup>39</sup> Stackhouse C, Gray C. Alternative Methods for Processing Arson Samples in Polyester Bags. *Journal of Forensic Science* 1998; 33(2):515-526.

---

<sup>40</sup> Stryjnik A, Hong-You R. Evaluation of the effectiveness of nylon bags as packaging for fire debris. Proceedings of the 56<sup>th</sup> Annual Meeting of the American Academy of Forensic Sciences 2004 Feb 16-21; Dallas, TX. Colorado Springs, CO: American Academy of Forensic Sciences, 2004

<sup>41</sup> USDA Guide I Principle of Home Canning: Complete Guide to Home Canning. July 1995. [http://www.uga.edu/nchfp/publications/usda/utah\\_can\\_guide\\_01.pdf](http://www.uga.edu/nchfp/publications/usda/utah_can_guide_01.pdf). Accessed November 2005.

<sup>42</sup> Prazen BJ, Bruckner CA, Synovec RE, Kowalski BR. Enhanced chemical analysis using parallel column gas chromatography with single-detector time-of-flight mass spectrometry and chemometric analysis. *Analytical Chemistry* 1999; 71:1093-1099.

<sup>43</sup> Bertsch W. Analysis of Accelerants in Fire Debris. Data Interpretation. *Forensic Science Review* 1997; 9:1-22.

<sup>44</sup> Doble P, Sandercock M, Du Pasquier E, Petoxz P, Roux C, Dawson M. Classification of premium and regular gasoline by gas chromatography/mass spectrometry, principal component analysis and artificial neural networks. *Forensic Science International* 2003; 132:26-39.

<sup>45</sup> Tan B, Hardy JK, Snaveley RE. Accelerant classification by gas chromatography/mass spectrometry and multivariate pattern recognition. *Analytica Chimica Acta* 2000; 422:37-46.

<sup>46</sup> Sandercock PML, DuPasquier E. Chemical fingerprinting of unevaporated automotive gasoline samples. *Forensic Science International* 2003; 134:1-10.

<sup>47</sup> Sandercock PML, DuPasquier E. Chemical fingerprinting of gasoline. 2. Comparison of unevaporated and evaporated automotive gasoline samples. *Forensic Science International* 2004; 140:43-59.

<sup>48</sup> Staniloae D, Petrescu B. Pattern Recognition Based Software for Oil Spills Identification by Gas-Chromatography and IR Spectrophotometry. *Environmental Forensics* 2001; 2:363-366.

<sup>49</sup> Frasinski L, Codling JK, Hatherly PA. Covariance mapping: a correlation method applied to multiphoton multiple ionization. *Science* 1989; 246:1029-1031.

<sup>50</sup> Jukes P, Buxey A, Jones AB, Stace A. Covariance images of the primary response from rare gas cluster ions to photoexcitation. *Journal of Chemical Physics* 1997; 106:1367-1372.

<sup>51</sup> Foltin M, Stueber GJ, Bernstein ER. Dynamics of neutral cluster growth and cluster ion fragmentation for toluene/water, aniline/argon, and 4-fluorostyrene/argon clusters: Covariance mapping of the mass spectral data. *Journal of Chemical Physics* 1998; 109:4342-4360.

- 
- <sup>52</sup> Feldman AB, Antoine M, Lin JS, Demirev PA. Covariance mapping in matrix-assisted laser desorption/ionization time-of-flight mass spectrometry. *Rapid Communications in Mass Spectrometry* 2003; 17:991-995.
- <sup>53</sup> Van Stipkonk MJ, Schweikert EA, Park MA. Coincidence Measurements in Mass Spectrometry. *Journal of Mass Spectrometry* 1997; 32:1151-1161.
- <sup>54</sup> Lindman HR. *Analysis of Variance in Experimental Design*. New York: Springer-Verlag; 1991.
- <sup>55</sup> Malinowski ER, Howery DG. *Factor Analysis in Chemistry*. New York: Wiley; 1980.
- <sup>56</sup> Barnett V, Lewis T. *Outliers in Statistical Data: Wiley Series in Probability and Mathematical Statistics*. Second Ed. New York: Wiley; 1984.
- <sup>57</sup> Sachs L, *Applied Statistics: A Handbook of Techniques*. New York: Springer-Verlag; 1984.
- <sup>58</sup> Lenth RV. Java Applets for Power and Sample Size [Computer software]. 2006. <http://www.stat.uiowa.edu/~rlenth/Power>. Retrieved July 4, 2006.
- <sup>59</sup> Almirall JR, Furton KG. Characterization of background and pyrolysis products that may interfere with the forensic analysis of fire debris. *Journal of Analytical and Applied Pyrolysis* 2004; 71: 51-67.
- <sup>60</sup> Mann DC, Gresham WR. Microbial Degradation of Gasoline in Soil. *Journal of Forensic Sciences* 1990; 35:913-923.